AD_____

Award Number: W81XWH–05–1-0035

TITLE: A double selection approach to achieve specific expression of toxin genes for ovarian cancer gene therapy

PRINCIPAL INVESTIGATOR: David T. Curiel, M.D., Ph.D.
Gene Siegal, M.D., Ph.D.
Minghui Wang, M.D.

CONTRACTING ORGANIZATION: University of Alabama
Birmingham, AL 35294-0111

REPORT DATE: November 2006

TYPE OF REPORT: Annual (Revised)

PREPARED FOR: U.S. Army Medical Research and Materiel Command
Fort Detrick, Maryland 21702-5012

REPORT DOCUMENTATION PAGE

Form Approved
OMB No. 0704-0188

1. REPORT DATE *(DD-MM-YYYY)*	**2. REPORT TYPE**	**3. DATES COVERED** *(From - To)*
01/11/06	Annual, Revised	1 Nov 2005 – 31 Oct 2006

4. TITLE AND SUBTITLE

A double selection approach to achieve specific expression of toxin genes for ovarian cancer gene therapy

5a. CONTRACT NUMBER

5b. GRANT NUMBER
W81XWH-05-1-0035

5c. PROGRAM ELEMENT NUMBER

6. AUTHOR(S)
David T. Curiel, M.D., Ph.D., Gene Siegal, M.D., Ph.D., Minghui Wang, M.D.

E-Mail: curiel@uab.edu

5d. PROJECT NUMBER

5e. TASK NUMBER

5f. WORK UNIT NUMBER

7. PERFORMING ORGANIZATION NAME(S) AND ADDRESS(ES)

University of Alabama
Birmingham, AL 35294-0111

8. PERFORMING ORGANIZATION REPORT NUMBER

9. SPONSORING / MONITORING AGENCY NAME(S) AND ADDRESS(ES)
U.S. Army Medical Research and Materiel Command
Fort Detrick, Maryland 21702-5012

10. SPONSOR/MONITOR'S ACRONYM(S)

11. SPONSOR/MONITOR'S REPORT NUMBER(S)

12. DISTRIBUTION / AVAILABILITY STATEMENT
Approved for Public Release; Distribution Unlimited

13. SUPPLEMENTARY NOTES

14. ABSTRACT: Gene therapy is a novel treatment modality which offers great potential for the control of carcinoma of the ovary. The efficacy of such approaches, however, is currently limited due to the inability of available gene delivery vehicles (vectors) to achieve efficient and selective gene transfer to target tumor cells. Proposed herein is a strategy to modify one candidate vector, recombinant adenovirus, such that it embodies the requisite properties of efficacy and specificity required for ovarian cancer gene therapy. This approach is based on targeting the delivered anti-cancer gene to tumor via two complimentary approaches. This strategy is based upon restricting the expression of the anti-cancer gene exclusively to ovarian cancer tumor cells ("transcriptional targeting") plus directing the binding of the viral vector particle exclusively to tumor cells ("transductional targeting").This "double targeting" approach is highly novel. We have advanced this double targeting approach in the current period. In the first regard, we have improved the infectivity of adenovirus (Ad) for ovarian cancer targets via a knob "switch" method exploiting fiber knobs of canine and ovine Ad fiber knobs. In the second instance, we have defined optimized tumor selective promoters for ovarian cancer (TSPs). In this period we have shown the utility of both of these modifications to improve adenovirus targeting for ovarian tumor cells in vitro and in vivo. These studies have provided the framework for testing our overall concept in the future funding period, for ascertaining therapeutic gains of double targeting in murine models of carcinoma of the ovary.

15. SUBJECT TERMS
Ovarian cancer, targeting, gene therapy

16. SECURITY CLASSIFICATION OF:			**17. LIMITATION OF ABSTRACT**	**18. NUMBER OF PAGES**	**19a. NAME OF RESPONSIBLE PERSON**
a. REPORT	**b. ABSTRACT**	**c. THIS PAGE**			USAMRMC
U	U	U	UU	109	**19b. TELEPHONE NUMBER** *(include area code)*

Standard Form 298 (Rev. 8-98)
Prescribed by ANSI Std. Z39.18

Table of Contents

Introduction

Ovarian cancer is one of the most common causes of cancer death in women. In large part this is due to the late presentation of the disease. On this basis, it is clear novel therapeutic approaches are warranted. In this regard, gene therapy represents one such novel approach which may be applied in the context of carcinoma of the ovary. For this technique to be successful clinically, highly efficient gene delivery vectors are necessary to deliver therapeutic genes specifically to tumor cells. Tropism-modified adenoviral vectors are the best agent for cell-specific gene delivery. Ovarian cancer-specific markers have been described which can be exploited as a means to achieve specific infection via "transductional targeting". The specificity of gene expression can be further improved by placing the gene under the control of an ovarian cancer-specific promoter via a "transcriptional targeting" approach. This "double-targeting" strategy achieves a synergistic improvement in specificity, thus enabling a therapeutic result to be obtained. This project seeks to develop an optimized gene delivery system based on a combination of the best available transductional and transcriptional targeting approaches for ovarian cancer. This system should result in highly efficient and specific expression of toxin encoding genes in tumor cells, enabling these cells to be selectivity eradicated and thus offering a novel technique for the achievement of ovarian cancer gene therapy.

Body

We are seeking to accomplish efficient and selective gene delivery to ovarian cancer tumor cells with our double targeting approach [1]. In the initial reporting period of this award we sought to identify candidate tumor selective promoters (TSPs) which exhibited the requisite "tumor on/liver off" induction profiles. In support of this goal, we developed a novel tissue slice method to evaluate the "tumor on" phenotype of candidate promoters in a stringent assay context [2]. Based upon these concepts, we extended these studies to the current period to compare candidate promoters in a head-to-head fashion to identify the optimal ovarian cancer TSPs to carry forward in the context of our vector designs. This was accomplished employing stringent assay based upon a tissue slice method of primary tumor analysis. Of note in this regard, we were also able to show the extended utility of our tissue slice method in characterizing vector-related hepatotoxicity [2]. In our studies during this period we were thus able to rigorously characterize candidate promoters, vis á vis the key parameters of "tumor on" and "liver off" whereby we could accomplish via vector targeting maximized expression of our therapeutic transgene and minimized hepatotoxicity.

We also sought to achieve maximized target cell infectivity. In this regard, tumor cell deficiency of the primary adenoviral receptor coxsackie-and-adenovirus receptor (CAR) dictates the need for adenovirus tropism modifications to achieve CAR-independent infection [3]. We initially employed a strategy of fiber knob serotype chimerism exploiting human serotype chimeras (Ad serotype 3) and xenotype chimeras (canine, ovine, porcine) [4,5]. These studies demonstrated that CAR-independent infection provides a means to achieve dramatic infectivity enhancement of tumor cells. Direct comparison of

the various modifications demonstrated that serotype chimerism of human type 3 adenoviruses achieved the highest target cell infectivity enhancements in the context of the broadest range of human ovarian cancer target cell lines and primary tumor samples [6, Fig.2]. Based on this recognition, we have endeavored studies to identify the cellular receptor for the type 3 fiber knob towards exploiting this information for further vector targeting gains [5]. Further, we have employed the optimized TSP with this optimal infectivity enhancement to achieve an improved therapeutic index for an adenovirus-based ovarian cancer gene therapy [6, Fig.6].

We have also sought to extend the gains of infectivity enhancement via a novel strategy of "complex mosaicism." In this approach, distinct capsid modifications capable of mediating CAR-independent infection are exploited in combination, in the context of a single viral particle [7, Fig.1]. We hypothesized that in a single capsid context the modifications would operate additively, or synergistically, to achieve infectivity enhancement. In our initial proof-of-principle studies we derived Ad vectors which incorporated both the serotype 3 knob and the sigma spike protein of reovirus [7, Fig.4]. These studies demonstrated a clear synergism of infectivity enhancement whereby augmented transduction of ovarian cancer targets could be demonstrated.

We also developed a method to incorporate targeting ligands into the adenovirus capsid via biotin cross-linking. This method allowed for cell specific targeting to ovarian cancer targets. In addition, imaging analysis confirmed the capacity of the vector modification to allow for human cell specific gene delivery *in vivo*.

Key Research Accomplishments

- Ovarian cancer tumor selective promoters (TSPs) were defined and compared head-to-head to define the optimal ovarian cancer TSP.
- Tissue slice analysis of human and murine liver allowed for pre-clinical assessment of vector related hepatotoxicity.
- Tropism modification via knob chimerism allowed for optimal tumor cell infectivity enhancement.
- The knob chimerism strategy of serotype chimerism for human adenovirus type 3 allowed for the highest levels of tumor cell transduction.
- The cellular receptor for the adenovirus serotype knob was identified.
- A novel strategy of capsid modification ("complex mosaicism") allowed for synergistic gains in infectivity enhancement for tumor cells.
- *In vivo* targeting of tumor cells was accomplished in murine model of human ovarian cancer.

Reportable Outcomes

1. Le LP, Le HN, Dmitriev IP, Davydova JG, Gavrikova T, Yamamoto S, Curiell DT, Yamamoto Y. Dynamic monitoring of oncolytkc adenovirus in vivo by genetic capsid labeling. JNCI, 2006 Feb 1;98(3):203-14.

2. Nakayama M, Both GW, Banizs B, Tsuruta Y, Yamamoto S, Kawakami Y, Douglas JT, Tani K, Curiel DT, Glasgow JN. An adenovirus serotype 5 vector with fibers derived from ovine atadenovirus demonstrates CAR-independent tropism and unique biodistribution in mice. Virology. 2006 Jun 20;350(1):103-15.

3. Pereboeva L, Komarova S, Roth J, Ponnazhagan S, Curiel DT. Targeting EGFR with metabolically biotinylated fiber-mosaic adenovirus. Gene Ther. Submitted.

4. Tsuruta Y, Pereboeva L, Glasgow JN, Rein DT, Kawakami Y, Alvarez RD, Rocconi RP, Siegal GP, Dent P, Fisher PB, Curiel DT. A mosaic fiber adenovirus serotype 5 vector containing reovirus σ1 and adenovirus serotype 3 knob fibers increase transduction in an ovarian cancer ex vivo system via a CAR-independent pathway. Clin Cancer Res. Submitted.

5. Zhang B, Liu J, Pan J, Hou Z, Han S, Hu G, Wang S, Zhu ZB, Curiel DT. A novel conditionally replicating adenovirus combined with cisplatin enhanced antitumor efficacy on ovarian cancer *in vitro* and *in vivo*. Clin Cancer Res. Submitted.

Conclusions

A strategy of double targeting to achieve selective gene delivery to tumor cells can be designed based upon the combination of transcriptional and transductional targeting methods. In the former regard, ovarian selective TSPs can be identified which exhibit the key tumor on/liver off profile. Further, stringent substrate assays can define the optimal TSP for our targeting goals. In the latter regard, we have validated that CAR-independent infection allows infectivity enhancement of tumor targets. Further, a strategy to achieve optimal infectivity enhancement gains can be realized based upon the complex mosaic paradigm. These optimized vector design advancements can now be combined in a double targeting configuration to allow for testing of our overall hypothesis vis à vis targeted *in vivo* transduction of tumor cells. We have thus completed Tasks 1-4, as listed on our Statement of Work. Task 5 will be completed during the final period of this award.

References

1. Glasgow JN, Everts M, Curiel DT. Transductional targeting of adenovirus vectors for gene therapy. Cancer Gene Ther. 2006;13:830-844. Review.

2. Stoff-Khalili MA, Rivera Aa, Le Lp, Stoff A, Everts M, Contreras JL, chen D, Teng L, Rotss HJ, Rocconi RP, Bauerschmitz GJ, Rein DT, Yamamoto M, Siegal GP, Dall P, Mathis JM, Curiel DT. Employment of liver tissue slice analysis to assay hepatotoxicity linke to replicative and nonreplicative adenoviral agents. Cancer Gene Ther. 2006;13:606-618.

3. Mathis JM, Stewart PL, Zhu ZB, Curiel DT. Advanced generation adenoviral agents embody enhanced potency based upon CAR-independent tropism. Clin Cancer Res. 2006 May;12(9):2651-2656.

4. Stoff-Khalili MA, Rivera AA, Glasgow JN, Le LP, Stoff A, Everts M, Tsuruta Y, Kawakami Y, Bauerschmitz GJ, Mathis JM, Pereboeva L, Seigal GP, Dall P, Curiel DT. A human adenoviral vector with a chimeric fiber from canine adenovirus type 1 results in novel expanded tropism for cancer gene therapy. Gene Ther. 2005;12:1696-1706.

5. Short, JJ, Chenthamarakshan V, Holterman MJ, Curiel DT, Pereboev A. Members of adenovirus species B utilize CD80 and CD86 as cellular attachment receptors. Virus Res. 2006;122:144-153.

6. Rocconi RP, Zhu ZB, Stoff-Khalili M, Rivera AA, Lu B, Wang M, Alvarez RD, Curiel DT, Makhija SK. Treatment of ovarian cancer with a novel dual targeted conditionally replicative adenovirus (CRAd). Gynecol Oncol. 2006 Dec 13; [Epub ahead of print]

7. Tsuruta Y, Pereboeva L, Glasgow JN, Rein DT, Kawakami Y, Alvarez RD, Rocconi RP, Siegal GP, Dent P, Fisher PB, Curiel DT. A mosaic fiber adenovirus serotype 5 vector containing reovirus σ1 and adenovirus serotype 3 knob fibers increase transduction in an ovarian cancer ex vivo system via a CAR-independent pathway. Clin Cancer Res. Submitted.

Appendices

1. Nakayama M, Both GW, Banizs B, Tsuruta Y, Yamamoto S, Kawakami Y, Douglas JT, Tani K, Curiel DT, Glasgow JN. An adenovirus serotype 5 vector with fibers derived from ovine atadenovirus demonstrates CAR-independent tropism and unique biodistribution in mice. Virology. 2006 Jun 20;350(1):103-15.

2. Pereboeva L, Komarova S, Roth J, Ponnazhagan S, Curiel DT. Targeting EGFR with metabolically biotinylated fiber-mosaic adenovirus. Gene Ther. Submitted.

3. Tsuruta Y, Pereboeva L, Glasgow JN, Rein DT, Kawakami Y, Alvarez RD, Rocconi RP, Siegal GP, Dent P, Fisher PB, Curiel DT. A mosaic fiber adenovirus serotype 5 vector containing reovirus σ1 and adenovirus serotype 3 knob fibers increase transduction in an ovarian cancer ex vivo system via a CAR-independent pathway. Clin Cancer Res. Submitted.

4. Zhang B, Liu J, Pan J, Hou Z, Han S, Hu G, Wang S, Zhu ZB, Curiel DT. A novel conditionally replicating adenovirus combined with cisplatin enhanced antitumor efficacy on ovarian cancer *in vitro* and *in vivo*. Clin Cancer Res. Submitted.

Available online at www.sciencedirect.com
SCIENCE DIRECT
Virology 350 (2006) 103–115
VIROLOGY
www.elsevier.com/locate/yviro

An adenovirus serotype 5 vector with fibers derived from ovine atadenovirus demonstrates CAR-independent tropism and unique biodistribution in mice

Masaharu Nakayama [a], Gerald W. Both [c], Boglarka Banizs [a,1], Yuko Tsuruta [a], Seiji Yamamoto [a], Yosuke Kawakami [a], Joanne T. Douglas [a,b], Kenzaburo Tani [d], David T. Curiel [a,b], Joel N. Glasgow [a,*]

[a] *Division of Human Gene Therapy, Departments of Medicine, Obstetrics and Gynecology, Pathology, Surgery, University of Alabama at Birmingham, 901 19th Street South BMR2-572, Birmingham, AL 35294-2180, USA*
[b] *Gene Therapy Center, University of Alabama at Birmingham, Birmingham, AL 35294, USA*
[c] *CSIRO Molecular and Health Technologies, North Ryde, NSW 2113, Australia*
[d] *Division of Molecular and Clinical Genetics, Medical Institution of Bioregulation, Kyushu University, Fukuoka 812-8582, Japan*

Received 30 November 2005; returned to author for revision 23 December 2005; accepted 26 January 2006
Available online 3 March 2006

Abstract

Many clinically important tissues are refractory to adenovirus (Ad) infection due to negligible levels of the primary Ad5 receptor the coxsackie and adenovirus receptor CAR. Thus, development of novel CAR-independent Ad vectors should lead to therapeutic gain. Ovine atadenovirus type 7, the prototype member of genus *Atadenovirus*, efficiently transduces CAR-deficient human cells in vitro, and systemic administration of OAdV is not associated with liver sequestration in mice. The penton base of OAdV7 does not contain an RGD motif, implicating the long-shafted fiber molecule as a major structural dictate of OAdV tropism. We hypothesized that replacement of the Ad5 fiber with the OAdV7 fiber would result in an Ad5 vector with CAR-independent tropism in vitro and liver "detargeting" in vivo. An Ad5 vector displaying the OAdV7 fiber was constructed (Ad5Luc1-OvF) and displayed CAR-independent, enhanced transduction of CAR-deficient human cells. When administered systemically to C57BL/6 mice, Ad5Luc1-OvF reporter gene expression was reduced by 80% in the liver compared to Ad5 and exhibited 50-fold higher gene expression in the kidney than the control vector. To our knowledge, this is the first report of a fiber-pseudotyped Ad vector that simultaneously displays decreased liver uptake and a distinct organ tropism in vivo. This vector may have future utility in murine models of renal disease.

Keywords: Gene therapy; Adenovirus; Targeting; Tropism modification; Coxsackie and adenovirus receptor (CAR); Liver tropism; Kidney tropism

Introduction

Vectors based on human adenovirus (Ad) serotypes 2 and 5 continue to show increasing promise as gene therapy delivery vehicles, especially for cancer gene therapy, due to several key attributes: Ad vectors display in vivo stability and excellent gene transfer efficiency to numerous dividing and non-dividing cell targets. In addition, Ad vectors are rarely linked to any severe disease in immunocompetent humans, providing rationale for further development of these vehicles.

The first step in Ad5 infection occurs via high-affinity binding of the virion fiber knob domain to its cognate cellular receptor known as the coxsackie and adenovirus receptor (CAR) (Henry et al., 1994; Xia et al., 1994; Bergelson et al., 1997; Tomko et al., 1997). Following knob-CAR binding, receptor-mediated endocytosis of the virion is dramatically increased by interaction of the penton base Arg–Gly–Asp (RGD) motif with cellular integrins αvβ3, αvβ5, αvβ1, α3β1 or other integrins (Bai et al., 1993; Wickham et al., 1993; Louis

* Corresponding author. Fax: +1 205 975 7949.
E-mail addresses: mnakayam@uab.edu (M. Nakayama), gerry.both@csiro.au (G.W. Both), bbanizs@uab.edu (B. Banizs), yuko.tsuruta@uab.edu (Y. Tsuruta), yamasei@uab.edu (S. Yamamoto), ykawaka@zj9.so-net.ne.jp (Y. Kawakami), jdouglas@uab.edu (J.T. Douglas), taniken@bioreg.kyushu-u.ac.jp (K. Tani), curiel@uab.edu (D.T. Curiel), jng@uab.edu (J.N. Glasgow).
[1] Current address: Department of Cell Biology, University of Alabama at Birmingham, Birmingham, AL 35294, USA.

0042-6822/$ - see front matter © 2006 Elsevier Inc. All rights reserved.
doi:10.1016/j.virol.2006.01.037

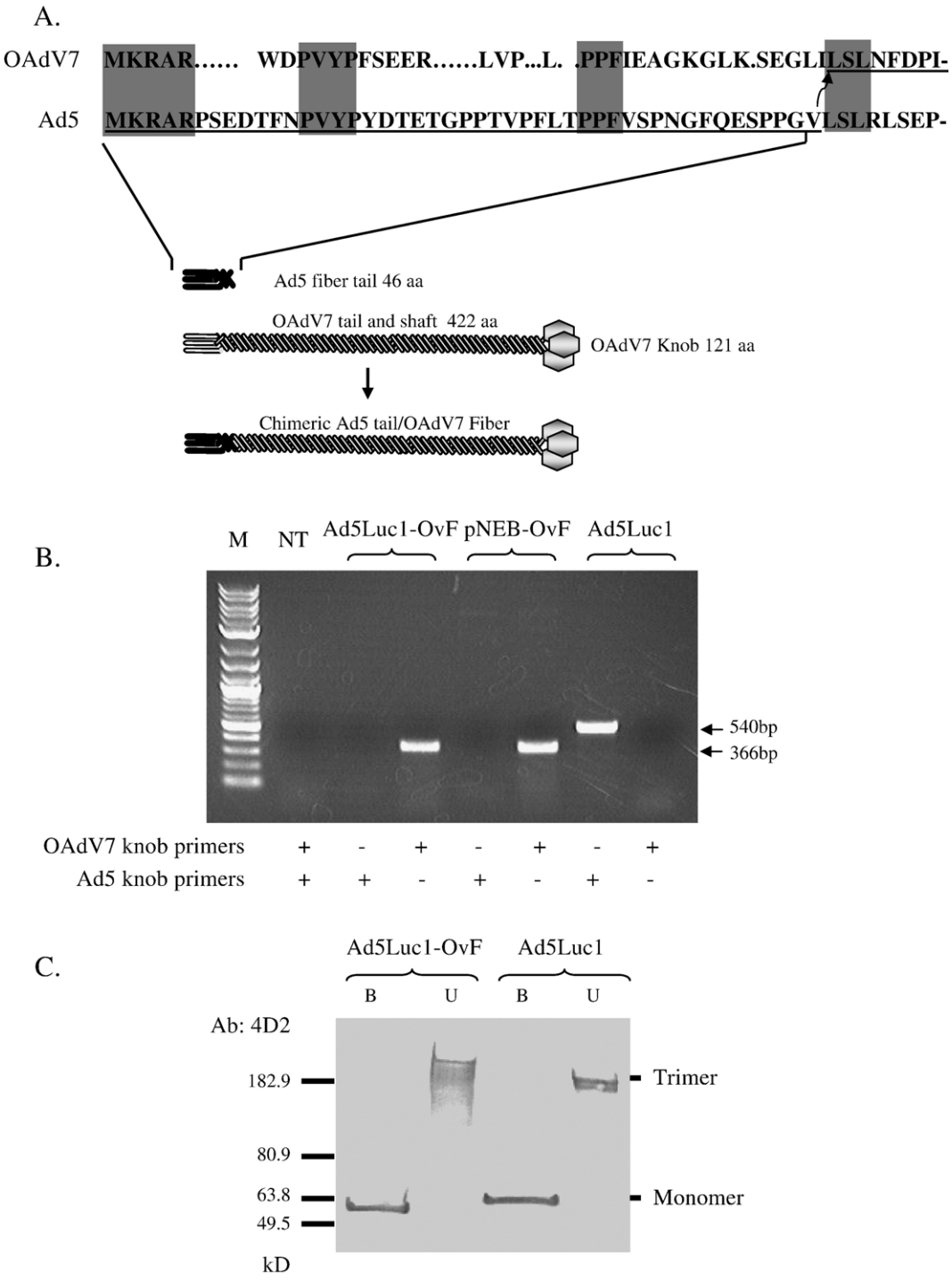

Fig. 1. Diagram depicting the design of the chimeric fiber and molecular validation of Ad5Luc1-OvF. (A) Construction of the 553-amino-acid chimeric fiber of Ad5Luc1-OvF, including the N-terminal amino acid sequences of the OAdV7 and human Ad5 fiber proteins. The LSL sequence common to both fibers that served as the junction for the replacement of the OAdV7 tail domain, as well as other common sequences, is highlighted. The final Ad5Luc1-OvF fiber sequence is underlined, and the arrow highlights that Val^{46} of the Ad5 tail domain is followed by Leu^{37} in the OAdV7 fiber. (B) PCR analysis of fiber genes using Ad genomes from rescued viral particles as the PCR templates. Ad5Luc1 virions and fiber shuttle plasmid pNEB.PK3.6-OvF (designated as pNEB-OvF in the figure) were used as controls. Lanes containing DNA size standards (M) and no PCR template (NT) are designated. Primers used are specific for the OAdV7 or Ad5 fiber gene knob domain. PCR products indicating the presence of the Ad5 or OAdV7 fiber knob domains are 540 and 366 bp, respectively. (C) Western blot analysis of fiber proteins from purified virions. 1×10^{10} vp of Ad5Luc1 with wild-type Ad5 fiber (lanes 3,4) or Ad5Luc1-OvF with chimeric OAdV7 fiber (lanes 1, 2) were resuspended in Laemmli buffer prior to SDS-PAGE and Western analysis with an anti-tail Ad5 fiber mAb. Samples in lanes 1 and 3 were heated to 99 °C prior to electrophoresis. Fiber monomers (M) and trimers (T) are indicated. Molecular mass markers indicate kilodaltons.

et al., 1994; Davison et al., 1997; Li et al., 2001; Salone et al., 2003).

Understanding of this two-step Ad entry pathway explains clinical findings by several groups that have demonstrated that cells expressing low levels of CAR are refractory to Ad infection and gene delivery. Native CAR-dependent tropism results in a scenario wherein non-target but high-CAR cells can be infected while target tissues, if low in CAR, are resistant to Ad infection. Essentially, while Ad delivery is uniquely efficient in vivo, the biodistribution of CAR is incompatible with many gene therapy interventions and in vivo co-localization of applied Ad vectors and the receptor is poor (Dmitriev et al., 1998; Miller et al., 1998; Fechner et al., 1999; Li et al., 1999; Cripe et al., 2001).

Based on a clear understanding of native Ad cell recognition, the development of CAR-independent Ad vectors has rationally focused on the fiber protein, the primary determinant of Ad tropism. Ad fiber pseudotyping, the genetic replacement of the knob domain or entire fiber with its structural counterpart from another human Ad serotype, has been employed as a means to derive Ad5-based vectors with CAR-independent tropism by virtue of the natural diversity in receptor recognition found in species B and D Ad fibers (Büchen-Osmond, 2002) and has identified chimeric vectors with superior infectivity to Ad5 in a variety of clinically relevant cell types (Gall et al., 1996; Shayakhmetov et al., 2000; Von Seggern et al., 2000; Chiu et al., 2001; Goossens et al., 2001; Havenga et al., 2001; Jakubczak et al., 2001; Havenga et al., 2002; Kanerva et al., 2002).

The development of non-human adenoviruses as gene therapy vehicles has been proposed (Khatri et al., 1997; Rasmussen et al., 1999; Reddy et al., 1999a, 1999b; Kremer et al., 2000; Loser et al., 2002; Hemminki et al., 2003). The rationale for these efforts has been three-fold: (1) no pre-existing humoral or cellular immunity will exist against "xeno" Ads in the majority of humans (Hofmann et al., 1999; Kremer et al., 2000), (2) several non-human Ads have been demonstrated to efficiently infect human cells without subsequent replication, including canine, bovine and murine mastadenoviruses (Gelhe and Smith, 1969; Nguyen et al., 1999; Rasmussen et al., 1999; Soudais et al., 2000) and ovine atadenovirus (Loser et al., 2000; Kumin et al., 2002) and (3) novel entry biologies of xeno Ads may circumvent CAR deficiency in clinically relevant human target tissues refractory to Ad5-based vectors.

Consistent with these considerations, the 287 isolate of the ovine adenovirus type 7 (OAdV7) has been evaluated as a potential human gene therapy vector (Voeks et al., 2002; Loser et al., 2003; Martiniello-Wilks et al., 2004; Wang et al., 2004). OAdV7 is the prototype isolate of a novel genus of viruses referred to as atadenovirus (Benko and Harrach, 1998). OAdV7 causes only mild symptoms in sheep and infects numerous human cell types efficiently, although replication in human cells is abortive due to the lack of viral promoter function (Boyle et al., 1994; Khatri et al., 1997; Rothel et al., 1997). OAdV7 displays CAR-independent tropism that is distinct from that of serotype 2 and 5 Ads, utilizing an unknown primary receptor(s) (Xu and Both, 1998). In addition, systemically applied OAdV7 exhibits a distinctive tissue distribution in vivo that is less hepatotropic in mice compared to Ad5-based vectors (Hofmann et al., 1999).

OAdV7 tropism is mediated via a 543-residue fiber molecule comprised of a 35 residue N-terminal tail region, a long shaft domain predicted to consist of 25 pseudorepeats and a relatively small 121-amino-acid C-terminal region comprising the knob domain (Vrati et al., 1995). In contrast to Ad5, the OAdV7 fiber does not contain the lysine-rich KKTK sequence found in the third repeat of the Ad5 fiber, a motif suggested to mediate hepatotropism of Ad5 vectors in rodents and primates in vivo (Smith et al., 2003a, 2003b). In addition, neither the penton nor fiber of OAdV7 contains an RGD sequence or other identifiable integrin-binding domain, suggesting that interaction with cell-surface integrins may not be required for infection (Vrati et al., 1996; Xu and Both, 1998). Thus, the fiber protein is the only structural determinant of OAdV7 tropism identified to date.

Based on the unique tropism of OAdV7 that combines CAR independence with a non-hepatotropic biodistribution profile, we hypothesized that an Ad5 vector, containing the OAdV7 fiber as well as its native penton base RGD, would achieve enhanced infectivity of Ad-refractory cell types in vitro and liver detargeted tropism in vivo.

Results

Generation of modified Ad5 containing the OAdV7 fiber

The OAdV7 fiber molecule is composed of homotrimers of a 543-amino-acid polypeptide. Predicted functional domains within the fiber are the tail domain spanning residues 1 to 35, the shaft domain from 36 to 422 containing approximately 25 pseudorepeats motifs and the 121-amino-acid fiber knob domain from 423 to 543 (Vrati et al., 1995). Most mammalian Ads contain a conserved threonine–leucine–tryptophan–threonine (TLWT) motif at the N-terminus of the fiber knob domain, and in human Ad2 and Ad5, a flexible region separating the shaft and the knob domains precedes this motif (van Raaij et al., 1999). The OAdV7 fiber does not contain this motif, thus the start of the knob domain is poorly defined.

Following examination of Ad5 and OAdV7 fiber polypeptide sequences, we identified a common leucine–serine–leucine (LSL) sequence common to both fibers immediately downstream of each tail domain (Fig. 1A). The LSL region was considered a common element in both fibers; therefore, we substituted the 44-amino-acid Ad5 tail domain for the native OAdV7 tail domain upstream of the LSL sequence to provide the correct penton base insertion domain for incorporation into the Ad5 capsid. This was accomplished using a two-plasmid rescue system essentially as described (Krasnykh et al., 1996; Glasgow et al., 2004). We constructed an E1-deleted recombinant Ad genome (Ad5Luc1-OvF) containing the chimeric Ad5 tail/OAdV7 fiber gene and a firefly luciferase reporter gene controlled by the CMV immediate early promoter/enhancer in the E1 region. Genomic clones of Ad5Luc1-OvF were sequenced, and two correct clones were chosen. Ad5Luc1-

Table 1
Ad5Luc1-OvF luciferase gene expression in various cancer cell lines

Cell line	Origin	CAR [a]	Fold increase in luciferase activity vs. Ad5 [b]	Reference
CHO	Hamster ovary	L/N	22	Soudais et al., 2000
RD	Rhabdomyosarcoma	L/N	1.5	Dmitriev et al., 1998; Cripe et al., 2001
PC-3	Prostate cancer	L/N	7.8	Okegawa et al., 2000
LNCaP	Prostate cancer	M	5% of Ad5	Okegawa et al., 2000
T24	Bladder cancer	L/N	9.8	Li et al., 1999
MCF7	Breast cancer	L/N	9.2	Y. Kawakami, unpublished data
HeLa	Cervical cancer	H	13% of Ad5	Bergelson et al., 1997
LoVo	Colon cancer	ND	60% of Ad5	
oLE	Ovine normal stroma	ND	2.7	
JS8JSRV	Ovine lung cancer	ND	5% of Ad5	
U118MG	Glioma	L/N	2.2	Kim et al., 2003
U118 CAR-tailless	Glioma	H	1% of Ad5	Kim et al., 2003
OV-3	Ovarian cancer	ND	23	
OV-4	Ovarian cancer	L/N	3.0	Hemminki et al., 2003
HEY	Ovarian cancer	L/N	6.5	Hemminki et al., 2003
SKOV	Ovarian cancer	ND	1	
SKOV3.ip1	Ovarian cancer	L/N	5.0	Hemminki et al., 2003
FaDu	Pharynx cancer	L/N	21% of Ad5	Blackwell et al., 1999
SCC-4	Tongue cancer	L/N	9.7	Blackwell et al., 1999
SCC-25	Tongue cancer	M	9% of Ad5	Blackwell et al., 1999
THLE-3	Normal liver epithelial	ND	10% of Ad5	
Primary Cells				
Patient 1	Ovarian cancer	ND	4	

[a] H, high levels of CAR; M, moderate; L/N, little or no CAR; ND, not determined. As determined by FACS analysis.
[b] 100 vp/cell, luciferase activity measured at 24 h post-infection.

OvF was rescued in 911 cells, and large-scale preparations of Ad5Luc1-OvF were purified by double CsCl gradient centrifugation. The concentration of Ad5Luc1-OvF was 2.7×10^{12} viral particles (vp)/ml, while the control vector Ad5Luc1 was 3.74×10^{12} vp/ml. Ad5Luc1 contains the wild-type Ad5 fiber and is isogenic to Ad5Luc1-OvF in all respects except for the fiber shaft and knob domains.

We confirmed the fiber knob genotype of Ad5Luc1-OvF via diagnostic PCR, using knob-domain-specific primer pairs and genomes from purified virions as PCR templates. Plasmids containing the fiber sequence of the wild-type OAdV7 fiber (data not shown) or the chimeric fiber gene were used as positive controls (Fig. 1B). To further confirm that Ad5Luc1-OvF virions contained trimeric fibers, we performed SDS-PAGE followed by Western blot analysis of vector particles. We used the monoclonal 4D2 primary antibody that recognizes the Ad5 fiber tail domain common to both the Ad5 and chimeric OAdV7 fiber molecules. We observed bands at approximately 185 kDa for Ad5Luc1-OvF and control Ad5Luc1 virions, corresponding to trimeric fiber molecules. Bands of boiled samples resolved at an apparent molecular mass of approximately 60–65 kDa, indicative of fiber monomers (Fig. 1C).

Ad5Luc1-OvF vector exhibits expanded tropism and enhanced gene transfer

We hypothesized that the incorporation of the OAdV7 fiber into the Ad5 capsid would provide augmented

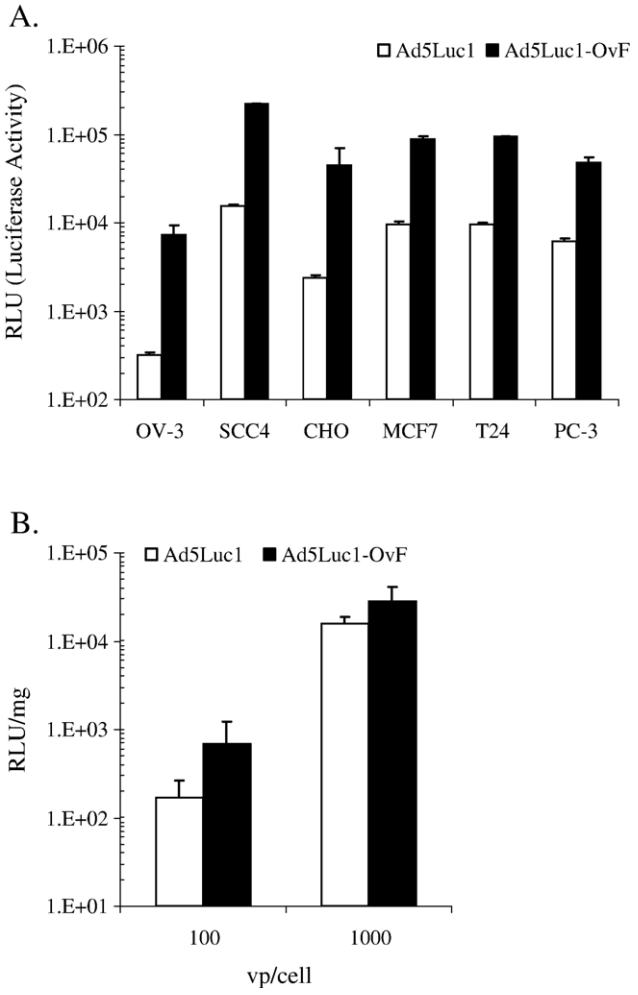

Fig. 2. Ad5Luc1-OvF-mediated gene transfer. Luciferase activities following transduction of a panel of CAR-deficient cell lines (A) and precision-cut human ovarian cancer tissue slices (B). Luciferase activity was determined 24 h post-transduction and is reported in relative light units (RLU) in panel A and RLU/mg cellular protein in panel B. Each column is average of 4 replicates using 100 vp/cell, and the error bar indicates the standard deviation.

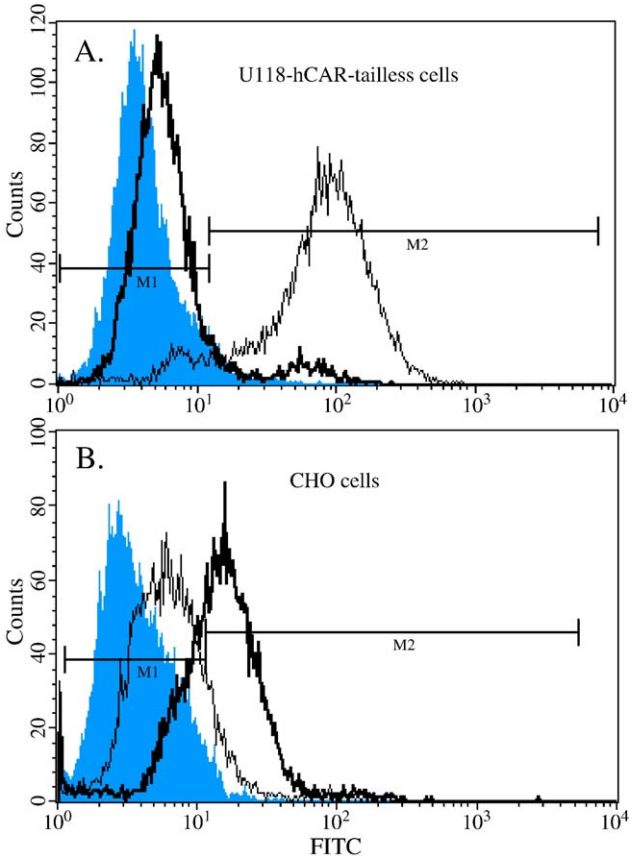

Fig. 3. FACS analysis of Ad5Luc1 and Ad5Luc1-OvF binding to U118-hCAR-tailless (upper panel) or CHO cells (lower panel). Aliquots of 2×10^5 cells were incubated with polyclonal rabbit anti-Ad5 antiserum following binding of virus to the cells at 4 °C (to block internalization). Cells were incubated in the presence of anti-rabbit FITC-labeled secondary antibody and subjected to flow cytometry analysis. The gray peaks in the histograms represent negative control cells incubated with primary and secondary antibodies only. The thin line indicates Ad5 cellular attachment, and the heavy line indicates Ad5Luc1-OvF attachment. In U118-hCAR-tailless cells, approximately 94% of cells were positive for Ad5Luc1 surface attachment (thin line), while only 8% of cells were positive for Ad5Luc1-OvF (heavy line) versus control cells receiving primary and secondary antibodies (gray peak). In CHO cells, 10% of cells were positive for Ad5Luc1 attachment compared to 60% of positive cells for Ad5Luc1-OvF.

transduction through expanded Ad vector tropism, including CAR-independent tropism. We therefore evaluated Ad5Luc1-OvF transduction of a panel of cell lines expressing variable levels of CAR (Table 1). As shown in Fig. 2A, Ad5Luc1-OvF provided augmented reporter gene delivery to several CAR-deficient cell lines, with augmentation up to 23-fold compared to Ad5Luc1. Furthermore, Ad5Luc1-OvF increased gene transfer to an unpassaged primary ovarian cancer patient sample as much as 5-fold versus Ad5Luc1 (Fig. 2B). Of interest, Ad5Luc1-OvF gene delivery augmentation to CAR-deficient RD cells (human rhabdomyosarcoma, 1.5-fold) was markedly lower than that of OV-3 cells (human ovarian cancer, 23-fold) and CAR-deficient CHO cells (Chinese hamster ovary, 22-fold), suggesting that RD cells do not express the requisite cell-surface molecule(s) for OAdV7 fiber recognition. We also evaluated Ad5Luc1-OvF transduction on a normal human liver epithelial cell line (THLE-3) and observed a 10-fold reduction in gene transfer compared to Ad5Luc1.

Ad5Luc1-OvF exhibits increased cell-surface binding in the absence of CAR

To investigate whether Ad5Luc1-OvF mediates increased gene transfer via enhanced cell-surface interaction and not altered intracellular trafficking, we performed cell-binding

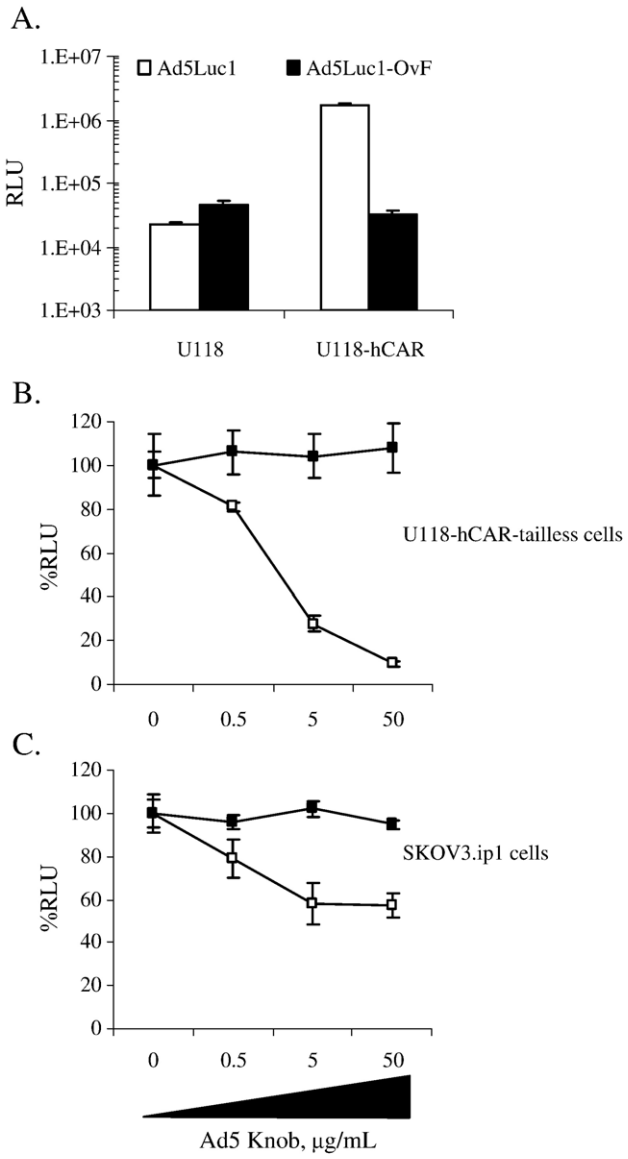

Fig. 4. Ad5Luc1 and Ad5Luc1-OvF-mediated gene transfer with Ad5 knob blocking. Luciferase activities following transduction of low-CAR U118MG cells and CAR-expressing U118-hCAR-tailless cells (A), transduction of U118-hCAR-tailless with Ad5Luc1 (white squares) or Ad5Luc1-OvF (black squares) with Ad5 knob block (B) and low-CAR SKOV3.ip1 cells with Ad5 knob block (C). Concentration of recombinant Ad5 fiber knob protein used to block transduction is indicated in µg/ml. Luciferase activity was determined 24 h post-transduction and is reported in relative light units (RLU) (A) or in percent total of unblocked luciferase activity for ease of comparison (B,C). Each column is average of 4 replicates using 100 vp/cell, and error bar indicates standard deviation.

assays employing FACS-based detection of surface-bound virions. We hypothesized that Ad5Luc1-OvF would display increased attachment to CAR-deficient cells, and possibly even CAR-positive cells, compared to Ad5 by virtue of novel virion/cell interaction. For these studies, we selected cell lines that exhibited maximally different gene transfer profiles between Ad5Luc1 and Ad5Luc1-OvF: CAR-deficient CHO cells and the CAR-positive U118-hCAR-tailless cell line that artificially expresses the extracellular domain of human CAR (Kim et al., 2002). Cells were incubated with Ad vectors at 4 °C to allow virion attachment, but not internalization, followed by labeling of bound virions with an anti-Ad primary antibody and an FITC-conjugated secondary antibody, with subsequent FACS analysis (see Materials and methods). As shown in Fig. 3A, surface-bound Ad5Luc1 was detected on 94% of U118-hCAR-tailless cells, while only 8% of these cells were positive for Ad5Luc1-OvF. This observation is consistent with the 100-fold disparity in gene transfer observed for these vectors in the same cell line (Table 1, Fig. 4A). In contrast, only 10% of CAR-negative CHO cells bound Ad5Luc1, while over 60% of CHO cells were positive for Ad5Luc1-OvF (Fig. 3B). These data indicate that a direct positive correlation exists between increased Ad5Luc1-OvF cell-surface interaction and enhanced gene delivery in CAR-deficient cells.

The OAdV7 fiber in Ad5Luc1-OvF dictates CAR-independent tropism

As shown in Table 1 and Fig. 3, Ad5Luc1-OvF gene transfer and cell binding were not dependent on the presence of CAR. To confirm this aspect of Ad5Luc1-OvF tropism, we performed knob-blocking assays using recombinant Ad5 fiber knob protein, a well-established method for demonstrating or ruling out CAR-mediated infection (Krasnykh et al., 1998; Einfeld et al., 2001; Glasgow et al., 2004). As shown in Fig. 4A, Ad5Luc1 exhibited clear CAR-dependent tropism as demonstrated by a 100-fold increase in transgene expression in U118-hCAR-tailless cells versus the CAR-deficient U118MG cell line. Furthermore, preincubation of cells with recombinant Ad5 knob protein at 50 μg/ml inhibited 90% and 50% of Ad5 Luc1 gene transfer to U118-hCAR-tailless cells and low-CAR SKOV3.ip1 cells, respectively (Figs. 4B, C). Conversely, Ad5Luc1-OvF gene delivery to U118MG cells was 2-fold higher than that of Ad5Luc1, and transduction of the highly CAR-positive variant line yielded no increase in luciferase values. Furthermore, competitive inhibition with Ad5 knob did not appreciably block Ad5Luc1-OvF-mediated gene transfer in either cell line, confirming the CAR-independent tropism of this vector.

Biodistribution of Ad5Luc1-OvF gene expression in mice

Following confirmation of our first hypothesis that the Ad5Luc1-OvF vector would exhibit enhanced infectivity in low CAR substrates via a novel, non-CAR based tropism, we next addressed the biodistribution profile of Ad5Luc1-OvF. Based on the biodistribution of intravenously applied OAdV7 in mice (Hofmann et al., 1999) and the lack of the putative heparin sulfate binding motif KKTK in the OAdV7 fiber shaft, we hypothesized that an Ad5 vector containing this fiber would demonstrate decreased hepatotropism in vivo. To this end, we evaluated the biodistribution of transgene expression of a panel of Ad vectors including Ad5Luc1-OvF, Ad5Luc1 and our Ad5Luc1-ΔKKTK vector (with the native KKTK sequence deleted from the fiber shaft) as a liver detargeted control vector,

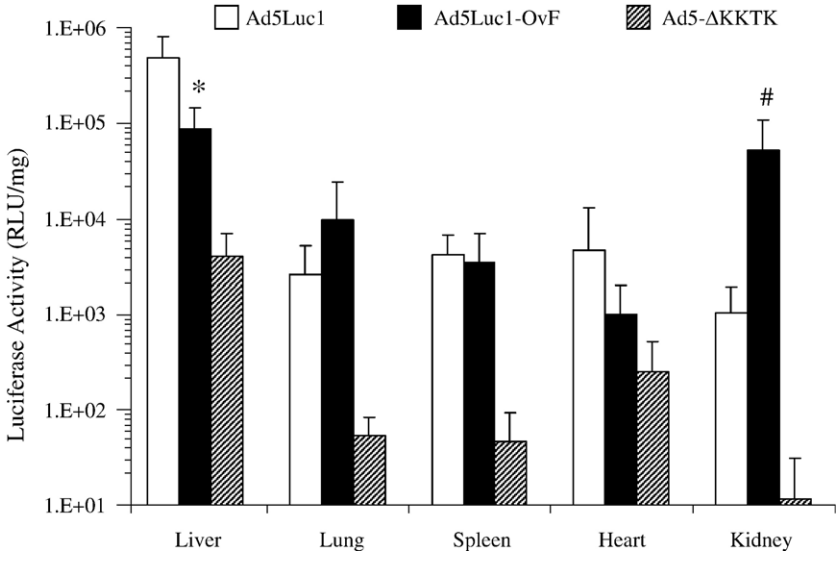

Fig. 5. In vivo biodistribution of Ad5-based vectors after intravenous injection into female C57BL/6 mice. Mice 6–8 weeks of age were injected with 1×10^{11} vp of Ad5Luc1 (open bars), Ad5Luc1-OvF (black bars) or Ad5-ΔdKKTK (cross-hatched bars). Luciferase activity was determined 48 h post-injection. Results from two individual experiments using different preparations of Ad5Luc1-OvF were combined and are presented as relative light units (RLU) normalized for total protein concentration for each individual organ. Each data point is an average of 8–10 mice (Ad5Luc1, $n = 10$; Ad5Luc1-OvF, $n = 8$; Ad5-ΔKKTK, $n = 10$), and error bars indicate standard deviation. *$P < 0.0028$ versus Ad5Luc1 in liver, #$P < 0.042$ versus Ad5Luc1 in kidney. For all tissues except heart, Ad5ΔKKTK luciferase values were significantly lower than Ad5Luc1, $P < 0.017$. In all cases, a two-tailed t test assuming unequal variance between groups was used for increased stringency.

similar to that described (Smith et al., 2003b). Mice were injected via the tail vein with 1×10^{11} viral particles. Forty-eight hours post-injection, the liver, spleen, lung, heart and kidney were harvested and homogenized, and luciferase activity and protein concentrations of cleared homogenates were measured. As expected, Ad5Luc1 produced the highest transgene expression in the liver, while Ad5-ΔKKTK vector gene expression in liver was reduced to 1% of control (Fig. 5). In all other organs examined, Ad5-ΔKKTK gene expression was markedly reduced to less than 7% of Ad5Luc1 control levels. Ad5Luc1-OvF gene expression was more evenly distributed among the major organs and was significantly decreased in the liver to approximately 18% of Ad5Luc1 levels ($P < 0.0028$). Ad5Luc1-OvF gene expression in the heart, spleen and lung was not significantly different from Ad5Luc1. Ad5Luc1-OvF gene expression in the kidney was increased 50-fold versus the Ad5Luc1 control vector ($P < 0.042$), resulting in a liver-to-kidney gene expression ratio of 0.59 for Ad5Luc1-OvF and 0.002 for Ad5Luc1, a difference of 280-fold. Of note, we observed a vector-specific difference in animal survival during the biodistribution studies. In this regard, all animals receiving control Ad survived the duration of the experiment; however, 3 of 11 mice receiving Ad5Luc1-OvF expired before the 48 h time point. Further analysis of this phenomenon is under investigation. In the aggregate, Ad5Luc1-OvF, a vector containing fibers from OAdV7 that are unable to bind CAR, demonstrates enhanced gene delivery to CAR-deficient human cells in vitro and displays a unique biodistribution characterized by attenuated liver transduction with significant kidney tropism.

Discussion

Despite a variety of avenues explored to improve human adenovirus serotype 5 as a therapeutic agent, this vector exhibits innate drawbacks of CAR dependency and hepatotropism. Of particular concern is that many clinically important tissues, including several cancer types, are refractory to Ad5 infection due to low CAR expression. Indeed, down-regulation of CAR has been reported for several tumor types, including glioma, ovarian, lung, breast and others (Miller et al., 1998; Hemminki and Alvarez, 2002; Bauerschmitz et al., 2002). As a consequence of limiting CAR levels in many clinically relevant target cells, high Ad vector dosage is often required for in vivo efficacy. Given that over 95% of systemically administered Ad particles are sequestered in the liver via hepatic macrophage (Kupffer cell) uptake (Tao et al., 2001) and hepatocyte transduction (Connelly, 1999) of both rodents and primates, therapeutically relevant Ad doses often result in vector-related liver toxicity (Peeters et al., 1996; Lieber et al., 1997; Sullivan et al., 1997; Worgall et al., 1997; Alemany et al., 2000; Shayakhmetov et al., 2004). Thus, Ad vectors exhibiting CAR-independent and/or expanded tropism coupled with low hepatotropism should prove valuable for maximal transduction of low-CAR targets at the lowest possible vector dose.

We sought to achieve this vector design mandate by replacing the Ad5 fiber with the corresponding structure from ovine atadenovirus serotype 7. The fiber of OAdV7 is the only identified structural determinant of native OAdV7 tropism, which is CAR-independent in vitro and non-hepatotropic when applied systemically. Genetic incorporation of the OAdV7 fiber molecule into the Ad5 virion ablated its CAR dependence as evidenced by competitive Ad5 knob blocking assays as well as increased cellular attachment to CAR-deficient CHO cells. Our results are consistent with previous findings showing that Ad5 and OAdV7 do not compete with each other for cell entry in cells that both viruses can infect (Xu and Both, 1998). Ad5Luc1-OvF exhibited enhanced infectivity in vitro, providing 3- to 23-fold increased gene transfer to several CAR-deficient cell lines and primary ovarian cancer tissue versus Ad5. However, Ad5Luc1-OvF gene transfer to other CAR-deficient human cancer cell lines such as SCC-25, FaDu and LNCaP, as well as the human THLE-3 normal liver cell line, was markedly reduced compared to the Ad5Luc1 control vector. These findings suggest that the receptor(s) for the OAdV7 fiber is not ubiquitously expressed, a biological phenomenon that may provide the basis of a level of cell- or tissue-type selectivity of potential utility.

Intravenous administration of Ad results in accumulation in the liver, spleen, heart, lung and kidneys of mice, although these tissues may not necessarily be the highest in CAR expression (Fechner et al., 1999; Reynolds et al., 1999; Wood et al., 1999). Instead, anatomic barriers, the structure of the vasculature and the degree of blood flow and in each organ probably contribute to the biodistribution, in addition to non-specific viral particle uptake by macrophages. This is true with regard to the liver in particular, which sequesters the majority of systemically administered Ad particles via hepatic macrophage (Kupffer cell) uptake (Tao et al., 2001) and hepatocyte transduction (Connelly, 1999), leading to cytokine release, inflammation and liver toxicity (Peeters et al., 1996; Lieber et al., 1997; Worgall et al., 1997; Shayakhmetov et al., 2004, 2005b). Thus, the nature of adenovirus–host interactions dictating the fate of systemically applied Ad has come under considerable scrutiny.

To this end, attempts to design Ad5 vectors that "detarget" the liver have been based on the assumption that CAR- and integrin-based interactions are required for liver uptake in vivo. The majority of attempts to inhibit hepatocyte and/or liver Kupffer cell uptake using Ad5 vectors with ablated CAR- or integrin-binding motifs in the Ad capsid have failed (Alemany and Curiel, 2001; Mizuguchi et al., 2002; Smith et al., 2002; Martin et al., 2003; Smith et al., 2003a), although some mutations of the Ad5 fiber knob have attenuated liver tropism of vectors following systemic administration (Einfeld et al., 2001; Koizumi et al., 2003; Yun et al., 2005). Indeed, recent studies focused on Ad vector biodistribution have demonstrated that Kupffer cell and hepatocyte uptake in vivo are largely CAR-independent (Liu et al., 2003; Shayakhmetov et al., 2004), confirming that native Ad5 tropism determinants at work in vitro contribute little to vector biodistribution in vivo.

The Ad fiber is a major structural determinant of liver tropism in vivo, even in the absence of knob/Ad receptor interaction (Nicklin et al., 2005). In this regard, Smith and co-

workers have examined the role of a putative heparan sulfate proteoglycan (HSPG)-binding motif, KKTK, in the third repeat of the native fiber shaft. Replacement of this motif with an irrelevant GAGA peptide sequence reduced reporter gene expression and Ad DNA in the liver by 90% in mice and non-human primates (Smith et al., 2003a). The authors postulated that removal of the KKTK inhibited Ad5 interaction with heparin sulfate proteoglycans (HSPG) in the liver; however, direct binding of this motif to HSPG has not been demonstrated.

Pseudotyping Ad5 with short-shafted fibers from Ad3, Ad35 or Ad40 that contain no native KKTK results in significant reduction of liver uptake (Table 2) (Nakamura et al., 2003; Sakurai et al., 2003; Vigne et al., 2003). Furthermore, the use of a shortened Ad5 fiber shaft that retains the native KKTK motif (Vigne et al., 2003) or replacement of the Ad5 shaft with the short Ad3 shaft domain (Breidenbach et al., 2004) was shown to attenuate liver uptake in vivo following intravenous delivery. Indeed, Shayakhmetov and co-workers have recently shown that short-shafted Ad vectors with either CAR- or non-CAR-interacting knob domains do not efficiently interact with hepatocytes in vivo and are not taken up by Kupffer cells (Shayakhmetov et al., 2004).

The Ad5Luc1-OvF fiber contains 25 pseudorepeats, no KKTK motif and likely forms a fiber at least as long as the native Ad5 fiber. Long-shafted Ads have been shown to accumulate within liver sinusoids and subsequently infect hepatocytes in a CAR-independent manner (Shayakhmetov et al., 2004). Thus, our result demonstrating marked reduction of in vivo liver gene expression appears to be unique for a long-shafted Ad vector and is comparable to results obtained with some short-shafted Ads (Table 2).

Recent evidence has highlighted the importance of serum factors in the hepatic uptake of systemically applied Ad vectors. Shayakhmetov and colleagues demonstrated that coagulation factor IX (FIX) and complement component C4-binding protein (C4BP) can direct Ad biodistribution in vivo by cross-linking Ad to hepatocellular HSGP and the LDL-receptor-related protein. Kupffer cell sequestration of Ad particles was likewise dependent on Ad association with FIX and C4BP (Shayakhmetov et al., 2005a). This work also demonstrated a key vector design approach whereby genetic modification of solvent-exposed loop structures in the Ad5 fiber knob attenuated serum factor binding resulting in reduced liver uptake in vivo. In addition to the Ad5Luc1-OvF vector, this serum-factor-ablated Ad vector is the only other long-shafted liver-detargeted Ad

Table 2
Fiber composition of Ad vectors displaying decreased liver localization in vivo

Ad Vector	Tail	Shaft	Knob	Liver detargeting	New in vivo tropism	Dose (vp)/Strain	Reference
Ad5Luc1	Ad5	Ad5 (22 repeats w/KKTK)	Ad5	No	–	1×10^{11}/C57BL/6	This report
Ad5Luc1-OvF	Ad5	OAdV7 (25 repeats, no KKTK)	OAdV7	20% of Ad5	Kidney, equal to liver	1×10^{11}/C57BL/6	This report
Ad5.Ad3.SH	Ad5	Ad3 (6 repeats, no KKTK)	Ad5	10% of Ad5	None reported	5×10^{10}/C57BL/6	Breidenbach et al., 2004
Ad5.Ad3.SH/knob3	Ad5	Ad3 (6 repeats, no KKTK)	Ad3	No	None reported	5×10^{10}/C57BL/6	Breidenbach et al., 2004
Ad5 DB6	Ad5	Ad3 (6 repeats, no KKTK)	Ad3	10% of Ad5	None reported	1×10^{11}/C57BL/6	Vigne et al., 2003
Ad5 BS1	Ad5	Ad5 (9 repeats, w/KKTK)	Ad5	10% of Ad5	None reported	1×10^{11}/C57BL/6	Vigne et al., 2003
Ad5.35F	Ad35	Ad35 (6 repeats, no KKTK)	Ad35	4% of Ad5	None reported	2×10^{11}/C57BL/6	Smith et al., 2003a,b
Ad5.5S35H	Ad5	Ad5	Ad35	No	None reported	2×10^{11}/C57BL/6	Smith et al., 2003a,b
Ad5.35S5H	Ad35	Ad35 (6 repeats, no KKTK)	Ad5	25% of Ad5	None reported	2×10^{11}/C57BL/6	Smith et al., 2003a,b
Ad5/35	Ad5	Ad35 (6 repeats, no KKTK)	Ad35	No	Kidney, 1% of liver	1×10^{10}/C57BL/6	Mizuguchi et al., 2002
Ad5.KO1	Ad5	Ad5	CAR-ablated Ad5	No	None reported	2×10^{11}/C57BL/6	Smith et al., 2003a,b
Ad5.S	Ad5	Ad5 (KKTK to GAGA)	Ad5	6% of Ad5	None reported	2×10^{11}/C57BL/6	Smith et al., 2003a,b
Ad5.K01.S	Ad5	Ad5 (KKTK to GAGA)	CAR-ablated Ad5	0.001% of Ad5	None reported	2×10^{11}/C57BL/6	Smith et al., 2003a,b
Ad5F35L	Ad5	Ad35 (6 repeats, no KKTK)	Ad35	0.001% of Ad5	None reported	1.5×10^{10}/C57BL/6	Sakurai et al., 2003
Ad5F/40S	Ad40	Ad40 (7 repeats, no KKTK)	Ad40	1% of Ad5	None reported	2×10^{10}/C57BL/6	Nakamura et al., 2003
Ad5/35L	Ad5	Ad5 (22 repeats, w/KKTK)	Ad35	No	None reported	1×10^{11}/C57BL/6	Shayakhmetov et al., 2004
Ad5/35S	Ad5	Ad35 (6 repeats, no KKTK)	Ad35	<10% of Ad5/35L	None reported	1×10^{11}/C57BL/6	Shayakhmetov et al., 2004
Ad5/9L	Ad5	Ad5 (22 repeats)	Ad9	No	None reported	1×10^{11}/C57BL/6	Shayakhmetov et al., 2004
Ad5/9S	Ad5	Ad9 (7 repeats, no KKTK)	Ad9	<10% of Ad5/9L	None reported	1×10^{11}/C57BL/6	Shayakhmetov et al., 2004

reported to date. Therefore, it is reasonable to posit that reduced liver uptake observed with Ad5Luc1-OvF is the result of the unique structure of the ovine fiber resulting in reduced and/or altered interaction with blood factors that mediate native Ad5 liver uptake.

Gene transfer to the kidney could have significant utility for the treatment of renal disease and in transplantation paradigms (Imai et al., 2004). While Ad, adeno-associated virus (AAV) and retroviral vectors transduce renal cells in vitro, systemic delivery of viral vectors has resulted in insufficient gene delivery to the kidney (Moullier et al., 1994; Takeda et al., 2004; Fujishiro et al., 2005). To increase in vivo gene transfer to the kidney, perfusion (Heikkila et al., 1996), catheter infusion (Takeda et al., 2004; Fujishiro et al., 2005) and direct interstitial injection (Ortiz et al., 2003) have been employed. Considering the established difficulty of generating Ad-mediated renal gene transfer via systemic injection, our result demonstrating abundant kidney gene expression by Ad5Luc1-OvF is notable. While the mechanism of enhanced kidney gene expression remains under investigation, we interpret this result as a consequence of unique, direct interaction(s) of Ad5Luc1-OvF with kidney and/or renal vasculature, and not solely as a result of decreased liver sequestration, since other Ad vectors exhibiting decreased hepatotropism have not demonstrated appreciable novel tissue tropism (Table 2).

The kidney is a complex organ with numerous specialized compartments including the glomeruli, tubules, interstitium and vasculature. The glomerular capillary endothelium is fenestrated, resulting in the "leaky" vasculature that would allow intravenous Ad vectors to contact the underlying filtration membrane and access to the epithelium of the renal tubule system. Indeed, injection of an Ad vector directly into the renal artery can result in gene transfer to cells of the proximal tubule (Moullier et al., 1994). Given the unique renal localization observed, we are currently extending our studies to determine the precise localization of Ad5Luc1-OvF gene expression within kidney substructures. An important issue related to the renal localization is the toxicity we observed while carrying out these studies. Given that only animals receiving Ad5Luc1-OvF vector expired before tissue harvest at 48 h post-injection and that liver gene expression was decreased in surviving animals, it is reasonable to suspect that the increased levels of Ad5Luc1-OvF in the kidney resulted in the toxicity. In this regard, further examination of renal tissue inflammation, apoptosis or other patho-physiology should provide the basis for understanding this effect observed in some animals.

To our knowledge, this is the first report of a fiber-pseudotyped Ad vector that simultaneously displays decreased hepatotropism and a distinct organ tropism in vivo. Furthermore, this novel redirection of vector biodistribution is directly attributable to fiber replacement with a non-CAR binding long-shafted fiber, an outcome seemingly at odds with recent fiber pseudotyping reports employing short-shafted vectors. In vitro, Ad5Luc1-OvF displays CAR-independent tropism with a positive correlation between increased Ad5Luc1-OvF cell-surface interaction and enhanced gene delivery in CAR-deficient cells, suggesting the use of as-yet unidentified receptor molecule(s). In addition, this vector may prove useful in murine models of renal disease.

Materials and methods

Cell lines

The Ad5 DNA-transformed 293 human embryonic cell line was purchased from Microbix (Toronto, ON, Canada). Human embryonic rhabdomyosarcoma RD cells, CAR-negative human U118MG glioma cells, PC-3 and LNCaP human prostate cancer cells, MCF7 human breast cancer cells, T24 human bladder cancer cells, Chinese hamster ovary cells (CHO), human squamous cell carcinoma SCC-4 and SCC-25 cells, FaDu human pharynx cancer cells, HeLa and SKOV ovarian cancer cells, LoVo colon cancer cells and OV-3 ovarian cancer cells were obtained from the American Type Culture Collection (ATCC) (Manassas, VA). The human ovarian adenocarcinoma cell lines Hey, SKOV3.ip1 and OV-4 were obtained from Drs. Judy Wolf, Janet Price (both of M.D. Anderson Cancer Center, Houston, TX) and Timothy J. Eberlein, (Harvard Medical School, Boston, MA), respectively. These cell lines were propagated in 50:50 mixture of Dulbecco's modified Eagle's medium and Ham's F-12 medium (DMEM/F-12) supplemented with 10% (v/v) fetal calf serum (FCS), L-glutamine (2 mM), penicillin (100 units/ml) and streptomycin (100 μg/ml). U118-hCAR-tailless cells, which express a truncated form of human CAR comprising the extracellular domain, transmembrane domain and the first two amino acids from the cytoplasmic domain (Wang and Bergelson, 1999), have been described previously (Kim et al., 2003) and were grown in DMEM/F12 as above except for the addition of 400 μg/ml G418. The ovine OLE stroma cell line and ovine lung cancer cell line JS8JSRV were generous gifts from Dr. Massimo Palmarini, University of Glasgow, UK. All cell lines were cultured at 37 °C in 5% CO_2 using culture media recommended by each respective supplier. FCS was purchased from Gibco-BRL (Grand Island, NY) and media, and supplements were from Mediatech (Herndon, VA).

Precision-cut human ovarian cancer slices

Human ovarian cancer tissue was obtained taken from ovarian cancer patients following institutional review board approval, essentially as described previously (Kirby et al., 2004). Briefly, excess material was received from the Department of Obstetrics and Gynecology, the University of Alabama at Birmingham Hospital. Precision-cut ovarian cancer slices were prepared using a Krumdiek Tissue Slicer (Alabama Research and Development, Munford, AL) fitted with a 4 mm coring device to produce a core biopsy of 4 mm diameter. The cores were then sliced to 150 μm thickness. Each slice was transferred into a well of a 24-well plate containing 1 ml William's Medium E and placed on a rocker. Tumor slices were maintained at 37 °C in a 5% CO_2 environment on a rocker and allowed to preincubate for 2 h before treatment. Ovarian cancer slices were infected with 100 and 1000 vp/cell with Ad5Luc1, Ad5/OAdV7 or no virus. Ovarian cancer slices were harvested

and frozen at 24 h after infection. Gene transfer was determined using a luciferase activity assay system (Promega, Madison, WI) according to the manufacturer's instructions.

Flow cytometry

Cells grown in T75 flasks were removed by addition of EDTA in PBS and resuspended in PBS containing 1% bovine serum albumin (BSA). Cells (2×10^5) were incubated with 3.5×10^9 viral particles of adenovirus, or buffer only, for 1 h at 4 °C in 250 μl PBS–BSA. Cells were then washed twice in 4 ml cold PBS–BSA and incubated with a 1:500 dilution of polyclonal rabbit anti-Ad5 antiserum (Cocalico Biologicals, Reamstown, PA) at 4 °C in 250 μl PBS–BSA. Cells were washed twice in 4 ml cold PBS–BSA and incubated in 250 μl of a 1:150 dilution of FITC-labeled goat anti-rabbit IgG secondary antibody (Jackson Immunoresearch Labs, West Grove, PA) for 1 h in PBS–BSA at 4 °C. Flow cytometry analysis was performed at the UAB FACS Core Facility using FACScan (Beckton Dickenson, San Jose, CA).

Plasmid construction

To create the chimeric fiber used in this study, we fused the Ad5 tail domain to the OAdV7 fiber shaft and knob domains. A 1553-bp PCR product containing a 5′ *Sca*I site, the OAdV7 fiber shaft and knob domains and a 3′ *Mun*I site was amplified from plasmid pAK containing the right hand *Bam*HI fragment of the OAdV7 genome cloned into Bluescribe M13+ *Bam*HI/*Hin*cII sites. The forward primer designated OAdS*Sca*IF was 5′-AGC GAA GGG TTA GTA CTA TCT TTA AAC-3′, and the reverse primer was designated OAd*Mun*I-R2 5′-TCA TAC AAT TGT TTA **TTA** TTG TCT GAA TTG-3′. The underlined bases indicate insertion of restriction sites, and the stop codon is shown in bold. Next, a PCR product containing a 5′ *Pac*I site, the Ad5 tail domain and a 3′ *Sca*I site was amplified from plasmid pNEB.PK.3.6, a pNEB193-based shuttle vector containing the Ad5 fiber (Krasnykh et al., 1996). The forward primer is designated NEB36*Pac*IF 5′-ATT ACG CCA AGC TTG CAT GCC TGC-3′ and reverse primer NEB36*Sca*IR 5′-GCA AAG AGA GTA CTC CAG GGG GAC-3′. This PCR product was then digested with *Pac*I and *Sca*I and gel-purified. Shuttle vector pNEB.PK.3.6-OvF was created by a 3-piece ligation of *Pac*I/*Mun*I-digested pNEB.PK.3.6 and the two digested PCR fragments containing the Ad5 tail region and the OAdV7 shaft and knob domains. Direct sequencing confirmed that the coding region for the chimeric fiber was correct.

Generation of recombinant adenovirus

Recombinant Ad5 genomes containing the chimeric OAdV7 fiber gene were derived by homologous recombination in *E. coli* BJ5183 with *Swa*I-linearized rescue plasmid pVK700 (Belousova et al., 2002) and the fiber-containing *Pac*I–*Kpn*I fragment of the shuttle vector pNEB.PK.3.6-OvF (described above) essentially as described (Krasnykh et al., 1998). pVK700 is derived from pTG3602 (Chartier et al., 1996) but contains an almost complete deletion of the fiber gene and contains a firefly luciferase reporter gene driven by the cytomegalovirus immediate early promoter in place of the E1 region. Genomic clones were sequenced and analyzed by PCR prior to transfection of 911 cells. Ad5Luc1 is a replication-defective E1-deleted Ad vector containing a firefly luciferase reporter gene in the E1 region driven by the cytomegalovirus immediate early promoter/enhancer (Krasnykh et al., 2001). All vectors were propagated on 911 cells and purified by equilibrium centrifugation in CsCl gradients by a standard protocol. Viral particle (vp) concentration was determined at 260 nm by the method of Maizel et al. (1968) by using a conversion factor of 1.1×10^{12} vp/absorbance unit.

Western blot analysis

Aliquots of Ad vectors containing 2.0×10^{10} viral particles were diluted into Laemmli buffer and incubated at room temperature or 99 °C for 15 min and loaded onto a 4–20% gradient SDS-polyacrylamide gel (Bio-Rad, Hercules, CA). Following electrophoretic protein separation, proteins were electroblotted onto a PVDF membrane. The primary antibody (monoclonal 4D2 recognizing the Ad5 fiber tail domain) was diluted 1:3000 (Lab Vision, Freemont, CA). Immunoblots were developed by addition of a secondary horseradish-peroxidase-conjugated anti-mouse immunoglobulin antibody at a 1:3000 dilution (Dako Corporation, Carpentaria, CA) followed by incubation with 3-3′-diaminobenzene peroxidase substrate (DAB; Sigma Company, St. Louis, MO).

Recombinant fiber knob proteins

The knob domain of Ad5 was expressed in *E. coli* with an N-terminus 6-histidine tag using the pQE81 expression plasmid (Qiagen, Hilden, Germany). The Ad5 fiber knob domain was PCR-amplified using primers that amplified the entire fiber knob domain and the three carboxy-terminal fiber shaft repeats using the following primers: Ad5 (fwd) 5′-CAAACAC***GG***ATCCCCT-TTTATTATTCTTGGGCAATGTATGA-3′ using plasmid pNEB.PK.3.6 as the template. The forward primer contains a 2-bp mutation (in bold) that creates a 5′-end *Bam*HI restriction site (underlined). The stop codon (TAA) and polyadenylation signal (AATAAA) are underlined in the reverse primer. The PCR products containing the Ad5 fiber knob region were digested with *Bam*HI, gel-purified and ligated into *Bam*HI–*Sma*I-digested pQE81. The resulting plasmid pQE81-Ad5 was sequenced to identify correct clones. The expression plasmid was introduced into *E. coli*, and 6-His-containing fiber knob proteins from bacterial cultures were purified on nickel-nitrilotriacetic acid (Ni-NTA) agarose columns (Qiagen). The ability to form trimers was confirmed by Western blot analysis of boiled and unboiled purified knob proteins using a mouse penta-His monoclonal antibody (Qiagen) and a horseradish-peroxidase-conjugated anti-mouse immunoglobulin antibody at a 1:3000 dilution (DAKO Corporation) followed by incubation with 3-3′-diaminobenzene peroxidase substrate (DAB; Sigma Company). Concentration of purified knob proteins was determined by the method of Lowry (Bio-Rad).

In vitro Ad-mediated gene transfer experiments

For virus gene transfer experiments using adherent cell lines, cells were grown in wells of 24-well plates and were incubated for 1 h at 37 °C with each Ad vector diluted to 100 vp/cell in 500 μl of transduction media containing 2% FCS. Following the incubation, cells were rinsed in transduction media and were maintained at 37 °C in an atmosphere of 5% CO_2. Cells were harvested 24 h post-transduction, and gene transfer was determined using a luciferase activity assay system (Promega, Madison, WI) according to the manufacturer's instructions.

For experiments containing blocking agents, recombinant fiber knob proteins at 0.5, 5.0 and 50 μg/ml final concentration were incubated with the cells at 37 °C in transduction media 15 min before the addition of the virus. Following the transduction, cells were rinsed with transduction media to remove unbound virus and blocking agent and were maintained at 37 °C in an atmosphere of 5% CO_2.

Animals

Mice were obtained at 4 to 6 weeks of age and quarantined at least 1 week before the study. Mice were kept under pathogen-free conditions according to the American Association for Accreditation of Laboratory Animal Care guidelines. Animal protocols were reviewed and approved by the Institutional Animal Care and Use Committee of UAB.

Biodistribution

Female C57BL/6 mice (Charles River Laboratories, Wilmington, MA), aged 6–8 weeks, were injected intravenously through the lateral tail vein with 1×10^{11} vp of Ad5Luc1, Ad5Luc1-OvF or Ad5-ΔKKTK in 100 μl of PBS. After 48 h, mice were sacrificed and livers, lungs, spleens, hearts and kidneys were harvested and representative sections were frozen in the liquid nitrogen immediately. The frozen organ samples were homogenized with a Mini Beadbeater (BioSpec Products, Inc., Bartlesville, OK) in 2 ml micro-tubes (Research Product International Corp., Mt. Prospect, IL) with 100 μl of 1.0 mm zirconia/silica beads (BioSpec Products, Inc.) and 1 ml of Cell Culture Lysis Buffer (Promega) then centrifuged at 14,000 rpm for 2 min. Luciferase activity was measured as before. Mean background luciferase activity was subtracted. All luciferase activities were normalized by protein concentration in the tissue lysates. Protein concentrations were determined using a Bio-Rad DC protein assay kit (Bio-Rad, Hercules, CA).

Statistics

Data were presented as mean values ± deviation. Statistical differences among groups were assessed by a two-tailed *t* test assuming unequal variance between groups for increased stringency; $P < 0.05$ was considered significant.

Acknowledgments

This work was supported by grants from the National Institutes of Health: 2R01CA083821 and 1P01HL076540, and from the US Department of Defense: DOD W81XWH-05-1-0035.

References

Alemany, R., Curiel, D.T., 2001. CAR-binding ablation does not change biodistribution and toxicity of adenoviral vectors. Gene Ther. 8 (17), 1347–1353.

Alemany, R., Suzuki, K., Curiel, D.T., 2000. Blood clearance rates of adenovirus type 5 in mice. J. Gen. Virol. 81 (Pt. 11), 2605–2609.

Bai, M., Harfe, B., Freimuth, P., 1993. Mutations that alter an Arg–Gly–Asp (RGD) sequence in the adenovirus type 2 penton base protein abolish its cell-rounding activity and delay virus reproduction in flat cells. J. Virol. 67 (9), 5198–5205.

Bauerschmitz, G.J., Barker, S.D., Hemminki, A., 2002. Adenoviral gene therapy for cancer: from vectors to targeted and replication competent agents (Review). Int. J. Oncol. 21 (6), 1161–1174.

Belousova, N., Krendelchtchikova, V., Curiel, D.T., Krasnykh, V., 2002. Modulation of adenovirus vector tropism via incorporation of polypeptide ligands into the fiber protein. J. Virol. 76 (17), 8621–8631.

Benko, M., Harrach, B., 1998. A proposal for a new (third) genus within the family Adenoviridae. Arch. Virol. 143 (4), 829–837.

Bergelson, J.M., Cunningham, J.A., Droguett, G., Kurt-Jones, E.A., Krithivas, A., Hong, J.S., et al., 1997. Isolation of a common receptor for Coxsackie B viruses and adenoviruses 2 and 5. Science 275 (5304), 1320–1323.

Blackwell, J.L., Miller, C.R., Douglas, J.T., Li, H., Reynolds, P.N., Carroll, W.R., et al., 1999. Retargeting to EGFR enhances adenovirus infection efficiency of squamous cell carcinoma. Arch. Otolaryngol. Head Neck Surg. 125 (8), 856–863.

Boyle, D.B., Pye, A.D., Kocherhans, R., Adair, B.M., Vrati, S., Both, G.W., 1994. Characterisation of Australian ovine adenovirus isolates. Vet. Microbiol. 41 (3), 281–291.

Breidenbach, M., Rein, D.T., Wang, M., Nettelbeck, D.M., Hemminki, A., Ulasov, I., et al., 2004. Genetic replacement of the adenovirus shaft fiber reduces liver tropism in ovarian cancer gene therapy. Hum. Gene Ther. 15 (5), 509–518.

Büchen-Osmond, C. 2002. The Universal Virus Database of the International Committee on Taxonomy of Viruses. http://www.ncbi.nlm.nih.gov/ICTVdb/index.htm.

Chartier, C., Degryse, E., Gantzer, M., Dieterle, A., Pavirani, A., Mehtali, M., 1996. Efficient generation of recombinant adenovirus vectors by homologous recombination in *Escherichia coli*. J. Virol. 70 (7), 4805–4810.

Chiu, C.Y., Wu, E., Brown, S.L., Von Seggern, D.J., Nemerow, G.R., Stewart, P.L., 2001. Structural analysis of a fiber-pseudotyped adenovirus with ocular tropism suggests differential modes of cell receptor interactions. J. Virol. 75 (11), 5375–5380.

Connelly, S., 1999. Adenoviral vectors for liver-directed gene therapy. Curr. Opin. Mol. Ther. 1 (5), 565–572.

Cripe, T.P., Dunphy, E.J., Holub, A.D., Saini, A., Vasi, N.H., Mahller, Y.Y., et al., 2001. Fiber knob modifications overcome low, heterogeneous expression of the coxsackievirus–adenovirus receptor that limits adenovirus gene transfer and oncolysis for human rhabdomyosarcoma cells. Cancer Res. 61 (7), 2953–2960.

Davison, E., Diaz, R.M., Hart, I.R., Santis, G., Marshall, J.F., 1997. Integrin alpha5beta1-mediated adenovirus infection is enhanced by the integrin-activating antibody TS2/16. J. Virol. 71 (8), 6204–6207.

Dmitriev, I., Krasnykh, V., Miller, C.R., Wang, M., Kashentseva, E., Mikheeva, G., et al., 1998. An adenovirus vector with genetically modified fibers demonstrates expanded tropism via utilization of a coxsackievirus and adenovirus receptor-independent cell entry mechanism. J. Virol. 72 (12), 9706–9713.

Einfeld, D.A., Schroeder, R., Roelvink, P.W., Lizonova, A., King, C.R., Kovesdi, I., et al., 2001. Reducing the native tropism of adenovirus vectors

requires removal of both CAR and integrin interactions. J. Virol. 75 (23), 11284–11291.
Fechner, H., Haack, A., Wang, H., Wang, X., Eizema, K., Pauschinger, M., et al., 1999. Expression of coxsackie adenovirus receptor and alphav-integrin does not correlate with adenovector targeting in vivo indicating anatomical vector barriers. Gene Ther. 6 (9), 1520–1535.
Fujishiro, J., Takeda, S., Takeno, Y., Takeuchi, K., Ogata, Y., Takahashi, M., et al., 2005. Gene transfer to the rat kidney in vivo and ex vivo using an adenovirus vector: factors influencing transgene expression. Nephrol. Dial. Transplant. 20 (7), 1385–1391.
Gall, J., Kass-Eisler, A., Leinwand, L., Falck-Pedersen, E., 1996. Adenovirus type 5 and 7 capsid chimera: fiber replacement alters receptor tropism without affecting primary immune neutralization epitopes. J. Virol. 70 (4), 2116–2123.
Gelhe, W.D., Smith, K.O., 1969. Abortive infection of human cell cultures by a canine adenovirus. Proc. Soc. Exp. Biol. Med. 131, 87–93.
Glasgow, J.N., Kremer, E.J., Hemminki, A., Siegal, G.P., Douglas, J.T., Curiel, D.T., 2004. An adenovirus vector with a chimeric fiber derived from canine adenovirus type 2 displays novel tropism. Virology 324 (1), 103–116.
Goossens, P.H., Havenga, M.J., Pieterman, E., Lemckert, A.A., Breedveld, F.C., Bout, A., et al., 2001. Infection efficiency of type 5 adenoviral vectors in synovial tissue can be enhanced with a type 16 fiber. Arthritis Rheum. 44 (3), 570–577.
Havenga, M.J., Lemckert, A.A., Grimbergen, J.M., Vogels, R., Huisman, L.G., Valerio, D., et al., 2001. Improved adenovirus vectors for infection of cardiovascular tissues. J. Virol. 75 (7), 3335–3342.
Havenga, M.J., Lemckert, A.A., Ophorst, O.J., van Meijer, M., Germeraad, W.T., Grimbergen, J., et al., 2002. Exploiting the natural diversity in adenovirus tropism for therapy and prevention of disease. J. Virol. 76 (9), 4612–4620.
Heikkila, P., Parpala, T., Lukkarinen, O., Weber, M., Tryggvason, K., 1996. Adenovirus-mediated gene transfer into kidney glomeruli using an ex vivo and in vivo kidney perfusion system—First steps towards gene therapy of Alport syndrome. Gene Ther. 3 (1), 21–27.
Hemminki, A., Alvarez, R.D., 2002. Adenoviruses in oncology: a viable option? BioDrugs 16 (2), 77–87.
Hemminki, A., Kanerva, A., Kremer, E.J., Bauerschmitz, G.J., Smith, B.F., Conductier, G., et al., 2003. A canine conditionally replicating adenovirus for evaluating oncolytic virotherapy in a syngeneic animal model. Mol. Ther. 7 (2), 163–173.
Henry, L.J., Xia, D., Wilke, M.E., Deisenhofer, J., Gerard, R.D., 1994. Characterization of the knob domain of the adenovirus type 5 fiber protein expressed in *Escherichia coli*. J. Virol. 68 (8), 5239–5246.
Hofmann, C., Loser, P., Cichon, G., Arnold, W., Both, G.W., Strauss, M., 1999. Ovine adenovirus vectors overcome preexisting humoral immunity against human adenoviruses in vivo. J. Virol. 73 (8), 6930–6936.
Imai, E., Takabatake, Y., Mizui, M., Isaka, Y., 2004. Gene therapy in renal diseases. Kidney Int. 65 (5), 1551–1555.
Jakubczak, J.L., Rollence, M.L., Stewart, D.A., Jafari, J.D., Von Seggern, D.J., Nemerow, G.R., et al., 2001. Adenovirus type 5 viral particles pseudotyped with mutagenized fiber proteins show diminished infectivity of coxsackie B-adenovirus receptor-bearing cells. J. Virol. 75 (6), 2972–2981.
Kanerva, A., Mikheeva, G.V., Krasnykh, V., Coolidge, C.J., Lam, J.T., Mahasreshti, P.J., et al., 2002. Targeting adenovirus to the serotype 3 receptor increases gene transfer efficiency to ovarian cancer cells. Clin. Cancer Res. 8 (1), 275–280.
Khatri, A., Xu, Z.Z., Both, G.W., 1997. Gene expression by atypical recombinant ovine adenovirus vectors during abortive infection of human and animal cells in vitro. Virology 239 (1), 226–237.
Kim, M., Zinn, K.R., Barnett, B.G., Sumerel, L.A., Krasnykh, V., Curiel, D.T., et al., 2002. The therapeutic efficacy of adenoviral vectors for cancer gene therapy is limited by a low level of primary adenovirus receptors on tumour cells. Eur. J. Cancer 38 (14), 1917–1926.
Kim, M., Sumerel, L.A., Belousova, N., Lyons, G.R., Carcy, D.E., Krasuykh, V., et al., 2003. The coxsackievirus and adenovirus receptor acts as a tumour suppressor in malignant glioma cells. Br. J. Cancer 88 (9), 1411–1416.
Kirby, T.O., Rivera, A., Rein, D., Wang, M., Ulasov, I., Breidenbach, M., et al., 2004. A novel ex vivo model system for evaluation of conditionally replicative adenoviruses therapeutic efficacy and toxicity. Clin. Cancer Res. 10 (24), 8697–8703.
Koizumi, N., Mizuguchi, H., Sakurai, F., Yamaguchi, T., Watanabe, Y., Hayakawa, T., 2003. Reduction of natural adenovirus tropism to mouse liver by fiber-shaft exchange in combination with both CAR- and alphav integrin-binding ablation. J. Virol. 77 (24), 13062–13072.
Krasnykh, V.N., Mikheeva, G.V., Douglas, J.T., Curiel, D.T., 1996. Generation of recombinant adenovirus vectors with modified fibers for altering viral tropism. J. Virol. 70 (10), 6839–6846.
Krasnykh, V., Dmitriev, I., Mikheeva, G., Miller, C.R., Belousova, N., Curiel, D.T., 1998. Characterization of an adenovirus vector containing a heterologous peptide epitope in the HI loop of the fiber knob. J. Virol. 72 (3), 1844–1852.
Krasnykh, V., Belousova, N., Korokhov, N., Mikheeva, G., Curiel, D.T., 2001. Genetic targeting of an adenovirus vector via replacement of the fiber protein with the phage T4 fibritin. J. Virol. 75 (9), 4176–4183.
Kremer, E.J., Boutin, S., Chillon, M., Danos, O., 2000. Canine adenovirus vectors: an alternative for adenovirus-mediated gene transfer. J. Virol. 74 (1), 505–512.
Kumin, D., Hofmann, C., Rudolph, M., Both, G.W., Loser, P., 2002. Biology of ovine adenovirus infection of nonpermissive cells. J. Virol. 76 (21), 10882–10893.
Li, Y., Pong, R.C., Bergelson, J.M., Hall, M.C., Sagalowsky, A.I., Tseng, C.P., et al., 1999. Loss of adenoviral receptor expression in human bladder cancer cells: a potential impact on the efficacy of gene therapy. Cancer Res. 59 (2), 325–330.
Li, E., Brown, S.L., Stupack, D.G., Puente, X.S., Cheresh, D.A., Nemerow, G.R., 2001. Integrin alpha(v)beta1 is an adenovirus coreceptor. J. Virol. 75 (11), 5405–5409.
Lieber, A., He, C.Y., Meuse, L., Schowalter, D., Kirillova, I., Winther, B., et al., 1997. The role of Kupffer cell activation and viral gene expression in early liver toxicity after infusion of recombinant adenovirus vectors. J. Virol. 71 (11), 8798–8807.
Liu, Q., Zaiss, A.K., Colarusso, P., Patel, K., Haljan, G., Wickham, T.J., et al., 2003. The role of capsid–endothelial interactions in the innate immune response to adenovirus vectors. Hum Gene Ther. 14 (7), 627–643.
Loser, P., Hillgenberg, M., Arnold, W., Both, G.W., Hofmann, C., 2000. Ovine adenovirus vectors mediate efficient gene transfer to skeletal muscle. Gene Ther. 7 (17), 1491–1498.
Loser, P., Huser, A., Hillgenberg, M., Kumin, D., Both, G.W., Hofmann, C., 2002. Advances in the development of non-human viral DNA-vectors for gene delivery. Curr. Gene Ther. 2 (2), 161–171.
Loser, P., Hofmann, C., Both, G.W., Uckert, W., Hillgenberg, M., 2003. Construction, rescue, and characterization of vectors derived from ovine atadenovirus. J. Virol. 77 (22), 11941–11951.
Louis, N., Fender, P., Barge, A., Kitts, P., Chroboczek, J., 1994. Cell-binding domain of adenovirus serotype 2 fiber. J. Virol. 68 (6), 4104–4106.
Maizel Jr., J.V., White, D.O., Scharff, M.D., 1968. The polypeptides of adenovirus: I. Evidence for multiple protein components in the virion and a comparison of types 2, 7A, and 12. Virology 36 (1), 115–125.
Martin, K., Brie, A., Saulnier, P., Perricaudet, M., Yeh, P., Vigne, E., 2003. Simultaneous CAR- and alpha V integrin-binding ablation fails to reduce Ad5 liver tropism. Mol. Ther. 8 (3), 485–494.
Martiniello-Wilks, R., Wang, X.Y., Voeks, D.J., Dane, A., Shaw, J.M., Mortensen, E., 2004. Purine nucleoside phosphorylase and fludarabine phosphate gene-directed enzyme prodrug therapy suppresses primary tumour growth and pseudo-metastases in a mouse model of prostate cancer. J. Gene Med. 6 (12), 1343–1357.
Miller, C.R., Buchsbaum, D.J., Reynolds, P.N., Douglas, J.T., Gillespie, G.Y., Mayo, M.S., et al., 1998. Differential susceptibility of primary and established human glioma cells to adenovirus infection: targeting via the epidermal growth factor receptor achieves fiber receptor-independent gene transfer. Cancer Res. 58 (24), 5738–5748.
Mizuguchi, H., Koizumi, N., Hosono, T., Ishii-Watabe, A., Uchida, E., Utoguchi, N., et al., 2002. CAR- or alphav integrin-binding ablated adenovirus vectors, but not fiber-modified vectors containing RGD peptide, do not change the systemic gene transfer properties in mice. Gene Ther. 9 (12), 769–776.
Moullier, P., Friedlander, G., Calise, D., Ronco, P., Perricaudet, M., Ferry, N.,

1994. Adenoviral-mediated gene transfer to renal tubular cells in vivo. Kidney Int. 45 (4), 1220–1225.

Nakamura, T., Sato, K., Hamada, H., 2003. Reduction of natural adenovirus tropism to the liver by both ablation of fiber-coxsackievirus and adenovirus receptor interaction and use of replaceable short fiber. J. Virol. 77 (4), 2512–2521.

Nguyen, T., Nery, J., Joseph, S., Rocha, C., Carney, G., Spindler, K., et al., 1999. Mouse adenovirus (MAV-1) expression in primary human endothelial cells and generation of a full-length infectious plasmid. Gene Ther. 6 (7), 1291–1297.

Nicklin, S.A., Wu, E., Nemerow, G.R., Baker, A.H., 2005. The influence of adenovirus fiber structure and function on vector development for gene therapy. Mol. Ther. 12 (3), 384–393.

Okegawa, T., Li, Y., Pong, R.C., Bergelson, J.M., Zhou, J., Hsieh, J.T., 2000. The dual impact of coxsackie and adenovirus receptor expression on human prostate cancer gene therapy. Cancer Res. 60 (18), 5031–5036.

Ortiz, P.A., Hong, N.J., Plato, C.F., Varela, M., Garvin, J.L., 2003. An in vivo method for adenovirus-mediated transduction of thick ascending limbs. Kidney Int. 63 (3), 1141–1149.

Peeters, M.J., Patijn, G.A., Lieber, A., Meuse, L., Kay, M.A., 1996. Adenovirus-mediated hepatic gene transfer in mice: comparison of intravascular and biliary administration. Hum. Gene Ther. 7 (14), 1693–1699.

Rasmussen, U.B., Benchaibi, M., Meyer, V., Schlesinger, Y., Schughart, K., 1999. Novel human gene transfer vectors: evaluation of wild-type and recombinant animal adenoviruses in human-derived cells. Hum. Gene Ther. 10 (16), 2587–2599.

Reddy, P.S., Idamakanti, N., Chen, Y., Whale, T., Babiuk, L.A., Mehtali, M., et al., 1999a. Replication-defective bovine adenovirus type 3 as an expression vector. J. Virol. 73 (11), 9137–9144.

Reddy, P.S., Idamakanti, N., Hyun, B.H., Tikoo, S.K., Babiuk, L.A., 1999b. Development of porcine adenovirus-3 as an expression vector. J. Gen. Virol. 80 (Pt. 3), 563–570.

Reynolds, P., Dmitriev, I., Curiel, D., 1999. Insertion of an RGD motif into the HI loop of adenovirus fiber protein alters the distribution of transgene expression of the systemically administered vector. Gene Ther. 6 (7), 1336–1339.

Rothel, J.S., Boyle, D.B., Both, G.W., Pye, A.D., Waterkeyn, J.G., Wood, P.R., et al., 1997. Sequential nucleic acid and recombinant adenovirus vaccination induces host-protective immune responses against *Taenia ovis* infection in sheep. Parasite Immunol. 19 (5), 221–227.

Sakurai, F., Mizuguchi, H., Yamaguchi, T., Hayakawa, T., 2003. Characterization of in vitro and in vivo gene transfer properties of adenovirus serotype 35 vector. Mol. Ther. 8 (5), 813–821.

Salone, B., Martina, Y., Piersanti, S., Cundari, E., Cherubini, G., Franqueville, L., et al., 2003. Integrin alpha3beta1 is an alternative cellular receptor for adenovirus serotype 5. J. Virol. 77 (24), 13448–13454.

Shayakhmetov, D.M., Papayannopoulou, T., Stamatoyannopoulos, G., Lieber, A., 2000. Efficient gene transfer into human CD34(+) cells by a retargeted adenovirus vector. J. Virol. 74 (6), 2567–2583.

Shayakhmetov, D.M., Li, Z.Y., Ni, S., Lieber, A., 2004. Analysis of adenovirus sequestration in the liver, transduction of hepatic cells, and innate toxicity after injection of fiber-modified vectors. J. Virol. 78 (10), 5368–5381.

Shayakhmetov, D.M., Gaggar, A., Ni, S., Li, Z.Y., Lieber, A., 2005a. Adenovirus binding to blood factors results in liver cell infection and hepatotoxicity. J. Virol. 79 (12), 7478–7491.

Shayakhmetov, D.M., Li, Z.Y., Ni, S., Lieber, A., 2005b. Interference with the IL-1-signaling pathway improves the toxicity profile of systemically applied adenovirus vectors. J. Immunol. 174 (11), 7310–7319.

Smith, T., Idamakanti, N., Kylefjord, H., Rollence, M., King, L., Kaloss, M., et al., 2002. In vivo hepatic adenoviral gene delivery occurs independently of the coxsackievirus–adenovirus receptor. Mol. Ther. 5 (6), 770–779.

Smith, T.A., Idamakanti, N., Marshall-Neff, J., Rollence, M.L., Wright, P., Kaloss, M., et al., 2003a. Receptor interactions involved in adenoviral-mediated gene delivery after systemic administration in non-human primates. Hum. Gene Ther. 14 (17), 1595–1604.

Smith, T.A., Idamakanti, N., Rollence, M.L., Marshall-Neff, J., Kim, J., Mulgrew, K., et al., 2003b. Adenovirus serotype 5 fiber shaft influences in vivo gene transfer in mice. Hum. Gene Ther. 14 (8), 777–787.

Soudais, C., Boutin, S., Hong, S.S., Chillon, M., Danos, O., Bergelson, J.M., et al., 2000. Canine adenovirus type 2 attachment and internalization: coxsackievirus–adenovirus receptor, alternative receptors, and an RGD-independent pathway. J. Virol. 74 (22), 10639–10649.

Sullivan, D.E., Dash, S., Du, H., Hiramatsu, N., Aydin, F., Kolls, J., et al., 1997. Liver-directed gene transfer in non-human primates. Hum. Gene Ther. 8 (10), 1195–1206.

Takeda, S., Takahashi, M., Mizukami, H., Kobayashi, E., Takeuchi, K., Hakamata, Y., et al., 2004. Successful gene transfer using adeno-associated virus vectors into the kidney: comparison among adeno-associated virus serotype 1–5 vectors in vitro and in vivo. Nephron. Exp. Nephrol. 96 (4), e119–e126.

Tao, N., Gao, G.P., Parr, M., Johnston, J., Baradet, T., Wilson, J.M., et al., 2001. Sequestration of adenoviral vector by Kupffer cells leads to a nonlinear dose response of transduction in liver. Mol. Ther. 3 (1), 28–35.

Tomko, R.P., Xu, R., Philipson, L., 1997. HCAR and MCAR: the human and mouse cellular receptors for subgroup C adenoviruses and group B coxsackieviruses. Proc. Natl. Acad. Sci. U.S.A. 94 (7), 3352–3356.

van Raaij, M.J., Mitraki, A., Lavigne, G., Cusack, S., 1999. A triple beta-spiral in the adenovirus fibre shaft reveals a new structural motif for a fibrous protein. Nature 401 (6756), 935–938.

Vigne, E., Dedieu, J.F., Brie, A., Gillardeaux, A., Briot, D., Benihoud, K., et al., 2003. Genetic manipulations of adenovirus type 5 fiber resulting in liver tropism attenuation. Gene Ther. 10 (2), 153–162.

Voeks, D., Martiniello-Wilks, R., Madden, V., Smith, K., Bennetts, E., Both, G.W., et al., 2002. Gene therapy for prostate cancer delivered by ovine adenovirus and mediated by purine nucleoside phosphorylase and fludarabine in mouse models. Gene Ther. 9 (12), 759–768.

Von Seggern, D.J., Huang, S., Fleck, S.K., Stevenson, S.C., Nemerow, G.R., 2000. Adenovirus vector pseudotyping in fiber-expressing cell lines: improved transduction of Epstein–Barr virus-transformed B cells. J. Virol. 74 (1), 354–362.

Vrati, S., Boyle, D., Kocherhans, R., Both, G.W., 1995. Sequence of ovine adenovirus homologs for 100K hexon assembly, 33K, pVIII, and fiber genes: early region E3 is not in the expected location. Virology 209 (2), 400–408.

Vrati, S., Brookes, D.E., Strike, P., Khatri, A., Boyle, D.B., Both, G.W., 1996. Unique genome arrangement of an ovine adenovirus: identification of new proteins and proteinase cleavage sites. Virology 220 (1), 186–199.

Wang, X., Bergelson, J.M., 1999. Coxsackievirus and adenovirus receptor cytoplasmic and transmembrane domains are not essential for coxsackievirus and adenovirus infection. J. Virol. 73 (3), 2559–2562.

Wang, X.Y., Martiniello-Wilks, R., Shaw, J.M., Ho, T., Coulston, N., Cooke-Yarborough, C., et al., 2004. Preclinical evaluation of a prostate-targeted gene-directed enzyme prodrug therapy delivered by ovine atadenovirus. Gene Ther. 11 (21), 1559–1567.

Wickham, T.J., Mathias, P., Cheresh, D.A., Nemerow, G.R., 1993. Integrins alpha v beta 3 and alpha v beta 5 promote adenovirus internalization but not virus attachment. Cell 73 (2), 309–319.

Wood, M., Perrotte, P., Onishi, E., Harper, M.E., Dinney, C., Pagliaro, L., et al., 1999. Biodistribution of an adenoviral vector carrying the luciferase reporter gene following intravesical or intravenous administration to a mouse. Cancer Gene Ther. 6 (4), 367–372.

Worgall, S., Wolff, G., Falck-Pedersen, E., Crystal, R.G., 1997. Innate immune mechanisms dominate elimination of adenoviral vectors following in vivo administration. Hum. Gene Ther. 8 (1), 37–44.

Xia, D., Henry, L.J., Gerard, R.D., Deisenhofer, J., 1994. Crystal structure of the receptor-binding domain of adenovirus type 5 fiber protein at 1.7 A resolution. Structure 2 (12), 1259–1270.

Xu, Z.Z., Both, G.W., 1998. Altered tropism of an ovine adenovirus carrying the fiber protein cell binding domain of human adenovirus type 5. Virology 248 (1), 156–163.

Yun, C.O., Yoon, A.R., Yoo, J.Y., Kim, H., Kim, M., Ha, T., et al., 2005. Coxsackie and adenovirus receptor binding ablation reduces adenovirus liver tropism and toxicity. Hum. Gene Ther. 16 (2), 248–261.

Targeting EGFR with Metabolically Biotinylated Fiber-Mosaic Adenovirus

Larisa Pereboeva[1,2], Svetlana Komarova[1], Justin Roth[1], Selvarangan Ponnazhagan[2] and David T. Curiel[1*]

Division of Human Gene Therapy, Departments of Medicine, Obstetric and Gynecology, Pathology, and Surgery, and the Gene Therapy Center, University of Alabama at Birmingham, Birmingham, Alabama 35294-2172 (1)

Department of Pathology and the Gene Therapy Center, University of Alabama at Birmingham, Birmingham, Alabama 35294 (2)

Running title: Targeting EGFR with fiber-mosaic Ad

Word count for the abstract: 201

Word count for the text:

*Corresponding author. Mailing address: Division of Human Gene Therapy, Departments of Medicine, Pathology and Surgery, and The Gene Therapy Center, The University of Alabama at Birmingham, Birmingham, AL, 35294

901 19th Street S., BMRII-508 University of Alabama at Birmingham, Birmingham, AL 35294. Phone: (205) 934-8627. Fax: (205) 975-7476. Email:david.curiel@ccc.uab.edu

SUMMARY

Adenovirus-based vectors are useful gene delivery vehicles for a variety of applications. Despite attractive properties, many in vivo applications require modulation of the viral tropism. Targeting approaches applied to adenoviral vectors included genetic modification of the viral capsid, controlled expression of the transgene, and combinatorial approaches that combine two or more targeting elements in single vectors. Most of these studies confirmed successful retargeting in cell cultures, however in vivo gains of targeted adenoviral vectors have not been widely demonstrated. We have developed a combinatorial retargeting approach utilizing metabolically biotinylated Ad, where the biotin acceptor peptide was incorporated in one of the fibers in the dual fiber viral particle resulting in metabolically biotinylated fiber-mosaic Ad (mBfMAd). We have utilized this vector in complex with EGF-Streptavidin to retarget fiber-mosaic virus to EGF receptor (EGFR) expressing cells in vitro and confirmed an increased infectivity of the retargeting complex. Most importantly, the utility of this strategy was demonstrated in vivo in two distinct animal models. In both models tested retargeted mBfMAd demonstrated an increased ratio of gene expression in target tissues compared to the liver expression profile. Thus, metabolically biotinylated fiber-mosaic virus in combination with appropriate adaptors can be successfully exploited for adenoviral retargeting strategies.

Key words: targeted delivery, EGFR, adenoviral vector, fiber-mosaic, metabolic biotinylation

INTRODUCTION

Adenovirus-based vectors remain one of the most useful gene delivery vehicles for a variety of clinical contexts and a preferable vector for cancer gene therapy. Despite the attractive properties, several limitations preclude safe and efficient Ad-based gene transfer, specifically for in vivo settings. One limitation is the broad tropism of adenovirus (Ad), due to the ubiquitous expression pattern of the primary cell receptor CAR and secondary integrin receptors, which leads to undesired virus uptake and gene expression in non-target tissues. Furthermore, low and inconsistent expression of CAR on tumor cells raises concerns about the efficacy of Ad-mediated gene therapy in cancer applications. Thus, for efficient and versatile use of adenovirus (Ad) as an in vivo gene therapy vector, modulation of the viral tropism is highly desirable.

Various targeting approaches have been designed to change viral tropism. One approach includes genetic modification of the viral capsid proteins via addition of foreign targeting ligands such as short peptides or polypeptide binding domains or the substitution of the fiber with other types of Ad fiber. In adapter-mediated approaches, the tropism of the virus is modified by a targeting moiety utilizing a ligand which associates with the Ad virion. Adapter molecules successfully used for Ad targeting include bispecific antibody (Ab) conjugates,[1] genetic fusions of single-chain Ab (scFv) with soluble CAR,[2] or scFv-scFv diabodies.[3]

The combined use of two or more targeting components in single vector has also been reported to significantly enhance the utility of individual targeting approaches. The Immunoglobulin (Ig)-binding domain of the Staphylococcus aureus protein A has been genetically-incorporated into Ad fiber, allowing antigen-specific Ig to serve as bifunctional adapter molecules. Another complex targeting system designed by Barry, Campos, and colleagues utilizes the high affinity biotin-avidin interaction.[4,5] This system exploits the incorporation of a biotin acceptor peptide (BAP) into the structural proteins of Ad, which allowed metabolic biotinylation of these vectors during propagation

in 293 cells. All of these studies have demonstrated successful retargeting of adenoviruses in vitro through alternative receptors. However, several limitations could be envisioned for the translation of these targeting approaches for in vivo applications. For instance, viruses with incorporated IgG-binding domains may face a competition with IgGs abundantly present in serum and other biological fluids. On the other hand, drastic modifications of adenoviral structural proteins usually hamper infection and subsequent steps in the viral life cycle, limiting the ability to scale up viral preparations. This could explain why no targeting gains have been reported to date using this strategy in vivo.

In this study we developed a variation of the combined retargeting approach utilizing metabolically biotinylated fibers in the context of a fiber-mosaic viral capsid. The fiber mosaic construct allows expression of two fibers: fiber-fibritin (FF) and the wild type (wt) fiber, both of which are incorporated into viral particles. We have previously demonstrated that inclusion of a second fiber with distinct binding properties can provide virus binding and infection.[6] In contrast to studies by Barry et al. the biotin acceptor peptide was incorporated into one of the fibers resulting in metabolically biotinylated fiber-mosaic Ad (mBfMAd). The wild type fiber facilitates the viral life cycle and allows the fiber-mosaic virus to be propagated to levels near that of the wild type adenovirus. In our study we have exploited biotinylated fiber-fibritin in complex with adapter EGF-Streptavidin to retarget the fiber-mosaic virus to EGF receptor (EGFR) expressing cells both in vitro and in vivo.

RESULTS

Design and characterization of metabolically biotinylated fiber-mosaic adenovirus (mBfMAd). The genome design of the metabolically biotinylated fiber-mosaic adenovirus Ad5FF.PSTCD.F5luc (mBfMAd) was similar to that previously described for AdFF6H.F5luc.[6] A minimal domain of the 1.3S subunit of *Propionibacterium shermanii* transcarboxylase (PSTCD) was added to the C-terminus of chimeric protein fiber-fibritin. This domain is naturally biotinylated at lysine 89, when expressed in *E.coli* and *Saccharomyces cerevisiae* by each organism's cellular biotin ligase enzyme[7] and is also metabolically biotinylated in mammalian cells.[8] Thus, the mBfMAd genome encodes two fibers in the L5 region: a chimeric fiber-fibritin containing a C-terminal 6His tag and the PSTCD domain (FF.PSTCD.6H) and the Ad5 wild type fiber (Fig. 1A). Both fibers contain the tail portion of Ad5 fiber, which anchors them to the penton of the virion and also allows both fibers to be detected with anti-fiber tail AB. The coding sequences of both fibers were spanned by untranslated 5' and 3' sequences of the wt fiber thereby providing equal transcription conditions (splicing, polyadenylation as well as regulation by the Major Late Promoter) for both fibers. The fiber-mosaic vector carries the firefly luciferase gene under the control of the CMV promoter in the E1 region of the Ad5 genome (Fig. 1A). The mBfMAd was rescued in 293 cells expressing the complementary E1 region for Ad5 growth. The titer of fiber-mosaic virus used for this study was 4.83×10^{12} vp/ml. 293 cell culture infected by these viruses at the same MOI exhibited similar rates of CPE development, indicating a comparable time course of infection. Furthermore, the total yield of mBfMad and physical titers calculated in vp were comparable to the preps of wt virus, indicating that viral yield was not affected. Several lots of the virus have been obtained in the standard lab preparations with the titers ranged from $1.5\text{-}10^{12}$ to $1.3\ 10^{13}$ vp/ml. Thus, the yield of mBfMAd was similar to the yield routinely observed for the recombinant Ad5 preparations with unmodified capsid,

suggesting that the additional fiber did not hamper virus propagation and packaging and allowed efficient production of the fiber-mosaic virus.

Fiber content in fiber-mosaic virions. To examine fiber incorporation into mosaic virions, we performed a series of Western blots where an equal number of viral particles ($2x10^9$) of Ad5luc, Ad5.FF6H.F5luc and Ad5FF.PSTCD.F5luc were loaded on SDS-PAGE (Fig. 1B). Incorporation of FF.PSTCD. 6H into viral particles was confirmed by the interaction with antibodies specific to fiber tail (4D2), trimeric fiber (2A6), and 6-His. Western blots with the 4D2 and 2A6 antibodies revealed fiber monomers and timers of the correct size. The anti-His Ab only reacted with chimeric fibers from mosaic virions: FF.6H and FF.PSTCD.6H. Attachment of biotin on FF.PSTCD.6H fiber was confirmed by interaction with streptavidin both in Western blot (Fig.1B) and ELISA, where mBfMAd was captured either by streptavidin or EGF-Streptavidin coated on plates (Fig1.C). In addition, the mBfMAd retained CAR binding through wt fiber as demonstrated in Fig1.D. Thus, the presence of the FF. PSTCD.6H in the capsid of the mosaic virus was detected by antibodies directed to all of the functional domains of the protein – fiber tail, fiber trimer, and 6His, thereby demonstrating that the additional fiber was incorporated into the virion and correctly displays all of its functional motifs. The presence of the biotin on this fiber has also been confirmed, thus enabling utilization of our vector in combination with bioltinylated adaptors for Ad retargeting strategies.

The fiber content in the mosaic virions was semi-quantitatively estimated by the protein band intensity after staining with 4D2 AB employing Image Tool software. This analysis showed that the average ratio of FF.PSTCD. 6H to wt fiber in mBFmAd was similar to average ratio of FF.6H to wt fiber in AdFF.6H and has been estimated as 1:5 (ranging from 1:3-1:6, where higher ratios were obtained analyzing fiber monomers and lower ratios were obtained based on fiber trimers). Therefore, it could be expected that fiber-mosaic has 1-3 vertices of the viral capsid that contained biotinylated fiber, which can be utilized in retargeting strategy.

Targeting metabolically biotinylated fiber-mosaic vectors to EGFR using the bi-functional adapter EGF-Streptavidin in vitro. Theoretically, any molecule equipped with bispecific binding affinities, one to biotin and another to a target cell-specific receptor, can function as an adapter to redirect biotinylated virus to specific cell types. The bispecific adaptor contained human EGF fused to the core-streptavidin[9] has been previously expressed in the bacterial system and its design and production was described in detail in.[10] This adaptor has been thoroughly characterized and used to retarget AAV to EGFR expressing cell lines. Thus, the availability of this adaptor enabled us to test the utility of our vector in an EGFR retargeting strategy. We first wanted to determine the infectivity of our vector when applied with the EGF-Streptavidin adaptor in vitro.

To analyze EGFR targeting *in vitro,* we evaluated adaptor–mediated infection by mBfMAd of several cell lines with different EGFR expression status. Cancer cell lines with low (MDA-MB-453) and high EGFR expression (A431, SKOV3ip1, A549) were transduced with Ad5luc or mBfMAd at 100 vp/cell. Viruses were preincubated with EGF-Streptavidin at concentration of 10 ug/ml and purified from excess of adaptor using Microcon filter tubes. The results are shown in Fig.2. On the cell line with low EGFR expression (MDA-MB-453), both viruses showed comparable infectivity as measured by luciferase transgene activity. However, EGF-Streptavidin targeted transduction of mBfMAd resulted in significantly enhanced luciferase activity on EGFR-positive cells compared to that obtained with Ad5luc. The increase in transduction varied from more than 10 fold in A431 to more than 30 fold in SKOV3ip1 cells (Fig.2A). Additional evidence of efficient in vitro retargeting with the bispecific adaptor was also obtained using stable cell lines that express the extracelular domain of human EGFR.[11] Murine fibroblasts NR6 (EGFR-deficient) or NR6wt (EGFR-expressing) were preincubated with either PBS (no adapter) or with increasing concentration of EGF-Streptavidin 1-25 μg/ml, washed, and then transduced with Ad5luc or mBfMAd. Addition of the adaptor enhanced the transduction of EGFR-positive cells in a dose–dependent manner, but had no

effect on cells lacking EGFR receptor expression. The highest concentration of adapter used for retargeting mBfMAd to EGFR positive NR6wt cells resulted in as 8-fold increase in transgene expression, while it only increased transduction of wt Ad by 3.2 folds at the same experimental conditions (Fig.2B). Thus, mBfMAd can achieve enhanced transduction via bispecific adapter in cell lines expressing target receptor.

Targeting metabolically biotinylated fiber-mosaic vectors to EGFR in vitro after blocking fiber-CAR interaction. Our EGFR retargeting strategy relies upon the incorporation of modified fiber-fibritin, which is one of the two fibers present in the capsid of the fiber-mosaic virus. Retaining the wt fiber gene in the viral genome (i.e. the wt fiber protein in the viral particle) gives the potential advantage of facilitation of viral life cycle and virus propagation. A possible disadvantage for retargeting is the presence of the wt fiber, which can direct the infection of fiber-mosaic via the CAR-mediated pathway on CAR-positive cell lines. To confirm that biotinylated fibers, which represent only a fraction in the context of viral capsid, are able to mediate virus infectivity and to confirm the dependence of transgene expression on EGF-EGFR interaction, we performed retargeting gene transfer experiments in the presence of the Ad5knob. Virus infectivity in conditions when the binding ability of the wt fiber is blocked would indicate the relative contribution of the second fiber to the overall virus infectivity.

The low EGFR-expressing cell line, MDA-MB-453, and cell lines overexpressing EGFR (A431, A549, SKOV3) were transduced with Ad5luc or mBfMAd at 50 pfu/cell preincubated either with PBS (no adaptor) or with EGF-Streptavidin at concentration of 10 ug/ml. To block the infection via wt fiber, cells were preincubated with 50 ug/ml of recombinant Ad5 knob protein. We have previously shown that this concentration of Ad5knob blocked infectivity of wt virus more than 95% on high CAR-expressing cell lines. The results are shown in the Fig.3. In line with previous experiments, an addition of the EGF-Streptavidin retargeting adapter augmented infectivity of the

fiber-mosaic virus only, whereas it did not influence infectivity of Ad5luc in any cell line tested. In general, mBfMAd demonstrated similar patterns of EGFR-dependent transduction as in previous in vitro experiment with significant gene transfer increase in EGFR-overexpressing cells (A431, SKOV3) and no effect in cells with low EGFR expression (MDA-MB-453). In the presence of Ad5 knob, Ad5luc had predicted pattern of infection block for all cell lines tested. The results of CAR blocking was particularly clear in the highly CAR positive cell line A549, where gene transfer was blocked by 99% in the presence of Ad5knob. Wt Ad infectivity remained at 20-50% of normal levels in other cell lines that express lower levels of CAR, presumably via infection through cellular integrins (A451, SKOV3). Ad5 knob-mediated blocking mBfMAd infection in the absence of adapter did not reduce infectivity as significantly as that for the Ad5luc, and was either similar to infectivity levels without blocking or only decreased to 37-45% of the initial infectivity levels. Most importantly, the fiber-mosaic virus demonstrated efficient adaptor-based retargeting in EGFR-positive cells in Ad5 knob blocking conditions. Infectivity was increased by approximately 300% in A431 cells and 200% in SKOV3 cells in blocking conditions, where wt fiber presumably did not participate in infection. The level of EGFR-based infectivity was higher on cell lines with high EGFR expression and moderate CAR expression, indicating that in the situation where CAR-mediated infection is negligible, transduction via a second fiber dominates and is sufficient to mediate infection. Thus, biotinylated fiber can mediate adapter-driven transduction in the context of mosaic virions.

Analysis of EGFR retargeting with mBfMAd in vivo using a murine model of ovarian carcinoma. Next, we wanted to test whether our retargeting strategy gives any benefits when applied in vivo. The SKOV3ip1 cell line has been previously shown to have a high expression of EGFR.[12] This cell line also demonstrated high levels of EGFR-mediated retargeting in our in vitro experiments. Thus, we utilized an intraperitoneal xenograft model of human ovarian cancer based on

i.p. injection of SKOV3ip1 cells into CB17 SCID mice for analysis of in vivo targeting by mBFmAd. After tumors have been developed, the animals were injected ip with Ad5luc or mBfMAd viruses with or without preincubation with the EGF-Streptavidin adapter. Expression of luciferase was measured 48 hr later in tumor and liver tissue lysates. As shown in Fig. 4A, EGFR-mediated infection with mBFmAd resulted in a statistically significant increase in luciferase expression in tumors. Addition of the adaptor augmented mBfMAd-mediated gene transfer in EGFR-expressing tumors by over 7 fold, with average of RLU/mg protein values of 1668000 ± 530100 and 223900 ± 38910 for groups with and without adapter respectively. Liver gene transfer was not influenced by addition of the adaptor in animals receiving mBfMAd with or without the adapter. Ad5luc showed higher levels of the gene transfer both in tumors and in livers (Fig. 4B) compared to mBfMAd. However, the pattern of retargeting with adaptor for Ad5luc was different from mBfMAd. Preincubation of Ad5luc with EGF-Strept resulted in only a slight increase of gene transfer noted for both tumors and livers in all groups, but this enhancement was not statistically significant. Despite of potential of adenoviral vectors for cancer gene therapy, a major impediment of Ad-based delivery is liver tropism of the vector. Vector modifications that could minimize liver uptake and maximize tumor transduction would enhance vector applicability. In this context, we were also interested how our retargeting efforts were reflected in changing the tumor-to-liver gene transfer ratio. The tumor-to-liver ratio was calculated for each individual animal and presented as individual dots on a graph in Fig. 4C. The mean values of these ratios for the two groups receiving Ad5luc with or without adapter were similar and corresponded to 9.4 and 8.9. The mean ratio calculated for the group receiving mBfMAd has increased from 39 for the group receiving virus without adaptor to 69 for the group receiving EGFR-retargeted virus. Large variations between the values calculated for individual animals within each group were noted, and rendered the differences between these two groups statistically insignificant. However, the EGF-mediated targeting capacities of mBfMAd and

Ad5luc as measured by the tumor-to-liver luciferase activity ratio, were statistically significant (P=0.01). Thus, these data demonstrate the gains of adapter-based retargeting to EGFR-expressing tumor xenografts in the model of localized tumor.

In vivo retargeting of mBfMAd to EGFR-expressing lung endothelium in EGFR transient transgenic hCAR mice. We also explored the feasibility of targeting mBFmAd to hEGFR expressed in the pulmonary vasculature of mice. For these experiments we have utilized the model recently developed in our group that is based on transient induction of the target molecule in the pulmonary endothelium. This is accomplished using a combination of the hCAR transgenic mice and Ad-based vectors that allowed endothelial cell-specific antigen expression via placing the transgene under control of the endothelial specific flt-1 promoter.

The hCAR transgenic mice express a truncated human CAR under control of the ubiquitin promoter, resulting in hCAR protein expression in all organs including the lungs and therefore sensitizing the animal to adenoviral infection.[13] The major benefit of this model for testing vector targeting gains is the accessibility of the antigen to systemically introduced targeted vectors. To transiently induce human EGFR in the pulmonary endothelium of hCAR transgenic mice we used the AdfltEGFR adenovirus. We have previously confirmed the functionality of this virus in vitro. Further, we confirmed the expression of hEGFR in the pulmonary vasculature of hCAR mice upon tail vein injection of AdflthEGFR (1×10^{11} vp) by staining for EGFR in lung sections (data not shown). To validate EGFR targeting *in vivo,* hCAR mice preconditioned with AdflthEGFR injection were reinjected 48 h later with 5.0×10^{10} vp of mBfMAd preincubated with either PBS or EGF-Streptavidin. The animals were sacrificed 48 h subsequent to the second injection, and luciferase activities in the lungs and livers were quantified. As shown in Fig. 5A, EGF-mediated luciferase activity of mBfMAd in the lungs of pre-treated animals was increased by almost 5-fold compared to that in animals receiving mBfMAd without the adapter (341587 vs. 70625 mean RLU/mg protein,

respectively). This indicates that mBfBAd complexed with molecular adapter was able to efficiently target cells expressing antigen in the lung of mice following intravenous administration. Furthermore, liver transduction by the targeted virus did not increase. This outcome provided a significantly higher lung-to-liver ratio for the EGFR-retargeted group versus the control virus infected group (6.5 vs. 1.3 mean ratios, respectively; P= 0.01) (Figure 5B). Therefore, the accessibility of EGFR expressed in the lung vasculature enables to augment EGFR-based transduction of targeted cells by systemically introduced mBfBAd. In aggregate, these results demonstrate the targeting capacities of our strategy in vivo.

DISCUSSION

In this study we evaluated a targeting approach, utilizing a genetically-modified Ad fiber and adapter-mediated retargeting, both combined in the context of a fiber-mosaic viral capsid. We applied this approach for EGFR targeting, to demonstrate the functionality of our strategy in vitro and to establish the potential of this system for in vivo targeting applications.

Bifunctional adapter molecules have been engineered with specificity for both the Ad capsid protein (mainly Ad fiber) and to alternative cellular receptors distinct from CAR. The main advantage of this system is in its flexibility for using high affinity binders, regardless of their nature and size. However, the necessity for producing complex adapter molecules, such as whole antibodies, antibody fragments, or recombinant fusion proteins, has always been regarded as an inherent drawback of this approach. Nevertheless, efficient adenovirus targeting in vivo has only been reported using adapter-based approaches.[14-16]

Genetically modified vectors have a theoretical advantage in that they don't require additional soluble components for infectivity. A number of viruses with fibers constructed in this manner have been reported ranging from minor modifications, including single amino acid substitutions[17] and addition of small peptides[18,19] to more substantial alterations, such as switching entire protein functional domains (knob, shaft),[20-22] and generation of artificial fiber-like scaffolds that retain the essential functional properties of the whole Ad fiber.[23,24] These vectors generally fulfill the basic targeting requirements on cells in vitro, but the expected targeting efficacy has not yet been translated to in vivo experiments. In fact, the genetically-modified single component vectors most often require careful optimization of vector design by trial and error. In view of these obstacles, we hypothesized that the fiber mosaic platform, where two fibers are included in the viral genome, presents a more flexible mode for Ad vector modification and may simplify optimization of targeting efforts.

Here, we engineered a novel fiber-mosaic Ad vector, which comprises two fiber types: the wt fiber and Fiber-Fibritin chimera fused to the biotin acceptor peptide (BAP). This strategy has previously been used to metabolically conjugate biotin to viral proteins in mammalian cells, which allows them to be coupled to retargeting adapter molecules that contain streptavidin.[4,5,25] However, the utility of biotin incorporation for virus retargeting has thus far only been demonstrated in vitro and, among all of the structural proteins tested, only fiber-incorporated biotin was capable of efficient retargeting.[5] These studies established that biotin attachment is determined by the locale for BAP incorporation and provided the rationale for our fiber-based retargeting strategy.

Although our fiber-mosaic vector does provide an alternative tropism, the native tropism is not completely ablated due to the retention of the wt fiber in the viral capsid. The targeting function is delegated to a recombinant fiber while keeping the structural and functional integrity of the wt fiber during all stages of viral life cycle. The presence of wt fiber served to amplify the fiber-mosaic Ad to titers as high as 10^{12}-10^{13} vp/ml in regular laboratory-scale preparations. The presence of wt fiber may undermine the efficiency of retargeting, since just a fraction of fibers present on the viral capsid will serve for retargeting purposes. However, efficient redirection of our vector towards cells expressing EGFR was validated in vitro. The adapter-driven mBfMAd increased transduction of EGFR-positive cell lines 10-23 fold, compared to transduction without adapter. This level of enhancement is comparable with previously reported values obtained utilizing a complex of the wt virus with different bispecific molecular adapters.[12,26] Similarly, adenovirus retargeted through an "adenobody" strategy demonstrated a 10-fold enhancement of infectivity on A431 cell line.[27] Efficient utilization of the retargeting fiber was demonstrated using blocking experiments. The mBfMAd vector complexed with EGF-Streptavidin maintained a high level of gene transfer in the presence of Ad5 fiber knob concentrations that blocked infectivity of the Ad5luc control virus in the presence or absence of the adapter. These data additionally support the ability of mBfMAd to

redirect infection through the EGFR pathway. Thus, we believe that the proposed mosaic virus can efficiently utilize one of the mosaic fibers to redirect virus to alternative receptor in vitro.

Retargeting of different viruses through cell growth factor receptors, such as epidermal growth factor receptor (EGFR), which is highly expressed on tumors of different origin, has been validated in several adapter-based studies.[12,26-29] All reported adapter constructs were effective at coupling Ad to EGFR and resulted in increased gene transfer to EGFR expressing cell lines. This proved that EGFR pathway is compatible with adenoviral infection cycle. EGF exhibits high affinity binding to EGFR, which leads to rapid internalization via the receptor-mediated endocytic pathway but no recycling of the receptor-ligand complex.[30] Thus, the EGFR pathway is one of the best studied and proven pathways for adenoviral retargeting in vitro. However, in vivo studies involving such experiments are scarce and primarily utilize intratumoral administration of retargeted viruses.[28,31] There is often a disconnect between the virus targeting efficacy *in vitro* and that *in vivo*, whereby the retargeting results obtained in cell culture does not translated into *in vivo* gains. Thus, we next wanted to test if our retargeting strategy using fiber-mosaic virus can be effective *in vivo* and retarget mBFmAd to EGFR expressing cells.

Initial in vivo studies for retargeting adenoviral vectors were carried out using adapter-mediated approaches in intraperitoneal models of human cancer in mice.[32,33] This approach allows evaluation of targeting without the major hurdle of systemic virus administration, sequestration of the injected virus by the liver. The SKOV3ip ovarian cancer cell line expresses a very high level of EGFR and thus presents a good model to test EGFR targeting. Depending on the experimental conditions, mBfmAd demonstrated a 5-20-fold increase in gene transfer on these cells in vitro. Thus, it seemed logical to test whether the targeting gains would be paralleled in vivo. When injected in mice with preestablished intraperitoneal SKOV3ip xenografts, EGFR-retargeted mBfmAd increased tumor luciferase expression 7-fold, while gene expression in the liver was not affected. Gene transfer

efficiency with the Ad5luc vector was also slightly enhanced by the presence of the adapter. We have noted similar effect of adapter on Ad5luc infectivity in vitro, but the adapter-based gene transfer enhancement of Ad5luc was lower than that of the mBFmAd. Moreover, the addition of the adapter to Ad5luc increased gene transfer in both tumor and liver to the same extent, which finally resulted in similar tumor-to-liver ratio for Ad5luc with or without adapter (9.4 vs 8.9), while the mean tumor-to-liver ratio calculated for the group receiving mBfMAd has increased from 39 to 69 for virus without adapter and EGFR-retargeted virus, respectively. Of note, previous publications on adapter-mediated Ad retargeting, under similar experimental conditions, report only qualitative data on targeting gains[32,34] or targeting gains of at most two-to-five fold. Thus, the retargeting strategy applied to mBFmAd allowed to achieve comparable increase in tumor gene transfer in the context of ovarian cancer xenografts.

Another approach to test retargeting properties of adenoviral vectors in an efficient manner was recently developed in our group.[2] Since systemically introduced vectors retargeted to tumors are to overcome multiple physiological barriers before reaching their targets, it has been proposed that the display of targeting molecules at accessible sites would facilitate testing of targeting gains of systemically administered adenoviral vectors. An hCAR-transgenic mouse model that is sensitized to Ad infection and is used to transiently express tumor antigens in the lung vasculature was recently reported to be efficient for evaluating vectors targeted to CD40 and carcinoembryonic antigen (CEA).[2,35] Thus, the hCAR mice were used to confirm whether our targeting strategy using the combination of two targeting modes in a single vector could efficiently target hEGFR expressed in the lungs. Expression of hEGFR was transiently induced in the mice pulmonary endothelium by systemic injection of recombinant adenovirus AdfltEGFR. In this model, mBFmAd retargeted to EGFR expressed in mouse lungs shown 5-fold enhancement in the lung gene transfer, which resulted in increased the lung-to-liver retargeting ratio from 1.3 for the virus without adapter to 6.3 for the

retargeted virus. The lung-to-liver ratios calculated in our experiment for the retargeted fiber-mosaic vector correlated well with the values obtained in a previous study utilizing this model for CD40 retargeting (lung-to-liver ratio of 5.2 for CD40-retargeted virus and 1.2 for irrelevant virus),[35] thus providing a good estimate of the level of transductional retargeting gains achievable in this *in vivo* model. Overall, this transient transgenic model system allowed our targeting strategy to be evaluated.

Despite the fact that statistically significant differences in gene transfer was obtained by targeted versus untargeted virus in both models tested, a considerable variation of gene transfer values were obtained for individual animals, particularly for the calculated tumor-to-liver or lung-to-liver ratios. Specifically, this was observed in the groups receiving mBFmAd with adapter. These variations could be associated with the individual in vivo conditions, experimental errors, or factors related to the retargeting system itself in its current design, such as uniformity of virus prep and virus-adapter formulation.

All experimental work included in this study was done using single mBFmAd and Ad5luc preps, which were characterized for vp and pfu content, as well as the degree of fiber incorporation and biotinylation. However, we would like to stress that the uniformity of viral preparation in terms of the fiber content of each individual viral particle remains unknown. It is likely that the preparation of fiber-mosaic virus could contain (i) truly fiber-mosaic particles having both fibers in one viral capsid, (ii) a mixture of viral capsids displaying just one of the fibers, (iii) a combination of both variants. This factor may affect the overall performance of the fiber-mosaic virus. Of note, native fiber-mosaic viruses of serotype 40 and 41 have equal presentation of both fibers and apparently display both fibers in a single viral particle.

Another possible cause for inconsistence of viral preps is potential recombination. Although we were trying to minimize homologous sequences in mosaic genome, the rearrangement at low level still exists. DNA isolated from several viral preps of mBFmAd was tested for the rearrangement and

reversion to the single fiber genome by PCR. A low level of PCR product with size corresponded to the recombination event was detected in viral preps, and in plasmid preps of mBFmAd Shuttle vector and Ad genome, which are the standard steps of designing adenoviral vector. We believe that recombination at some low level occurred in the plasmid DNA while it is being propagated in bacteria, thus mBFmAd viral prep also may carry low level of contamination with viruses with one fiber. To minimize recombination in improved generations of fiber-mosaics, silent point mutations can be introduced into fiber tail sequences. In addition, we also can not exclude possible batch to batch variation of mBFmAd preps in terms of biotinylated fiber incorporation. For this experiment virus was pre-incubated with the adapter without any additional purification. However, further optimization for obtaining the virus-adapter complex can be considered. The crude viral prep obtained after the first virus CsCl banding can be further purified on avidin columns to eliminate virions lacking the recombinant fibers fibers. We are currently testing the consistency of fiber-mosaic virus preparations. Several lots of virus preparation did show a similar ratio of wt fiber to biotinylated fiber incorporation as described previously. However, different experimental and viral amplification conditions may bias or favor incorporation of the retargeting fiber and influence the overall efficiency of the retargeting strategy.

In this study we have demonstrated enhanced gene transfer based on transductional retargeting of our vector. It would be of a considerable interest to investigate to which extent it will translate to therapeutic endpoints. Several publications indicated the feasibility of conversion of the vector targeting gains to the treatment benefits in experimental animal models.[28,33] Thus, our future goal will include the introduction of an anti-cancer therapeutic gene in the context of the proposed fiber-mosaic platform to test therapeutic efficacy of our retargeting strategy.

In summary, we have confirmed that mBfMAd complexed with EGF-Streptavidin could successfully retarget virus to EGFR-expressing cancer cell lines. Most importantly, the evidence of

utility of this strategy was demonstrated in vivo. The targeting potential of mBfMAd complexed with EGF-Streptavidin was tested on two in vivo models that overexpress EGFR in different tissues. First, we utilized a mouse model of locoregional EGFR-positive ovarian xenografts. Secondly, the retargeting capacity of mBfMAd/EGF was tested on a “transient transgenic” mouse model with transient expression of hEGFR in the mouse lung vasculature. mBfMAd/EGF achieved a higher transduction level in the lung compared to mBfMAd without adapter. Moreover, tumor-to-liver or lung-to-liver gene expression ratios for retargeted mBfMAd increased in both models tested. Thus, we demonstrated that additional fiber in fiber-mosaic could be used for biotinylation and this modification, in combination with appropriate adapters, can be successfully exploited for adenoviral retargeting strategies. Importantly, our study demonstrated the proof of preclinical utility of our targeting strategy in animal models.

MATERIALS AND METHODS

Cells. The 293 human kidney cell line was purchased from Microbix (Toronto, Ontario, Canada). The human ovarian carcinoma cell line SKOV3.ip1 was obtained from Janet Price (M.D. Anderson Cancer Center, Houston, TX.). The human epidermoid carcinoma (A-431), human ovarian carcinoma (SKOV3), lung carcinoma (A549) and human breast cancer (MDA-MB-453) cell lines were from the American Type Culture Collection (Manassas, Va.). NR6 and NR6wt cell lines were obtained from Dr. Alan Wells (University of Pittsburgh, Pittsburgh, PA). These cell lines represent 3T3-derived fibroblasts lacking endogenous EGFRs (NR6) or the same cell line retrovirally transduced with the complete human EGFR (NR6wt).[11]

Antibodies. Monoclonal antibodies against the Ad5 fiber tail (4D2) and the fiber trimer (2A6) were purchased from Lab Vision (Fremont, CA). Anti-His antibody was obtained from QIAGEN (Valencia, CA). Secondary goat anti-mouse IgG HRP conjugated antibody was obtained from DAKO (Carpinteria, CA). Streptavidin and biotinylated HRP for Western blot were from Vector Labs (components of Vectastain ABC kit). Streptavidin for ELISA was from Southern Biotechnology Association, Birmingham, AL.

Recombinant proteins. Recombinant soluble CAR protein was provided by Dr. Igor Dmitriev, The Gene Therapy Center, University of Alabama at Birmingham.[12] The fiber-knob domain of Ad5 fibers was produced in Escherichia coli with N-terminal tags of six consecutive histidine residues (6-His), using the pQE30 expression vector (Qiagen, Valencia, CA). Recombinant EGF-Streptavidin was obtained as described in Ponnazhagan et al.[10] Briefly, this adapter was obtained by cloning coding sequences of EGF in frame with core-streptavidin in the vector pSTE2-215 Yol. For large-scale production of the fusion protein, 1 L of bacterial culture was induced with 20 μM IPTG (isopropyl-ß-D-thiogalactopyranoside) for 5 h at 30°C. Protein was purified from both soluble periplastic extract and remaining inclusion bodies. To obtain soluble periplasmic extract of

recombinant protein cell pellet was resuspended in 1/100 of the original culture volume in a buffer containing 50 mM Tris-HCl and 20% sucrose (pH 8.0). To purify protein from inclusion bodies, the pellet remaining after previous step was resuspended in 1/50 volume (to that of the original culture) of a buffer containing 6 M guanidine-HCl and 100 mM Tris (pH 7.0) and left rotating overnight. Following centrifugation at 13,000 rpm for 30 min, the supernatant containing the fusion protein was affinity purified with an Ni-nitrilotriacetic acid (Ni-NTA) column (Qiagen) according the manufacture manual. The eluted fusion protein was dialyzed against a buffer containing 100 mM Tris and 400 mM L-arginine and stored as frozen in aliquots at -20°C.

Viruses. Adenoviral vector having wild type fiber (Ad5luc) was used as a control for infectivity assessment of fiber-mosaic virus. Fiber mosaic virus AdFF/F5[6] genetically encoding two fibers: Fiber-fibritin containing 6-His at C-teminus[23] and wt fiber was used in virus binding experiments. Both viral genomes are isogenic to mBfMAd except the fiber region and contain the firefly luciferase gene under CMV promoter in E1 region. AdfltEGFR was used for transient expression of human EGFR in mouse lung vasculature in experiments testing systemic targeting of mBfMAd. The design of this virus is similar to the virus AdfltCEA described in,[2] where EGFR cDNA replaced CEA. EGFR cDNA was amplified from plasmid pcDNA3-EGFR.[36] All viruses were CsCl purified and viral particle titer was determined according to standard procedure.

Generation of metabolically biotinylated fiber-mosaic adenovirus (mBfmAd). The design of the genome of metabolically biotinylated fiber-mosaic adenovirus Ad5FF.PSTCD.F5luc (mBfMAd) was similar to that described previously for AdFF6H.F5luc,[6] where the virus genome encodes two fibers in the L5 region: chimeric fiber-fibritin containing C-terminal 6His (FF6H)[37] and Ad5 wild type fiber. The coding sequences of both fibers are spanned by untranslated 5' and 3' sequences of wt fiber, with intent to provide equal transcription conditions for both fibers (splicing, polyadenylation and regulation by the Major Late Promoter). To create Ad5FF.PSTCD.F5luc we

added a minimal domain of the 1.3S subunit of Propionibacterium shermanii transcarboxylase (PSTCD) to the chimeric protein fiber-fibritin. This domain is naturally biotinylated at lysine 89, when expressed in E.coli and Saccharomyces cerevisiae by each organism's cellular biotin ligase enzyme[7] and also can be metabolically biotinylated in mammalian cells.[8] DNA of PSTCD domain was amplified by PCR from the PinPoint-Xa2 plasmid (Promega) using primers 5'-GGCTCTAGAGCCGGTAAGGCCGGAGAG and 5'-CCGTCTAGAGAGATCCCCGATCTTGATG. The amplified fragment was then inserted into the XbaI site of plasmid pZeroFF6H, to obtain FF.PSTCD.6H. The cDNA of the resulting fiber FF.PSTCD.6H was amplified and cloned into a fiber mosaic shuttle vector pTGbx using ClaI and SwaI sites, therefore the shuttle plasmid finally has tandem fibers: FF.PSTCD.6H and Ad5 wt fiber flanked by Ad sequences. The Ad5 fiber-mosaic genome was obtained by homologous recombination of the mosaic shuttle vector (pTGbx FF.PSTCD.6H) with SwaI-linearized Ad5 genome backbone plasmid pVK700[38] in Escherichia coli BJ5183. The pVK700 plasmid contains cytomegalovirus (CMV) promoter-driven firefly luciferase gene in the E1 region as a reporter gene. The plasmid obtained was designated as pAdFF.PSTCD.6H.F5luc. The fiber-mosaic virus AdFF.PSTCD.6H.F5luc was rescued in 293 cells and purified by a standard CsCl gradient protocol. Titers of viral preps were determined in physical (vp) units, and infectious (pfu) units by TCID50 method according to the AdEasy protocol (Strategene, La Jolla, CA). Single virus preps of both Ad5luc and mBfMAd were used throughout the entire study. The physical titers obtained were $4.15x10^{12}$ and $4.83x10^{12}$ vp/ml for Ad5luc and the mBfMAd vector, while the infectious titers were $4.50x10^{11}$ and $8.97x10^{9}$ pfu/ml, respectively. Ratio of vp/pfu for Ad5luc and mBfMAd was 1:9 and 1:530, respectively.

Western blot analysis. Western blot to detect virus fibers and confirm fiber biotinylation was performed as described.[6] Briefly, aliquots of Ad vectors equal to $5x10^9$ viral particles (vp) were loaded on sodium dodecyl sulfate 4-20% gradient PAGE (BioRad, Hercules, CA) either boiled or unboiled. After separation, viral proteins were electroblotted onto a polyvinylidene difluoride (PVDF) membrane and detected with 4D2, 2A6, anti-His monoclonal AB followed by secondary antibody conjugated with HRP or strepavidin/biotinylated HRP for detection of fiber biotinylation. The blots were developed with 3,3'-diaminobenzidine (DAB).

ELISA. To test the binding properties of fiber-mosaic Ad, solid-phase binding enzyme-linked immunosorbent assay (ELISA) was performed. Binding attributed to wild type Ad fiber was confirmed by interaction with CAR as described.[6] Binding properties of the mosaic virus attributed to the biotinylated fiber were tested in interaction with streptavidin and EGF-streptavidin, which were coated on plastic at 50 μg/ml and 5 μg/ml correspondingly in 100 μl of 100 mM carbonate buffer (pH 9.5) during overnight incubation at 4°C. After washing and blocking, the wells were incubated with the virus followed the secondary antibodies.

Ad-mediated gene transfer assay. Infectivity of the mBfMAd in tumor cell lines was determined by gene transfer assay. Amount of mBfMAd or Ad5luc was calculated for each gene transfer experiment depending on cell numbers in the experimental protocol to correspond to the desired MOI. Viruses were preincubated with EGF-Streptavidin at the concentration of 10 μg/ml in 300 ul of PBS for 1h at room temperature and purified from excess of adaptor using Microcon Centrifugal Filter Devices YM-100 (molecular weight cut-off 100 kDa) (Amicon Bioseparation,. Millipore, Bedford, MA, USA). Viruses used as no adaptor control underwent the same procedure as above except PBS was added instead of the adaptor. Aliquots of the prepared viruses in DMEM-F12 containing 2% fetal bovine serum (FBS) were added to the cells and infection was carried out for 2 hr at 37°C. The cells were incubated in complete media with 10% FBS at 37°C to allow expression

of the luciferase gene for twenty four hours. Luciferase activity in the cell lysates was analyzed by using the Promega (Madison, Wis.) luciferase assay system and a Berthold (Gaithersburg, Md.) luminometer.

In the system with artificial expression of human EGFR, mouse fibroblast cells NR6 or NR6wt stably transduced with human EGFR were first preincubated for 10 min at RT with either PBS (no adaptor) or with increasing concentration of EGF-Streptavidin (1-25 ug/ml). After washing with PBS cells were transduced with Ad5luc or mBfMAd at 50 pfu/cell. Luciferase assay was performed as described above.

Competitive inhibition assay. Cell lines with low (MDA-MB-453) or high EGFR expression (A431, A549, SKOV3) were plated in 24-well plates at a density of $1x10^6$ cells/well. On the following day the cells were preincubated with recombinant Ad5 knob at 50 ug/ml for 10 min at room temperature to block infection via the wt fiber. Viruses were prepared as described in previous section and applied to cells, after the blocking step was completed, at MOI 50 pfu/cell for 2 hr at 37°C. Unbound virus was washed away with PBS, and medium with 10% FBS was added to each well. Forty hours later, the cells were processed for luciferase assay as described above.

In vivo retargeting of mBfMAd to EGFR using animal model of ovarian carcinoma. CB17 SCID female mice 6-8 weeks of age (Charles River) were injected intraperitoneally (ip) with $10x10^6$ SKOV3ip1 cells to establish intraperitoneal ovarian tumors. At day 21 after SKOV3ip injection, mice (n=7 per group) were followed with ip injection of Ad5luc or mBfMAd viruses at $1x10^{10}$ vp/animal preincubated either with adaptor EGF-Streptavidin (10 μg) or PBS. Mice were sacrificed 48 hr later, all visible tumor nodules (combined and treated as one tumor sample from each animal) and livers were excised and luciferase assay was performed in tissue lysates. Same lysates were used to determine protein concentration by Bio-Rad assay.

In vivo retargeting of mBfMAd to EGFR-expressing lung endothelium in EGFR transient transgenic hCAR mice. The transgenic hCAR mice were a generous gift from Dr. Sven Pettersson (Karolinska Institute, Sweden). These mice express truncated human CAR (hCAR) under the control of the human ubiquitin-C promoter, thus allowing hCAR expression in a variety of tissues, including the lungs, kidneys, liver, heart, brain, and muscle.[13] In this study, 8–12-week-old hCAR mice screened for presence of hCAR using PCR and flow cytometry were used. First, hCAR transgenic mice were preconditioned to achieve transient EGFR expression in lung endothelium. For that mice were injected via tail vein with $1x10^{11}$ vp of AdfltEGFR per animal. Transient expression of Ad transgene in lung endothelium under these conditions has been first demonstrated by Everts et al.[2] Forty-eight hours after the first injection, each mouse was injected iv with $5x10^{10}$ vp of mBfMAd preincubated either with EGF-Streptavidin (100 ng) or PBS. All animals were sacrificed 48 hours after last viral injection. Lung and liver luciferase activities were measured and normalized for protein content determined by Bio-Rad assay.

Animal experiments and protocols were reviewed and approved by the Institutional Animal Care and Use Committee of University of Alabama at Birmingham.

Statistics. Student's t-test was employed for statistical analysis where $p < 0.05$ was considered to be statistically significant.

ACKNOWLEDGEMENTS:

We thank Joel Glasgow and Alex Pereboev for proofing the manuscript and helpful critique.

This study was supported, in part, by NIH grants RO1CA083821-06, 1P01HL076540, 1P01CA104177-01A2, CA075930-07 and DOD grant W81XWH-05-1-0035 and Muscular Dystrophy Association.

REFERENCES

1 Reynolds PN, Zinn KR, Gavrilyuk VD, Balyasnikova IV, Rogers BE, Buchsbaum DJ *et al.* A targetable, injectable adenoviral vector for selective gene delivery to pulmonary endothelium in vivo. *Mol Ther* 2000; **2:** 562-578.

2 Everts M, Kim-Park SA, Preuss MA, Passineau MJ, Glasgow JN, Pereboev AV *et al.* Selective induction of tumor-associated antigens in murine pulmonary vasculature using double-targeted adenoviral vectors. *Gene Ther* 2005; **12:** 1042-1048.

3 Nettelbeck DM, Miller DW, Jerome V, Zuzarte M, Watkins SJ, Hawkins RE *et al.* Targeting of adenovirus to endothelial cells by a bispecific single-chain diabody directed against the adenovirus fiber knob domain and human endoglin (CD105). *Mol Ther* 2001; **3:** 882-891.

4 Campos SK, Parrott MB, Barry MA. Avidin-based targeting and purification of a protein IX-modified, metabolically biotinylated adenoviral vector. *Mol Ther* 2004; **9:** 942-954.

5 Campos SK, Barry MA. Comparison of adenovirus fiber, protein IX, and hexon capsomeres as scaffolds for vector purification and cell targeting. *Virology* 2006.

6 Pereboeva L, Komarova S, Mahasreshti PJ, Curiel DT. Fiber-mosaic adenovirus as a novel approach to design genetically modified adenoviral vectors. *Virus Res* 2004; **105:** 35-46.

7 Cronan JE, Jr. Biotination of proteins in vivo. A post-translational modification to label, purify, and study proteins. *J Biol Chem* 1990; **265:** 10327-10333.

8 Parrott MB, Barry MA. Metabolic biotinylation of recombinant proteins in mammalian cells and in mice. *Mol Ther* 2000; **1:** 96-104.

9 Sano T, Pandori MW, Chen X, Smith CL, Cantor CR. Recombinant core streptavidins. A minimum-sized core streptavidin has enhanced structural stability and higher accessibility to biotinylated macromolecules. *J Biol Chem* 1995; **270:** 28204-28209.

10 Ponnazhagan S, Mahendra G, Kumar S, Thompson JA, Castillas M, Jr. Conjugate-based targeting of recombinant adeno-associated virus type 2 vectors by using avidin-linked ligands. *J Virol* 2002; **76:** 12900-12907.

11 Chen P, Murphy-Ullrich JE, Wells A. A role for gelsolin in actuating epidermal growth factor receptor-mediated cell motility. *J Cell Biol* 1996; **134:** 689-698.

12 Dmitriev I, Kashentseva E, Rogers BE, Krasnykh V, Curiel DT. Ectodomain of coxsackievirus and adenovirus receptor genetically fused to epidermal growth factor mediates adenovirus targeting to epidermal growth factor receptor-positive cells. *J Virol* 2000; **74:** 6875-6884.

13 Tallone T, Malin S, Samuelsson A, Wilbertz J, Miyahara M, Okamoto K *et al.* A mouse model for adenovirus gene delivery. *Proc Natl Acad Sci U S A* 2001; **98:** 7910-7915.

14 Gu DL, Gonzalez AM, Printz MA, Doukas J, Ying W, D'Andrea M *et al.* Fibroblast growth factor 2 retargeted adenovirus has redirected cellular tropism: evidence for reduced toxicity and enhanced antitumor activity in mice. *Cancer Res* 1999; **59:** 2608-2614.

15 Fisher KD, Stallwood Y, Green NK, Ulbrich K, Mautner V, Seymour LW. Polymer-coated adenovirus permits efficient retargeting and evades neutralising antibodies. *Gene Ther* 2001; **8:** 341-348.

16 Lanciotti J, Song A, Doukas J, Sosnowski B, Pierce G, Gregory R *et al.* Targeting adenoviral vectors using heterofunctional polyethylene glycol FGF2 conjugates. *Mol Ther* 2003; **8:** 99-107.

17 Roelvink PW, Mi Lee G, Einfeld DA, Kovesdi I, Wickham TJ. Identification of a conserved receptor-binding site on the fiber proteins of CAR-recognizing adenoviridae. *Science* 1999; **286:** 1568-1571.

18 Dmitriev I, Krasnykh V, Miller CR, Wang M, Kashentseva E, Mikheeva G *et al.* An adenovirus vector with genetically modified fibers demonstrates expanded tropism via utilization of a coxsackievirus and adenovirus receptor-independent cell entry mechanism. *J Virol* 1998; **72:** 9706-9713.
19 Wickham TJ, Tzeng E, Shears LL, 2nd, Roelvink PW, Li Y, Lee GM *et al.* Increased in vitro and in vivo gene transfer by adenovirus vectors containing chimeric fiber proteins. *J Virol* 1997; **71:** 8221-8229.
20 van Beusechem VW, van Rijswijk AL, van Es HH, Haisma HJ, Pinedo HM, Gerritsen WR. Recombinant adenovirus vectors with knobless fibers for targeted gene transfer. *Gene Ther* 2000; **7:** 1940-1946.
21 Magnusson MK, Hong SS, Boulanger P, Lindholm L. Genetic retargeting of adenovirus: novel strategy employing "deknobbing" of the fiber. *J Virol* 2001; **75:** 7280-7289.
22 Mercier GT, Campbell JA, Chappell JD, Stehle T, Dermody TS, Barry MA. A chimeric adenovirus vector encoding reovirus attachment protein sigma1 targets cells expressing junctional adhesion molecule 1. *Proc Natl Acad Sci U S A* 2004; **101:** 6188-6193.
23 Krasnykh V, Belousova N, Korokhov N, Mikheeva G, Curiel DT. Genetic targeting of an adenovirus vector via replacement of the fiber protein with the phage T4 fibritin. *J Virol* 2001; **75:** 4176-4183.
24 Belousova N, Korokhov N, Krendelshchikova V, Simonenko V, Mikheeva G, Triozzi PL *et al.* Genetically targeted adenovirus vector directed to CD40-expressing cells. *J Virol* 2003; **77:** 11367-11377.
25 Parrott MB, Adams KE, Mercier GT, Mok H, Campos SK, Barry MA. Metabolically biotinylated adenovirus for cell targeting, ligand screening, and vector purification. *Mol Ther* 2003; **8:** 688-700.
26 Haisma HJ, Grill J, Curiel DT, Hoogeland S, van Beusechem VW, Pinedo HM *et al.* Targeting of adenoviral vectors through a bispecific single-chain antibody. *Cancer Gene Ther* 2000; **7:** 901-904.
27 Watkins SJ, Mesyanzhinov VV, Kurochkina LP, Hawkins RE. The 'adenobody' approach to viral targeting: specific and enhanced adenoviral gene delivery. *Gene Ther* 1997; **4:** 1004-1012.
28 Hemminki A, Dmitriev I, Liu B, Desmond RA, Alemany R, Curiel DT. Targeting oncolytic adenoviral agents to the epidermal growth factor pathway with a secretory fusion molecule. *Cancer Res* 2001; **61:** 6377-6381.
29 van Beusechem VW, Grill J, Mastenbroek DC, Wickham TJ, Roelvink PW, Haisma HJ *et al.* Efficient and selective gene transfer into primary human brain tumors by using single-chain antibody-targeted adenoviral vectors with native tropism abolished. *J Virol* 2002; **76:** 2753-2762.
30 Kolibaba KS, Druker BJ. Protein tyrosine kinases and cancer. *Biochim Biophys Acta* 1997; **1333:** F217-248.
31 Liang Q, Dmitriev I, Kashentseva E, Curiel DT, Herschman HR. Noninvasive of adenovirus tumor retargeting in living subjects by a soluble adenovirus receptor-epidermal growth factor (sCAR-EGF) fusion protein. *Mol Imaging Biol* 2004; **6:** 385-394.
32 Printz MA, Gonzalez AM, Cunningham M, Gu DL, Ong M, Pierce GF *et al.* Fibroblast growth factor 2-retargeted adenoviral vectors exhibit a modified biolocalization pattern and display reduced toxicity relative to native adenoviral vectors. *Hum Gene Ther* 2000; **11:** 191-204.
33 Rancourt C, Rogers BE, Sosnowski BA, Wang M, Piche A, Pierce GF *et al.* Basic fibroblast growth factor enhancement of adenovirus-mediated delivery of the herpes simplex virus

thymidine kinase gene results in augmented therapeutic benefit in a murine model of ovarian cancer. *Clin Cancer Res* 1998; **4:** 2455-2461.

34 Tanaka T, Huang J, Hirai S, Kuroki M, Watanabe N, Tomihara K *et al.* Carcinoembryonic antigen-targeted selective gene therapy for gastric cancer through FZ33 fiber-modified adenovirus vectors. *Clin Cancer Res* 2006; **12:** 3803-3813.

35 Izumi M, Kawakami Y, Glasgow JN, Belousova N, Everts M, Kim-Park S *et al.* In vivo analysis of a genetically modified adenoviral vector targeted to human CD40 using a novel transient transgenic model. *J Gene Med* 2005; **7:** 1517-1525.

36 Bonner JA, Buchsbaum DJ, Russo SM, Fiveash JB, Trummell HQ, Curiel DT *et al.* Anti-EGFR-mediated radiosensitization as a result of augmented EGFR expression. *Int J Radiat Oncol Biol Phys* 2004; **59:** 2-10.

37 Krasnykh V, Belousova N, Korokhov N, Mikheeva G, Curiel DT. Genetic targeting of an adenovirus vector via replacement of the fiber protein with the phage T4 fibritin. *J Virol* 2001; **75:** 4176-4183.

38 Belousova N, Krendelchtchikova V, Curiel DT, Krasnykh V. Modulation of adenovirus vector tropism via incorporation of polypeptide ligands into the fiber protein. *J Virol* 2002; **76:** 8621-8631.

TITLES AND LEGENDS TO FIGURES

Fig. 1. **Design and characterization of metabolically biotinylated fiber-mosaic adenovirus (mBfMAd)**

A) Diagram of fiber-mosaic adenovirus Ad.FF.PSTCD.6H.F5luc (mBfMAd) genome. Modification of L5 region of Ad genome includes tandem of fiber genes: fiber-fibritin with biotin acceptor peptide PSTCD and 6His tag and wt Ad5 fiber.

(B) Fiber content in fiber-mosaic AdFF6H.F5luc virions. Equal amounts of Ad5luc AdFF6H.F5luc and Ad.FF.PSTCD.6H.F5luc ($5x10^9$ vp) in SDS sample buffer were loaded on gradient (4–20%) SDS gel either boiled or unboiled. Electrophoretically separated viral proteins were transferred to PVDF membrane and developed with monoclonal antibodies specific to fiber tail (4D2), fiber trimer (2A6), 6His-Tag and Streptavidin-HRP.

(C, D) Binding characteristics of mBfMAd. Binding of mBfMAd to streptavidin (C) and recombinant CAR (D) was tested in ELISA. The number of virus particles used for binding experiments was within the range of 1×10^7–2×10^{10} which corresponded to 0.01-5 μg of viral protein per well. Control lane shown represents nonspecific binding of mBfMAd to the plastic surface in the absence of CAR.

Fig. 2. **Increased gene transfer to EGFR-expressing cell lines.**

(A) Cancer cell lines with low (MDA-MB-453) and high (A431, SKOV3ip1, A549) EGFR expression were transduced with Ad5luc or mBfMAd at 100 vp/cell.

Viruses were preincubated with EGF-Streptavidin at concentration of 10 μg/ml, purified from excess of adaptor using centricon tubes and applied on cells. Results are presented as % of increase of luciferase expression with adaptor. Mean luciferase expression of the same virus without adaptor was designated as 100 %.

(B) Murine fibroblasts NR6 or NR6wt EGFR, expressing extracellular domain of human EGFR, were preincubated with either PBS (no adaptor) or with increasing concentration of EGF-Streptavidin 1-25 μg/ml. Cells has been were transduced with Ad5luc or mBfMAd at 50 pfu/cell. Results are presented as increase of luciferase expression with adaptor. Mean luciferase expression of the same virus without adaptor was designated as 100 %.

Fig. 3. **Infectivity of mBfMAd Ad after blocking fiber-CAR interaction.**

Cell lines with low EGFR expression (MDA-MB-453) and cell lines overexpressing EGFR (A431, A549, SKOV3) were transduced with Ad5luc or mBfMAd at 50 pfu/cell preincubated either with PBS (no adaptor) or with EGF-Streptavidin at concentration of 10 ug/ml. To block infection via wt fiber cells were preincubated with Ad5 knob recombinant protein at 50 ug/ml. Twenty-four hours later the cells were processed for luciferase assay. Results are presented as % of luciferase expression compared to infection of this virus without adaptor or knob blocking. Data presented are mean average of triplicates plus sample standard deviation.

Fig. 4. **In vivo retargeting of mBfMAd to EGFR using animal model of ovarian carcinoma.**

CB17 SCID mice were injected ip with $10x10^6$ SKOV3ip1 cells to establish intraperitoneal ovarian tumors. At day 21 after SKOV3ip injection, four groups of mice (n=7) were injected with Ad5luc or mBfMAd viruses either without adaptor or preincubated with EGF-streptavidin. Viruses were injected ip at $1x10^{10}$ vp/animal. Mice were sacrificed 48 hr later, tumors and livers were excised and luciferase assay was performed in tissue lysates. Results are presented as luciferase expression (RLU) normalized for protein content (mg protein) for mBfMAd (A) and Ad5luc (B), and as tumor-to-liver ratio of luciferase expression (C). Tumor-to-liver ratio was calculated for individual animals

and represented as one dot on a graph. Bars represent averages of values in each group (n=7), P=0.01.

Fig. 5. **In vivo retargeting of mBfMAd to EGFR-expressing lung endothelium in EGFR transient transgenic hCAR mice.**

hCAR transgenic mice were injected with AdfltEGFR at 10^{11} vp/mice via tail vein for expression of EGFR in lung endothelium followed by second injection of mBfMAd with or without adaptor at $5x10^{10}$ vp/animal via tail vein 48 hr later. 48 hours after mBfMAd all animals were sacrificed.

A) Lung and liver luciferase activities 48 hr after intravenous administration of mBfMAd with or without EGF-Streptavidin adaptor. Results are presented as lung and liver luciverase expression (RLU) normalized for protein content (mg protein).

B) Lung-to–liver ratios of luciferase activities in individual animals (n=7). Bars represent averages of values in each group (P=0.01).

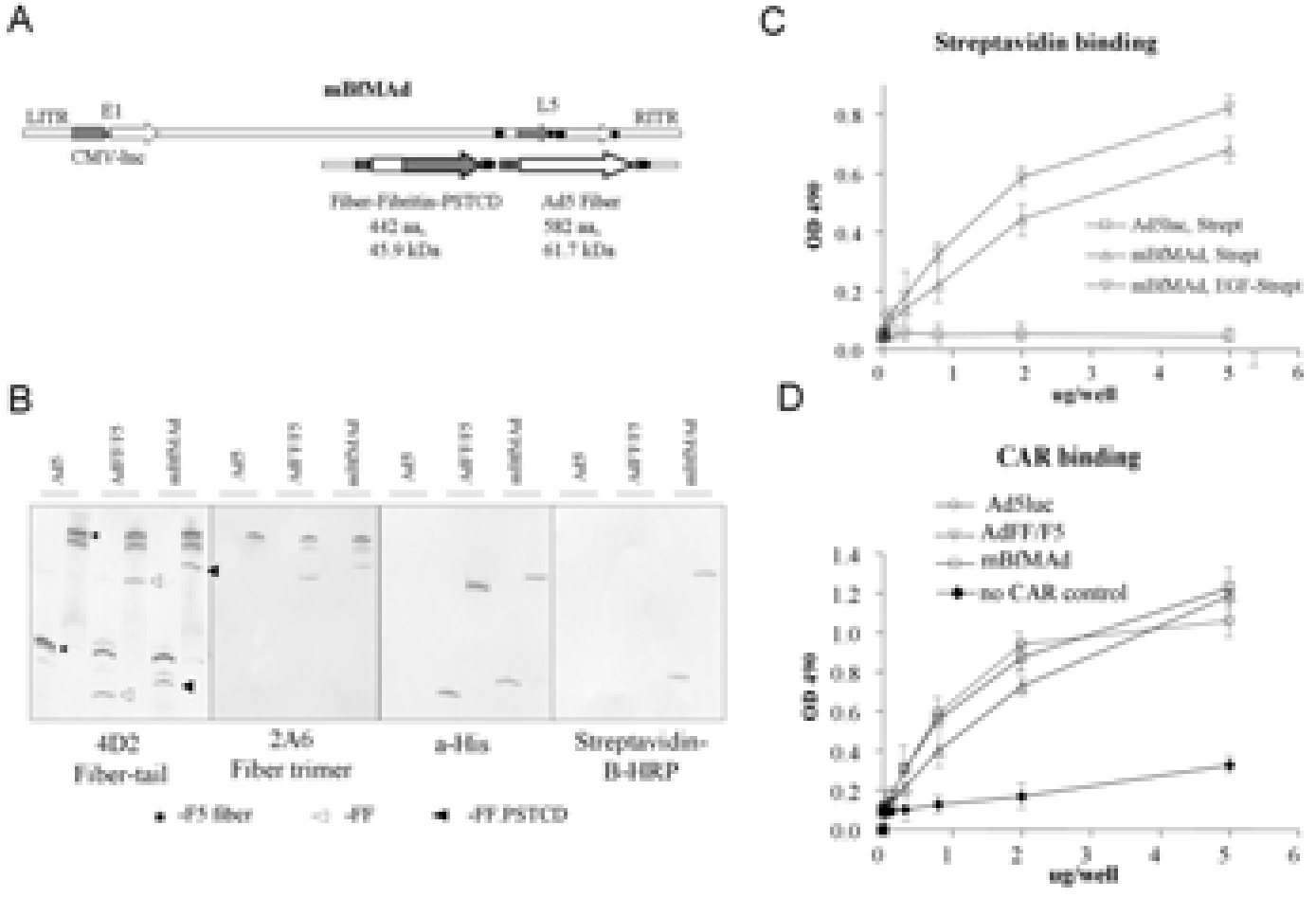
A
mBIMAd
L3
L3TR
E1
R3TR
CMV-luc
Fiber-Fibritin-PSTCD
442 aa,
45.9 kDa
Ad5 Fiber
582 aa,
61.7 kDa
B
Ad5
AdFF1/5
mBIMAd
4D2
Fiber-tail
2A6
Fiber trimer
a-His
Streptavidin-
B-HRP
-F5 fiber
-FF
-FF PSTCD
C
Streptavidin binding
OD 450
ug/well
Ad5luc, Strept
mBIMAd, Strept
mBIMAd, EGF-Strept
D
CAR binding
Ad5luc
AdFF/F5
mBIMAd
no CAR control
OD 450
ug/well

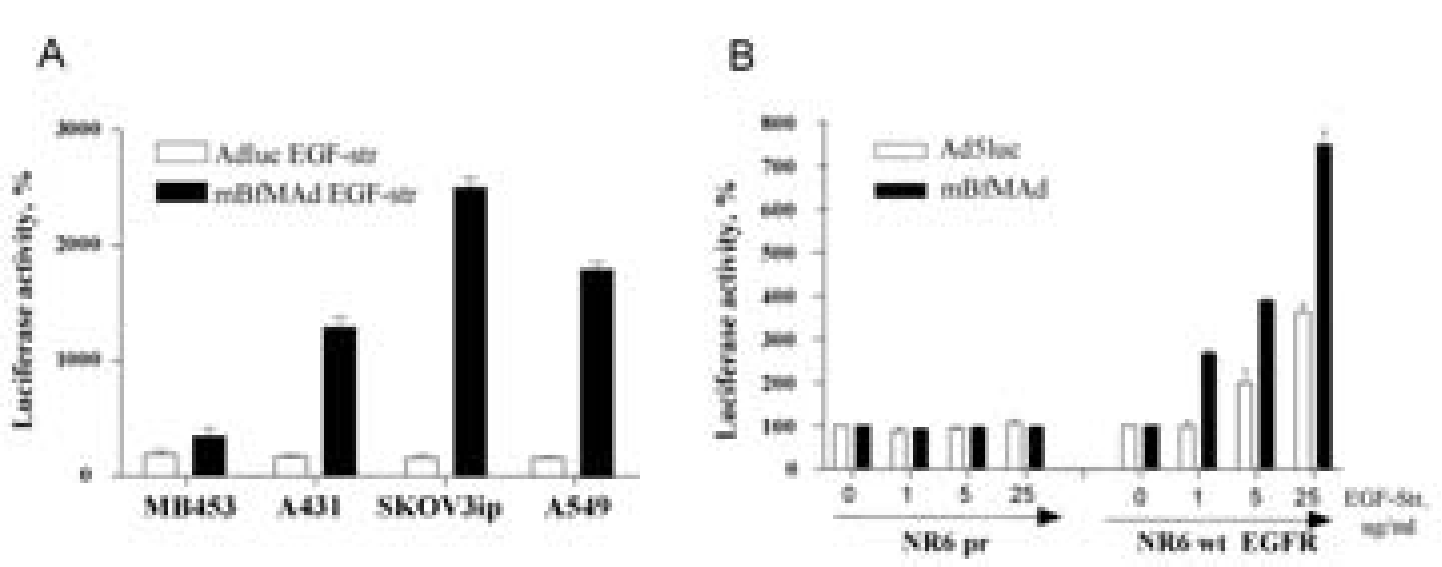
A
Adluc EGF-str
mB/MAd EGF-str
Luciferase activity, %
MB453
A431
SKOV3ip
A549
B
Ad5luc
mB/MAd
Luciferase activity, %
0
1
5
25
NR6 pr
NR6 wt EGFR
EGF-Str, ng/ml

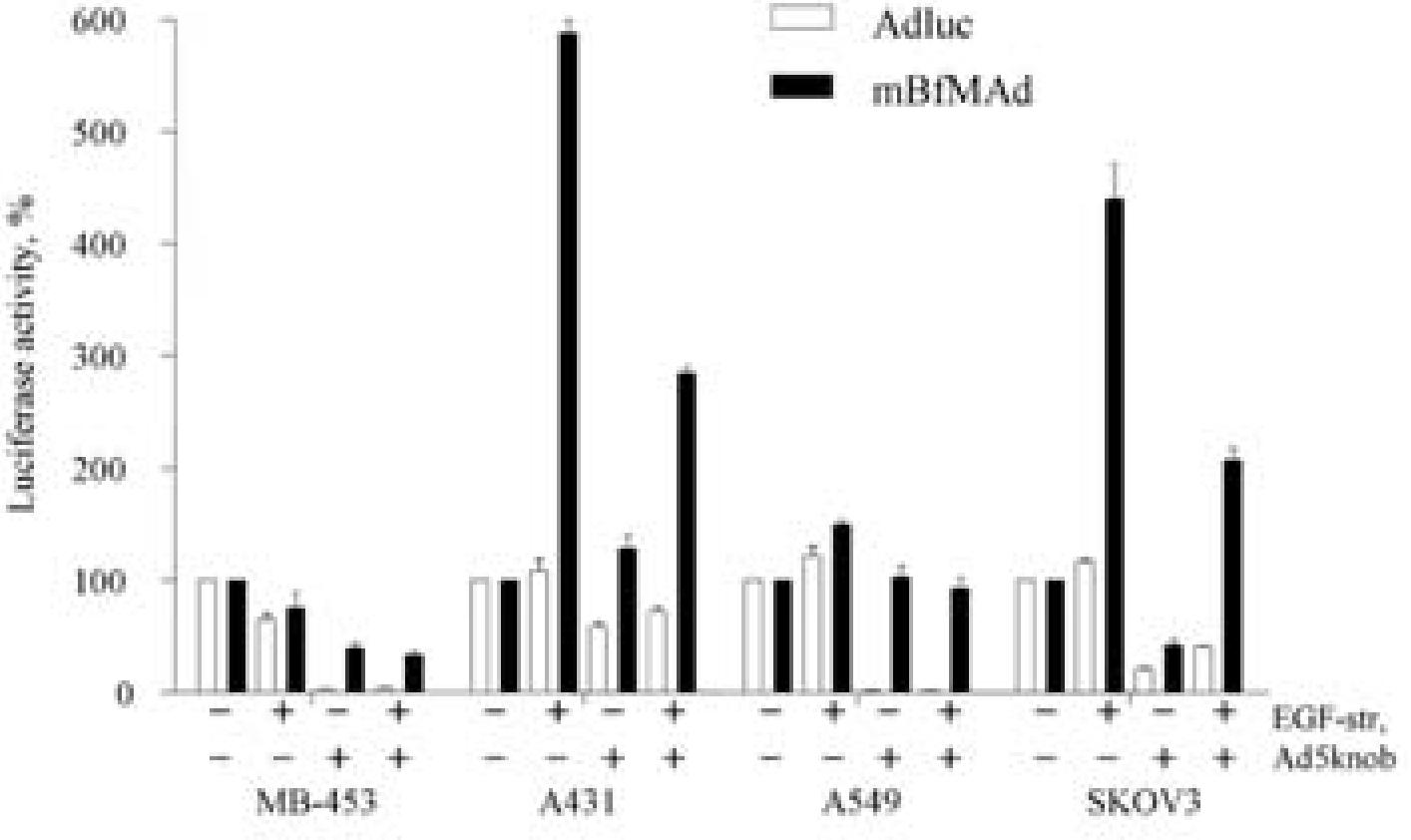
Adluc
mBfMAd
Luciferase activity, %
600
500
400
300
200
100
0
EGF-str.
Ad5knob
MB-453
A431
A549
SKOV3

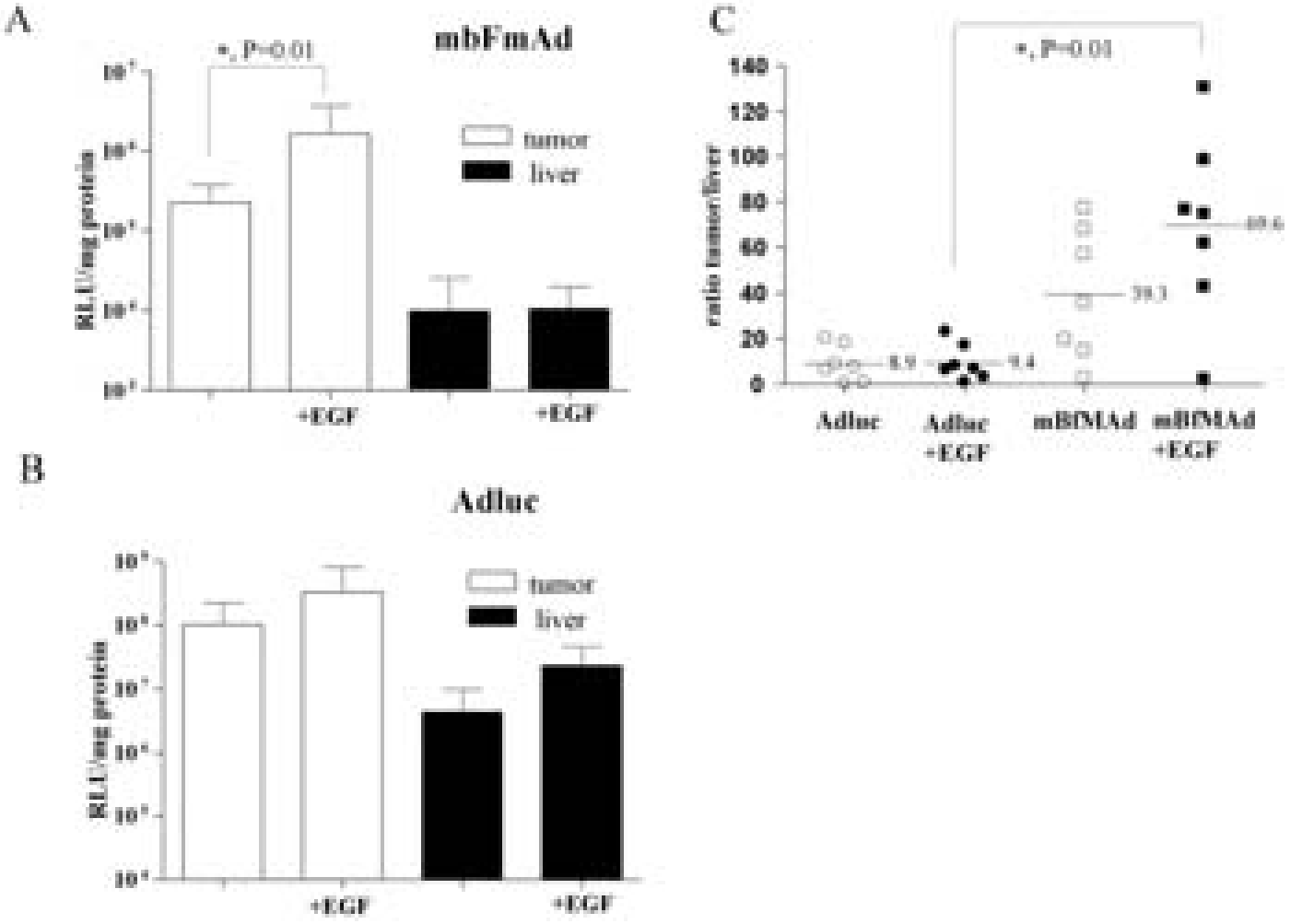
A
mbFmAd
*, P<0.01
tumor
liver
RLU/mg protein
+EGF
+EGF
B
Adluc
tumor
liver
RLU/mg protein
+EGF
+EGF
C
*, P<0.01
ratio tumor/liver
8.9
9.4
39.3
69.6
Adluc
Adluc +EGF
mBfMAd
mBfMAd +EGF

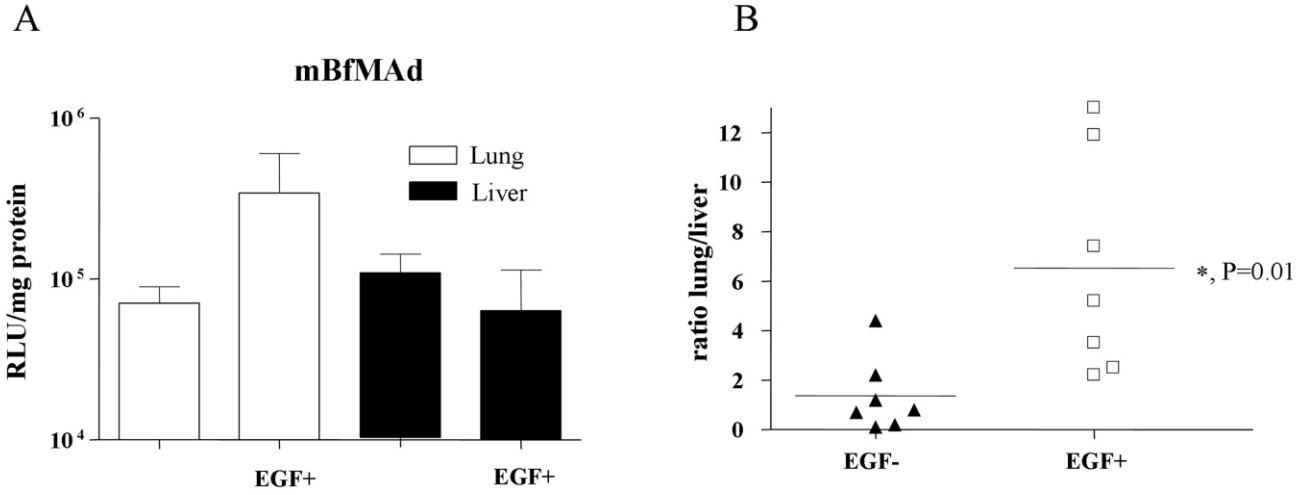
A
mBfMAd
RLU/mg protein
10^6
10^5
10^4
Lung
Liver
EGF+
EGF+
B
ratio lung/liver
12
10
8
6
4
2
0
*, P=0.01
EGF-
EGF+

Title: A Mosaic Fiber Adenovirus Serotype 5 Vector Containing Reovirus σ1 and Adenovirus Serotype 3 Knob Fibers Increases Transduction in an Ovarian Cancer Ex Vivo System via a CAR-Independent Pathway

Authors: Yuko Tsuruta, [1] Larisa Pereboeva, [1,2] Joel N. Glasgow, [1,2,3] Daniel T. Rein, [1,6] Yosuke Kawakami, [1] Ronald D. Alvarez, [2,4] Rodney P. Rocconi, [4] Gene P. Siegal, [2,5] Paul Dent [7], Paul B. Fisher, [8] and David T. Curiel [1,2]

Author's affiliations: [1] Division of Human Gene Therapy, Departments of Medicine, Obstetrics and Gynecology, Pathology, Surgery, [2] UAB Gene Therapy Center, [3] Division of Cardiovascular Disease, [4] Department of Obstetrics and Gynecology, [5] Departments of Pathology, Cell Biology and Surgery, The University of Alabama at Birmingham, Birmingham, AL; [6] Department of Obstetrics and Gynecology, University of Düsseldorf Medical Center, Düsseldorf, Germany; [7] Department of Biochemistry, Massey Cancer Center, Virginia Commonwealth University, Richmond, VA; and [8] Departments of Pathology, Neurosurgery and Urology, Herbert Irving Comprehensive Cancer Center, Columbia University Medical Center, College of Physicians and Surgeons, New York, NY

Grant support: This work was supported by the following grants from the National Institute of Health: CA35675, CA97318, CA104177, and CA83821; DOD grant W81XWH-05-1-0035, and the Waxman Foundation for Cancer Research.

Request for reprints: Dr. David T. Curiel, Division of Human Gene Therapy, Departments of Medicine, Obstetrics and Gynecology, Pathology, and Surgery, and The Gene Therapy Center, The University of Alabama at Birmingham, 901 19th Street South, BMR2-508, Birmingham, AL, 35294-2172. Phone: (205) 934-8627; Fax: (205) 975-7476; E-Mail: curiel@uab.edu.

Running title: Enhanced infectivity of mosaic fiber adenovirus in ovarian cancer

Key words: ovarian cancer; adenovirus; reovirus; σ1 spike protein; tumor tissue slice

Abstract

Purpose: Adenovirus serotype 5 (Ad5) has been used for gene therapy with limited success due to insufficient infectivity in cells with low expression of the primary receptor, the coxsackie and adenovirus receptor (CAR). Evidence that Ad serotype receptors other than CAR may be of use was presented in previous studies that showed the Ad3 receptor is expressed at high levels in ovarian cancer cells. We hypothesized that combined use of unique chimeric fibers in the context of novel mosaic Ad vectors would enhance infectivity via non-CAR pathways in ovarian cancer cells.

Experimental Design: We constructed and characterized Ad5 vectors that utilize Ad3 knob and reovirus fibers to generate a fiber mosaic virion. Serotype 3 Dearing reovirus utilizes a fiber-like σ1 protein to infect cells expressing sialic acid and junction adhesion molecule 1 (JAM1). We, therefore, constructed a fiber mosaic Ad5 vector, designated Ad5/3-σ1, encoding two fibers: A σ1 chimeric fiber, and the chimeric Ad5/3 fiber composed of an Ad3 knob.

Results: Functionally, Ad5/3-σ1 utilized sialic acid, JAM1, and Ad3 receptor for cell transduction and achieved maximum infectivity enhancement in ovarian cancer cells with low CAR expression. Furthermore, Ad5/3-σ1 achieved infectivity enhancement in primary tissue slices of human ovarian tumor.

Conclusions: We have developed a new type of Ad5 vector with the novel tropism, possessing fibers from Ad3 and reovirus, that exhibits enhanced infectivity via CAR independent pathway(s). In addition, the flexible genetic platform of vector allows different combination of fiber variants that can be incorporated within the same particle.

Introduction

Ovarian cancer is the most fatal gynecologic malignancy in the United States, and its incidence is reported to be increasing (1). Poor prognosis is associated with delayed diagnosis until advanced stage. Five-year survival rates in patients diagnosed with advanced stage disease continue to be less than 30 % despite aggressive surgical debulking and chemotherapy. Cancer gene therapy has been widely investigated in the last decade as one of the new approaches for ovarian cancer. Adenoviral vectors, in particular vectors based on human serotype 5 (Ad5), have shown a great applicability in preclinical evaluations (2). Despite exciting preclinical data, adenoviral gene therapy approaches have yet to display significant clinical benefit. Although, limited treatment-related toxicities of this vector have been demonstrated in completed phase I gene therapy trials for ovarian cancer patients, the therapeutic efficacy of these protocols was not satisfactory (3). In general, poor therapeutic results have been attributed in large part to insufficient transduction of tumor cells. Human tumor cells frequently express little to none of the primary Ad receptor, coxsackie and adenovirus receptor (CAR) (4, 5). This CAR deficiency renders many tumor cells resistant to Ad infection, undermining cancer gene therapy strategies that require efficient tumor cell transduction. To address this issue, strategies are being developed that aim at modifying the Ad vector tropism to achieve CAR-independent transduction.

Genetic capsid modification has rationally focused on the fiber knob domain, which is the primary determinant of Ad tropism, to achieve CAR-independent cell entry. We previously demonstrated that a fiber mosaic Ad5 vector provided viral entry via two different pathways, resulting in an additive gain in infectivity in a variety of transformed

cells, including ovarian cancer cells (6). We derived a fiber mosaic Ad5 vector that incorporates two distinct fibers: the Ad5 fiber and a chimeric reovirus fiber (6). The chimeric reovirus fiber includes the fiber-like σ1 protein, which is a receptor-binding molecule of serotype 3 Dearing (T3D) reovirus. The σ1 protein has been reported to utilize the coreceptors JAM1 and sialic acid for cellular binding (7, 8). These receptors are clearly distinct from the Ad5 receptor and together determine T3D reovirus tropism. Of note, this fiber mosaic modification greatly enhanced vector infectivity in cancer cells compared to the wild-type Ad5 fiber. To further increase infectivity of the fiber mosaic Ad5 vector, and to gain more specific infectivity for ovarian cancer, we replaced the Ad5 wild-type fiber gene in a tandem-fiber cassette with the gene for a chimeric Ad5/3 fiber. The Ad5/3 fiber contains the tail and shaft domains of Ad serotype5 and the knob domain of serotype 3. It has been suggested that the Ad3 receptor is expressed at high levels in ovarian cancer cells. Ad5 vectors, that express a chimeric fiber consisting of the Ad serotype 3 knob domain (Ad5/3) have been shown to significantly increase infectivity in ovarian cancer cells. Thus, we engaged in the construction and characterization of Ad5 vectors that were mosaics Ad3 knob and reovirus fibers. The goal being a newly developed fiber mosaic Ad vector, which could bind to ovarian cancer cells using the Ad3 receptor, JAM1, and sialic acid cell receptors, thus establishing a novel strategy to achieve infectivity enhancement based on a CAR-independent tropism.

A noteworthy aspect of our fiber mosaic strategy is the flexibility whereby different combinations of fiber variants can be incorporated within the same particle. On this basis, fiber mosaic virions can be proposed which embody ever greater potential for enhancement of vector infectivity.

To evaluate the efficacy of the newly established Ad vector, we introduced a thin-slice tumor model technique that has been evaluated in our group. In this regard, Kirby et al. has clarified that the thin-slice tumor model system represents a stringent method of *ex vivo* evaluation of novel adenoviral vectors (9). For this technique, the Krumdieck tissue slicer is a novel instrument, which was introduced in 1980s to cut precise tissue slices from an organ of interest (10). Tissue slices thus obtained including those of human derivation are capable of maintaining their original *in vivo* structure and composition. The study provided a means for rigorous preclinical analysis of adenovirus-based replication on patient tumors. We explored the infectivity efficacy of our newly developed mosaic fiber Ad vector utilizing this established technique for preclinical evaluation, thus providing a powerful tool to determine the therapeutic index for clinical translation.

Materials and Methods

Cell lines. The 293 cells were purchased from Microbix (Toronto, Ontario, Canada). Human ovarian cancer cell lines ES-2 and OV-3 were obtained from the American Type Culture Collection (ATCC, Manassas, VA). Human ovarian adenocarcinoma cell lines OV-4 and Hey were a kind gift from Dr. Timothy J. Eberlein (Harvard Medical School, Boston, MA) and Dr. Judy Wolf (M.D. Anderson Cancer Center, Houston, TX), respectively. L929 cells were maintained as described previously (8). All other cell lines were cultured in media recommended by suppliers (Mediatech, Herndon, VA and Irvine Scientific, Santa Ana, CA). FBS was purchased from Hyclone (Logan, UT). All cells were grown at 37°C in a humidified atmosphere of 5% CO_2.

Generation of the σ1 chimeric fiber construct. A schematic of the σ1 chimeric fiber structure is shown in Figure 1A. To design the σ1 chimeric fiber, the fiber tail domain of Ad5 was fused in its whole length to the entire σ1 coding region in frame with a carboxy-terminally encoded 6-histidine (6-His) sequence, resulting in F5S1H as described previously (6).

Generation of shuttle plasmids for the fiber mosaic Ad5 genome. We previously created a shuttle vector, pNEB.PK.FSPF5S1/F5, which contained tandem fiber genes for the σ1 chimeric fiber, F5S1H and the wild-type Ad5 fiber (6). The current shuttle vector was based on pNEB.PK.FSPF5S1/F5. We replaced the Ad5 knob sequence of the wild-type Ad5 fiber with the Ad3 knob coding sequence in frame, resulting in pNEBσ5/3. Technically, a fiber shuttle vector, pNEB.PK.F5/3 (11), containing an Ad5 tail, Ad5

shaft, and an Ad3 knob was utilized to extract the coding sequence of the Ad3 knob with *Nhe*I-*Mun*I-digestion. Another shuttle vector, pNEB.PK.FSPF5S1/F5, was digested with *Nhe*I and *Mun*I for removal of the Ad5 knob sequence. A *Nhe*I /*Mun*I fragment containing the coding sequence of the Ad3 knob from pNEB.PK.F5/3 was cloned into the *Nhe*I-*Mun*I-digested pNEB.PK.FSPF5S1/F5, resulting in pNEBσ5/3, containing the σ1 chimeric fiber, F5S1H, and the chimeric Ad5/3 fiber genes in tandem.

Generation of recombinant Ad. A schematic of the viruses used in this study is shown in Fig.1B. Recombinant Ad5 genomes containing the tandem fiber genes were derived by homologous recombination in *E. coli* BJ5183 with *Swa*I-linearized rescue plasmid pVK700 and the *Pac*I and *Kpn*I-fragment of pNEBσ5/3 containing tandem fibers, essentially as described previously (12). The recombinant region of the genomic clones was sequenced prior to transfection into 293 cells. All vectors were propagated in 293 cells and purified using a standard protocol (13). The resultant fiber mosaic virus was Ad5/3-σ1. Viral particle (v.p.) concentration was determined by the OD_{260} method as described by Maizel, et al. (14). The infectious titer was determined according to the AdEasy Vector System (Qbiogene, Inc. Carlsbad, CA).

PCR amplification of viral genome fragments. Viral DNA was amplified using the Taq PCR Core Kit (Qiagen Inc., Valencia, CA). The sequences of the primers were as follows: Ad5tail-sense 5'-ATGAAGCGCGCAAGACCGTCTGAAGAT; Ad3knob-antisense 5'-GTCATCTTCTCTAATATAGGAAAAGGTAAATGGGG; and σ1head-antisense 5'-ATTCTTGCGTGA AACTACGCGG.

Protein electrophoresis and Western blotting. To detect the incorporation and the trimerization of fibers in virus particles, Ad vectors equal to 1.0×10^{10} to 1.0×10^{11} v.p. were resolved by SDS-PAGE and Western blotting as described previously (15).

Recombinant proteins. The fiber-knob domains of Ad5 and Ad3 fibers were produced and purified as described previously (11). The protein concentrations in all experiments were determined by the Bradford method (Bio-Rad Laboratories, Hercules, CA).

In Vitro Gene Transfer Assays. Cells were infected with viruses at 37°C for 1 hour and unbound virus was washed away. A luciferase assay was performed 24 hours later (Promega, Madison, WI) according to the manufacturer's instructions. Data are presented as mean values ± standard deviation.

Competitive inhibition assay. Recombinant Ad3 fiber knob proteins or anti-JAM1 polyclonal antibody (c-15, Santa Cruz Biotechnology, Inc., Santa Cruz, CA) were incubated with the cells at 37ºC for 15 minutes prior to infection. Alternatively, cells were treated with 333 milliunits/ml of *Clostridium perfringens* neuraminidase type X (Sigma-Aldrich Co, St. Louis, MO) at 37°C for 30 minutes to remove cell-surface sialic acid, followed by two washes with PBS. Cells were then exposed to viruses at 37°C for 1 hour. Unbound virus and blocking agents were washed away. After 24 hours of incubation at 37°C, the cells were processed for performance a luciferase assay, as previously described. Subsequent procedures were the same as described previously. Data are presented as mean values ± standard deviation.

Precision-cut human ovarian tumor slices.

Following institutional review board approval, primary human ovarian tumors were obtained from newly diagnosed ovarian cancer patients who underwent debulking surgery as primary treatment. The ovarian tumor was kept in RPMI medium supplemented with 10% FBS, 2mM L-glutamine, 100 U penicillin/ml, and 100 µg/ml streptomycin on ice until dissection. Precision-cut ovarian tumor slices (diameter 8 mm, thickness 150 µm) were prepared using a Krumdiek Tissue Slicer (Alabama Research and Development, Munford, AL) (9). Sequential slices were transferred into 6-well plates containing 2 ml of complete culture medium and placed on a rocker plate. These tumor slices were maintained at 37°C in a 5% CO_2 environment on the rocker plate and allowed to preincubate for 2 hours before treatment. The ovarian tumor slices were then infected with 100 vp/cell of each virus at 37°C for 1 hour on the rocker plate, after which unbound viruses were washed away. The tumor slices were processed for a luciferase assay after 24 hours of incubation at 37°C, as described previously (16).

Results

Construction of fiber mosaic viruses. To create a chimeric fiber structurally compatible with Ad5 capsid incorporation, the σ1 chimeric fiber (F5S1H) was designed to comprise the amino-terminal tail segment of the Ad5 fiber sequence genetically fused to the entire T3D σ1 protein, and a carboxy-terminal 6-His tag was included as a detection marker (Fig.1A) (6). Our previous fiber mosaic virus (Ad5-σ1) contained tandem fiber genes, wherein the F5S1H σ1 chimeric fiber was positioned in front of the Ad5 wild type fiber gene. We replaced the Ad5 wild type fiber gene of the tandem-fiber cassette with the genome of the chimeric Ad5/3 fiber containing the tail and shaft domains of Ad serotype5 and the knob domain of serotype 3 (11). Our current tandem-fiber cassette contained tandem fiber genes, wherein the F5S1H σ1 chimeric fiber was positioned in front of the chimeric Ad5/3 fiber gene in the L5 region of the Ad5 genome (Fig.1B). In this configuration, each fiber was positioned before the untranslated sequences of the wild-type fiber to provide equal transcription, splicing, polyadenylation, and regulation by the major late promoter. We constructed E1-deleted recombinant Ad genomes (Ad5/3-σ1) containing the σ1 chimeric fiber (F5S1H), the chimeric Ad5/3 fiber, and a firefly luciferase reporter gene controlled by the CMV immediate early promoter/enhancer. Following virus rescue and large scale propagation in 293 cells, we obtained Ad5/3-σ1 vector at concentrations of 6.48×10^{12} v.p. per ml. These concentrations compared favorably with that of Ad5Luc1 at 3.74×10^{12} v.p. per ml, Ad5/3Luc1 at 8.7×10^{11} v.p. per ml, and Ad5-σ1 vector at 5.31×10^{12} v.p. per ml. In addition, the v.p. per Plaque Forming Unit (PFU) ratios determined for Ad5/3-σ1, Ad5Luc1, Ad5/3Luc1, and Ad5-σ1 were 13.8, 13.3, 2.76, and 22, respectively, indicating

excellent virion integrity for both species. Of note, the control vectors used throughout this study, Ad5Luc1 and Ad5/3Luc1 each contained one fiber and are isogenic to Ad5/3-σ1 in all respects except for the fiber locus.

Definition of fiber gene configurations for fiber mosaic Ad. We confirmed the fiber genotype of Ad5/3-σ1 via diagnostic PCR, using the σ1 chimeric fiber or the chimeric Ad5/3 fiber primer pairs and genomes from purified virions as PCR templates (Fig. 2A). To confirm that Ad5/3-σ1 virions contained both trimerized fibers, we performed SDS-PAGE followed by Western blot analysis on viral particles. The 4D2 anti-Ad5 fiber tail monoclonal antibody (Neomarkers, Fremont, CA) was used and fiber bands were observed at approximately 180 kDa for unboiled samples of Ad5Luc1, Ad5/3Luc1, and Ad5/3-σ1 virions, corresponding to fiber trimers (Fig. 2B, lanes 1, 3 and 5). In boiled samples, the 4D2 antibody detected bands of apparent molecular mass of approximately 60 kDa, indicative of fiber monomers (lanes 2, 4 and 6). The fiber mosaic viruses were difficult to resolve by Western blotting, due to the near-identical sizes of the σ1 chimeric and the chimeric Ad5/3 fiber proteins.

To confirm the presence of the σ1 chimeric fiber protein in virions, we used the anti-Penta His monoclonal antibody (QIAGEN Inc.) which recognizes 6-His tags (Fig. 3C). Fiber bands corresponding to both trimeric and monomeric σ1 chimeric fiber protein were observed using the anti-Penta His antibody. (Fig. 3C, lanes 1 and 2). These results confirm that the trimeric F5S1H σ1 chimeric fiber was incorporated into Ad5/3-σ1 virions.

The Ad5/3-σ1 vector exhibits sialic acid-, JAM1-, and Ad3 receptor-dependent tropism. Our hypothesis was that inclusion of both the σ1 chimeric fiber (F5S1H) and the chimeric Ad5/3 fiber into an Ad5 vector would enhance infectivity of Ad-refractory cell types via expanding the vector tropism. To test the Ad5/3-σ1 tropism, we performed neuraminidase treatment to remove cell-surface sialic acid, and performed competitive blocking experiments using an anti-JAM1 antibody or recombinant Ad3 knob protein. Ad5/3Luc1 was used as a positive control for the chimeric Ad5/3 fiber function. For this analysis, we used the low CAR expressing human ovarian cancer cell line, Hey, due to its high sialic acid, JAM1, and Ad3 receptor expression (6). Transduction with Ad5/3-σ1 was inhibited 12% using the anti-JAM1 antibody, which increased to 25% when combined with neuraminidase (Fig. 3A). Combined treatment with neuraminidase, anti-JAM1 antibody, and the Ad3 knob protein reduced transduction by 78%, compared to controls receiving no blocking agent (Fig. 3A). Together, these data confirm that the Ad5/3-σ1 vector utilizes sialic acid, the JAM1 binding domain of the σ1 chimeric fiber (F5S1H), and the Ad3 receptor binding domain of the chimeric Ad5/3 fiber for cell transduction. These findings indicate that Ad5/3-σ1 created *sialic acid-, JAM1-, and Ad3 receptor-dependent* tropism, confirming the functionality of the σ1 chimeric fiber (F5S1H) and the chimeric Ad5/3 fiber in our fiber mosaic Ad5.

Ad5/3-σ1 vector exhibits increased transduction of CAR-deficient cells. To determine the contribution of the σ1 chimeric fiber to the expanded Ad tropism, we evaluated Ad5/3-σ1 infectivity in L929 murine fibroblast cells that are commonly used for propagating reovirus. L929 cells express both the sialic acid and JAM1 σ1 receptors but

no detectable CAR. As expected, Ad5/3-σ1 resulted in the maximum increase level of gene transfer (57-fold), relative to both Ad5Luc1 and Ad5/3Luc1 in L929 cells (Fig. 3B).

Ad5/3-σ1 vector exhibits increased transduction of low-CAR ovarian cancer cells. In our previous study, we confirmed that the Hey, OV-4, ES-2, and OV-3 ovarian cancer cell lines were sialic acid/JAM1-positive but low-CAR (6). Ad5/3-σ1 results in a 33-fold (OV-3) to 62-fold (Hey) increase in luciferase activity compared to Ad5Luc1. Luciferase activities were also enhanced in OV-4 (1.74-fold) and OV-3 (3.43-fold) cells using Ad5/3-σ1, compared to Ad5/3Luc1 (Fig. 4A). Many clinically relevant tissues are refractory to Ad infection, including ovarian cancer cells, due to negligible CAR levels (17). To more closely model the clinical situation with the most stringent substrate, we analyzed Ad5/3-σ1 transduction of primary human ovarian carcinoma cells. Importantly, Ad5/3-σ1 increased gene transfer to precision cut ovarian cancer tissue slices from 1.7- to 59-fold versus Ad5Luc1 (Fig. 4B). Herein, we have outlined the construction, rescue, purification, and initial tropism characterization of a novel vector containing a non-Ad fiber molecule. Our results show that in low-CAR cells, Ad5/3-σ1 provides novel tropism and results in increased gene transfer rates, compared to wild-type Ad5. This is accomplished using the reovirus coreceptors JAM1 and sialic acid, in combination with the Ad3 receptor. The novel tropism of this vector represents a crucial attribute for Ad-based gene therapy vectors.

Discussion

One of the major strategies to enhance the therapeutic potential of Ad5-based cancer gene therapy has been to engineer novel adenoviral vector systems which alter the tropism of adenoviruses away towards receptors that are more abundant than its primary receptor, CAR, on the surface of primary tumor cells. Variable, but usually low expression of CAR has been documented in many cancer cell types, including glioma, rhabdomyosarcoma, and ovarian cancer (18-20). We have reported that a fiber mosaic Ad5 vector strategy allowed viral entry via two different pathways with additive gains in infectivity in a variety of cell types (6). In this study, we evaluated the use of a fiber mosaic Ad5 vector that utilizes both the Ad3 (Ad5/3) and reovirus receptors, which are independent of coventional Ad5 tropism. This vector was based on the previously reported fiber mosaic Ad5 vector that incorporates two distinct fibers: the Ad5 fiber and a chimeric reovirus fiber. The current fiber mosaic Ad5 vector was generated by substituting the Ad3 knob in place of the Ad5 knob domain. We constructed an Ad5 genome utilizing a tandem fiber cassette, which resulted in an Ad5 vector that expressed both the Ad5/3 fiber and the σ1 chimeric fiber. We confirmed that the fiber mosaic Ad5 virions incorporated both fibers by Western Blot analysis and by the functional ability of both fibers to utilize the appropriate receptor(s) for viral transduction. This is the first vector which contains non-CAR binding fibers from two different virus families to replace Ad5 tropism.

We further confirmed that the addition of the σ1 chimeric fiber contributed to augmentation of gene transfer compared to Ad vectors with single fiber in cells lacking the Ad5 and Ad3 receptors. Ad5/3-σ1 provided a 57-fold increase in gene transfer

relative to both the wild-type fiber control virus, the Ad5Luc1 and the single Ad5/3 fiber control virus, Ad5/3Luc1, in L929 cells that lack Ad5 and Ad3 receptor expression.

Consistent with our hypothesis of enhanced infectivity, we observed augmented gene transfer with Ad5/3-σ1 in all ovarian cancer cell lines tested, ranging from 33-fold to 62-fold, when compared to the wild-type fiber control virus, Ad5Luc1. However, compared to the single Ad5/3 fiber control virus, Ad5/3Luc1, augmented gene transfer on the same cell lines was modest ranging from 1.74-fold to 3.43-fold.

Importantly, the enhanced infectivity of the Ad5/3-σ1 virus was observed on more stringent clinical substrates, human primary ovarian tumor tissue slices, although the augmentation of gene transfer was variable. The thin-sliced tissue culture is an ideal method for preclinical *ex vivo* infectivity analysis because it allows evaluation of adenoviruses in primary tumors derived from cancer patients (9). Consistent with our hypothesis of enhanced infectivity, we observed augmented gene transfer with Ad5/3-σ1 in all patient tumor slices tested, ranging from 1.7-fold to 59-fold. This augmentation was variable, and often occurred in tumor slices with supposedly diverse receptor expression profiles. We believe this variation is due to variable receptor expression between tumor slices. Clearly it would be of interest to directly correlate receptor expression with the degree of infectivity in clinical specimens. Unfortunately, this was not possible with the samples studied here, because the whole tumor specimen was necessary for analysis of infectivity enhancement. However, we have demonstrated a good correlation between primary receptor density, infectivity and oncolysis in our previous *in vitro/ vivo* studies using cell lines (18, 21-25).

There are two possible explanations for the modest level of Ad5/3-σ1 gene transfer compared to the single Ad5/3 fiber control virus, Ad5/3Luc1. At first it may be due to reduced levels of the σ1 chimeric fiber incorporation compared to the chimeric Ad5/3 fiber in fiber mosaic Ad5 particles. We previously confirmed that both 4D2 anti-Ad5-tail antibody and 6-His antibody could detect fibers with similar band intensity in Western blot when equal numbers of virus particles were loaded. Figure 2B and 2C showed the presence of both fibers on Ad5/3-σ1. However, to detect the σ1 chimeric fiber in our fiber mosaic Ad5 vector using 6-His antibody, we had to load ten times the number of virus particles compared to the chimeric Ad5/3 fiber as detected by using 4D2 anti-Ad5-tail antibody. This result suggests that incorporation of the σ1 chimeric fiber is insufficient compared to that of the chimeric Ad5/3 fiber on Ad5/3-σ1. This would explain the limited additivity of transductional efficiency by the σ1 chimeric fiber in ovarian cancer cells. Another explanation is that the Ad3 receptor in ovarian cancer was generally expressed at higher levels, and most of the cells infected with fiber mosaic Ad5/3-σ1 were able to accomplish this via the A5/3 fiber (18). Even when JAM1 or sialic acid is expressed on ovarian cancer cells, the binding may be negligible since the σ1 chimeric fiber was incorporated less efficiently in the fiber mosaic Ad5/3-σ1 as described above. Because the Ad3 receptor is widely expressed on ovarian cancer cell surfaces of epithelial origin, the σ1 chimeric fiber could have played a minimum role in the increased transductional efficiency, compared to control virus with Ad5/3 fiber, Ad5/3Luc1, infection.

Thus, we have used the “fiber mosaicism” concept, the use of two separate fibers with distinct receptor recognition, to combine the use of multiple receptors to enhance viral

infectivity (6). In this study, the mosaic fiber Ad5/3-σ1 vector provided enhanced infectivity in low-CAR expressing ovarian cancer cell lines. This was the result of multiple non-CAR receptor binding properties provided by the fiber elements of different virus families. Ad gene therapy vectors with CAR-independent tropism may prove valuable for maximal transduction of low-CAR expressing tumors using minimal vector doses. Furthermore, this study utilized a preclinical assay that involved primary human ovarian tumor tissue to evaluate the fiber mosaic Ad vectors and proved further evidence of a preclinical screening strategy for examining improved gene therapy agents.

Acknowledgments

We thank Dr. Victor Krasnykh for providing plasmids pVK700, pNEB.PK.F5/3, and pNEB.PK.3.6. We also thank Dr. Justin C. Roth for his critical reading of the manuscript.

References

1. Greenlee RT, Hill-Harmon MB, Murray T, Thun M. Cancer statistics, 2001. CA Cancer J Clin 2001;51: 15-36.
2. Gomez-Navarro J, Curiel DT, Douglas JT. Gene therapy for cancer. Eur J Cancer 1999;35: 867-85.
3. Vorburger SA, Hunt KK. Adenoviral gene therapy. Oncologist 2002;7: 46-59.
4. Krasnykh V, Dmitriev I, Navarro JG, *et al.* Advanced generation adenoviral vectors possess augmented gene transfer efficiency based upon coxsackie adenovirus receptor-independent cellular entry capacity. Cancer Res 2000;60: 6784-7.
5. Glasgow JN, Bauerschmitz GJ, Curiel DT, Hemminski A. Transductional and transcriptional targeting of adenovirus for clinical applications. Current Gene Therapy 2004;4: 1-14.
6. Tsuruta Y, Pereboeva L, Glasgow JN, *et al.* Reovirus sigma1 fiber incorporated into adenovirus serotype 5 enhances infectivity via a CAR-independent pathway. Biochem Biophys Res Commun 2005;335: 205-14.
7. Barton ES, Forrest JC, Connolly JL, *et al.* Junction adhesion molecule is a receptor for reovirus. Cell 2001;104: 441-51.
8. Chappell JD, Gunn VL, Wetzel JD, Baer GS, Dermody TS. Mutations in type 3 reovirus that determine binding to sialic acid are contained in the fibrous tail domain of viral attachment protein sigma1. J Virol 1997;71: 1834-41.
9. Kirby TO, Rivera A, Rein D, *et al.* A novel ex vivo model system for evaluation of conditionally replicative adenoviruses therapeutic efficacy and toxicity. Clin Cancer Res 2004;10: 8697-703.
10. Krumdieck CL, dos Santos JE, Ho KJ. A new instrument for the rapid preparation of tissue slices. Anal Biochem 1980;104: 118-23.
11. Krasnykh VN, Mikheeva GV, Douglas JT, Curiel DT. Generation of recombinant adenovirus vectors with modified fibers for altering viral tropism. J Virol 1996;70: 6839-46.
12. Belousova N, Krendelchtchikova V, Curiel DT, Krasnykh V. Modulation of adenovirus vector tropism via incorporation of polypeptide ligands into the fiber protein. J Virol 2002;76: 8621-31.
13. Graham F, Prevec L. Manipulation of adenovirus vectors. In: Murray EJ, Walker JM, editors. Methods in molecular biology. Clifton, N.J.: Humana Press; 1991. p. 109-28.
14. Maizel JV, Jr., White DO, Scharff MD. The polypeptides of adenovirus. I. Evidence for multiple protein components in the virion and a comparison of types 2, 7A, and 12. Virology 1968;36: 115-25.
15. Pereboeva L, Komarova S, Mahasreshti PJ, Curiel DT. Fiber-mosaic adenovirus as a novel approach to design genetically modified adenoviral vectors. Virus Research 2004;105: 35-46.
16. Breidenbach M, Rein DT, Schondorf T, *et al.* A new targeting approach for breast cancer gene therapy using the Heparanase promoter. Cancer Lett 2005.

17. Kelly FJ, Miller CR, Buchsbaum DJ, *et al.* Selectivity of TAG-72-targeted adenovirus gene transfer to primary ovarian carcinoma cells versus autologous mesothelial cells in vitro. Clin Cancer Res 2000;6: 4323-33.
18. Kanerva A, Mikheeva GV, Krasnykh V, *et al.* Targeting adenovirus to the serotype 3 receptor increases gene transfer efficiency to ovarian cancer cells. Clin Cancer Res 2002;8: 275-80.
19. Kim M, Sumerel LA, Belousova N, *et al.* The coxsackievirus and adenovirus receptor acts as a tumour suppressor in malignant glioma cells. Br J Cancer 2003;88: 1411-6.
20. Cripe TP, Dunphy EJ, Holub AD, *et al.* Fiber knob modifications overcome low, heterogeneous expression of the coxsackievirus-adenovirus receptor that limits adenovirus gene transfer and oncolysis for human rhabdomyosarcoma cells. Cancer Res 2001;61: 2953-60.
21. Yamamoto M, Davydova J, Wang M, *et al.* Infectivity enhanced, cyclooxygenase-2 promoter-based conditionally replicative adenovirus for pancreatic cancer. Gastroenterology 2003;125: 1203-18.
22. Kanerva A, Zinn KR, Chaudhuri TR, *et al.* Enhanced therapeutic efficacy for ovarian cancer with a serotype 3 receptor-targeted oncolytic adenovirus. Mol Ther 2003;8: 449-58.
23. Kanerva A, Wang M, Bauerschmitz GJ, *et al.* Gene transfer to ovarian cancer versus normal tissues with fiber-modified adenoviruses. Mol Ther 2002;5: 695-704.
24. Douglas JT, Kim M, Sumerel LA, Carey DE, Curiel DT. Efficient oncolysis by a replicating adenovirus (ad) in vivo is critically dependent on tumor expression of primary ad receptors. Cancer Res 2001;61: 813-7.
25. Hemminki A, Dmitriev I, Liu B, Desmond RA, Alemany R, Curiel DT. Targeting oncolytic adenoviral agents to the epidermal growth factor pathway with a secretory fusion molecule. Cancer Res 2001;61: 6377-81.

Figure Legends

Fig. 1. Schema of fiber mosa*ic Ad5 genomes.* (A) Key components of the σ1 chimeric fiber. In the σ1 chimeric fiber, the tail of Ad5 fiber is fused to the reovirus fiber protein σ1 and a six-histidine (6-His) tag is fused to the carboxy-terminus of the σ1 chimeric fiber through a linker (designated F5S1H). (B) Map of Ad5 genomes with fiber modification. In all vectors, the E1 region is replaced by CMV promoter/luciferase transgene cassette. Ad5/3-σ1 is a fiber mosaic vector that carries the σ1 chimeric fiber with a carboxy-terminal 6-His tag (F5S1H) as well as the chimeric Ad5/3 fiber. Ad5/3Luc1 is a control virus that carries the chimeric Ad5/3 fiber. Ad5-σ1 is a fiber mosaic vector that carries the σ1 chimeric fiber with a carboxy-terminal 6-His tag (F5S1H) as well as the wild-type Ad5 fiber. Ad5Luc1 is a control virus that carries the wild-type Ad5 fiber.

Fig. 2. *Analysis of fibers in rescued viral particles.* (A) Detection of fiber genes in the Ad genome. Rescued viral particles were analyzed with PCR, using pairs of the σ1 chimeric fiber primers or the chimeric Ad5/3 fiber primers. pNEBσ5/3 was used as a positive control for both fibers. Absence of a PCR template was designated as the "Control". (B)–(C) Western blot analysis of fiber proteins in purified virions. (B) A total of 1.0×10^{10} v.p. per lane of Ad5Luc1 with the wild-type Ad5 fiber (lane 1, 2), Ad5/3Luc1 with the chimeric Ad5/3 fiber (lane 3, 4) or Ad5/3-σ1 with dual fibers (lane 5, 6) were resuspended in Laemmli buffer prior to SDS-PAGE, electrotransfer, and detection with the 4D2 anti-Ad5 fiber tail antibody. The samples in lanes 2, 4 and 6 were

boiled (b), while lanes 1, 3 and 5 (unboiled (u)) contain proteins in their native trimeric configuration. (C) A total of 1.0×10^{11} v.p. per lane of Ad5/3-σ1 (lane 1, 2), and Ad5-σ1 (lane 3, 4) with dual fibers were probed with an anti-6-His antibody. Lane 1: unboiled Ad5/3-σ1 virions, lane 2: boiled Ad5/3-σ1 virions, lane 3: unboiled Ad5-σ1 virions, lane 4: boiled Ad5-σ1 virions, and lane 5: recombinant Ad5 knob with a 6-His tag as a positive antibody control.

Fig. 3. *Evaluation of the efficacy and receptor specificity of Ad5/3-σ1 mediated gene transfer*. (A) Analysis of Ad5/3-σ1 receptor usage in Hey cells. *C. perfringens* neuraminidase (NM), an anti-JAM1 antibody (JAM1 Ab), and recombinant Ad3 fiber knob protein (Ad3 knob) were employed to block Ad5/3-σ1 infection. Hey cells were either untreated or treated with 100 μg/ml anti-JAM1 antibody, both an anti-JAM1 and antibody 333 milliunits/ml neuraminidase, or combined reagents with neuraminidase, anti-JAM1 antibody and 50 μg/ml recombinant Ad3 fiber knob protein. Cells were incubated with 100 v.p./cell of Ad5/3Luc1 (gray bar) or Ad5/3-σ1 (black bar) and harvested 24 hours later for luciferase activity. All luciferase values were normalized against the activity of controls receiving no blocking treatment valued at 100%. Each data point is an average of four replicates. The error bars indicate standard deviation. (B) Mouse fibroblast cells (L929) were incubated with Ad5Luc1 (blank bar), Ad5-σ1 (dotted bar), Ad5/3Luc1 (gray bar) or Ad5/3-σ1 (black bar) at 10, 100, and 1000 v.p./cell. Luciferase activity was determined 24 hours post-infection and is expressed as relative light units (RLU). Each bar represents the mean of three experiments. The error bars indicate standard deviation.

Fig. 4. *Infectivity profiles of Ad5/3-σ1*. (A) Representative ovarian cancer cell lines, Hey, OV-4, ES-2, and OV-3 were infected with Ad5/3Luc1 (gray bar) and Ad5/3-σ1 (black bar) at 10 and 100 v.p./cell. Luciferase activity was measured 24 hours post-infection and is expressed as relative light units (RLU). Each bar represents the mean of three experiments plus the standard deviation. (B) Human tumor slices of ovarian cancer patient were infected with Ad5Luc1 (blank bar), Ad5-σ1 (dotted bar), Ad5/3Luc1 (gray bar) or Ad5/3-σ1 (black bar) at 100 v.p./cell. Luciferase activity was measured 24 hours post-infection and is expressed as RLU/mg protein. Each bar represents the mean of four experiments plus the standard deviation.

A novel conditionally replicating adenovirus combined with cisplatin enhanced antitumor efficacy on ovarian cancer *in vitro* and *in vivo*

Bei Zhang[1], Jiayin Liu[1*] Jinshun Pan[2], Zhen Hou[1], Suping Han[1], Gang Hu[2], Shuyi Wang[3], Zeng B. Zhu[4] and David T. Curiel[4]

[1]Department of Obstetric and gynecology, Affiliated Hospital of Nanjing Medical University, Nanjing 210029, China

[2]Department of Pharmacology, Nanjing Medical University, Nanjing 210029, China

[3]Departments of Medicine, University of Alabama at Birmingham, USA

[4]Division of Human Gene Therapy, Department of Medicine, Pathology, Surgery, OB/Gyn and the Gene Therapy Center, The University of Alabama at Birmingham, Birmingham, Alabama, USA.

*To whom correspondence should be addressed

*Correspondence author: jyliu@njmu.edu.cn

Fax number: 86-025-86863159

Tel number: 86-025-86862884

Abstract

Purpose：To investigate the combined effect of using a novel survivin promoter-based conditionally replicating adenovirus (CRAd-S.RGD) plus *cis*-diamminedichloroplatinum (cisplatin, CDDP) on ovarian cancer *in vitro* and *in vivo*. **Methods:** The viability of SKOV3 ovarian cancer cells was performed by using the MTT assay after infection with different doses of CRAd-S.RGD and CDDP. Specifically, 10 pfu/cell of CRAd-S.RGD, 10 μg/ml of CDDP and 10 pfu/cell of CRAd-S.RGD plus 10 μg/ml of CDDP were compared, respectively. Antitumor efficacy and survival curves were evaluated after treatment with CRAd-S.RGD (i.t. 10^8 pfu /d, days 1-5), CDDP (i.p. 4 mg/kg/d, days 1, 3, 5), combined treatment of CRAd-S.RGD plus CDDP, or a PBS control administered in subcutaneously in a SKOV-3 xenograft animal model. Apoptosis was determined by TUNNEL assay following the different treatments. **Results:** *In vitro*, the CRAd-S.RGD killed SKOV3 cells by oncolysis in a dose-dependent manner. *In vivo*, superior tumor inhibition and animal survival rates were obtained with a synergistic effect seen using combined treatment with CRAd-S.RGD plus CDDP compared to single treatment with CRAd-S.RGD or CDDP. Apoptosis was also increased following combined treatment. **Conclusion:** The results clearly demonstrate that CRAd-S.RGD combined with CDDP synergistically increases the therapeutic efficacy. The same therapeutic efficacy could be obtained by using combined treatment with CRAd-S.RGD plus CDDP at two lower doses that minimize the drug toxicity to host tissues. This strategy is a potential therapeutic modality for treatment of ovarian cancer.

Introduction

Virotherapy represents an exciting and novel interventional strategy for range of neoplastic disorders, including ovarian cancer. In this strategy, a virus is rendered conditionally replicative in tumor cells whereby direct oncolytic target cell killing is achieved (1). A variety of viral species have been adapted as virotherapy agents with the majority of clinical trials to date exploiting conditionally replicating herpes simplex virus (HSV) and adenovirus (2,3). Of note, transition of promising virotherapy strategies from the bench-to-bed has proceeded with unpredictable speed. Unfortunately, therapeutic efficacy has been limited by poor infectivity, tumor cell specificity, and high host cell toxicity. The toxicity of adenoviral vectors is a key point in the field of gene therapy since these viruses localize to the liver when systemically administered (4). This could lead to severe or lethal liver dysfunction (5).

To minimize the toxicity of the therapeutic agents, one exciting modality is combined with two or three treatments in one patient to gain therapeutic efficiency and limit toxicity. Recently, Adusumilli *et al.*(6) reported that CDDP-induced GADD34 expression and selectively enhanced the tumor cell killing effect of the $\gamma_1$34.5-deficient oncolytic virus, NV1066. In their report the authors clearly demonstrated synergistic gains in oncolytic killing of human mesothelioma tumor targets via a combination of NV1066 plus CDDP. Lu et al.(7) described survivin as a therapeutic target for irradiation (IR) sensitization in lung cancer. The authors showed solid data that combined inhibition of survivin and irradiation resulted in significantly decreased lung cancer cell survival. The evidences that IR and CDDP will increase the activity of the survivin promoter in human glioma cell lines (8,9) and cervical cancer cell lines (Rein *et al.*, unpublished data) have been studied in Curiel's group. Recently, a study has also been exploited by Zhang *et al.* in which the IR and CDDP stimulated the activity of a survivin promoter in an adenovirus type 5 vector, reAdGL3BSurvivin, in

ovarian cancer cell lines and in primary ovarian cancer cells (manuscript has been submitted to Gynecology Oncology). The tumor cell killing effect of combined treatment with the survivin promoter-based CRAd and chemotherapy, however, has not been exploited in ovarian cancer.

In this study, a novel CRAd agent, CRAd-S.RGD, was used for combined treatment with CDDP for ovarian cancer approach. CRAd-S.RGD is an adenoviral vector in which the E1 expression and viral replication are regulated with the survivin promoter and the viral infectivity is enhanced with a capsid modification, RGD. Combined treatment with the CRAd-S.RGD and CDDP resulted in the enhanced cell killing *in vitro*, retarded tumor growth, and increased animal survival rates in xenograft model. The synergistic effect of the combined treatment was observed as tumor growth inhibition 40 days post treatment. In addition, the percentage of apoptosic tumor cells was increased by the combined treatment. The results clearly demonstrate that CRAd-S.RGD combined with CDDP results in a synergistic increase in the therapeutic efficacy. Thus, the same therapeutic efficacy could be reached by combined treatment of both CRAd-S.RGD and CDDP at lower doses that minimize toxicity to host tissues. This could be a potential therapeutic modality for treatment of ovarian cancer.

Materials and Methods

Cells, chemicals and animals

The human ovarian cancer SKOV3 cell line was purchased from Institute of Biochemistry and Cell Biology, Chinese Academy of Sciences (SIBS CAS, Shanghai, China). The cells were cultured in RPMI-1640 medium (GIBCO, Grand Island, NJ). Each medium was also supplemented with 10 % heat inactivated fetal calf serum (Hyclone, Logan, Utah), penicillin (100 iu/ml), streptomycin (100 μg/ml) (Sigma, St. Louis, Missouri). Cells were incubated at 37° C in a 5% CO_2 environment under humidified conditions. Cis-diamminedichloroplatinum (cisplatin, CDDP) was purchased from Sigma Chemical Co. (St. Louis, Missouri). The Balb/c nude mice (female, 6–8 weeks old) used in this study and were purchased from Shanghai SLAC Laboratory Animal Co. Ltd (Shanghai, China).

Recombinant Adenoviruses Two plamids, pShuttle-Scs/PA/S-S and pVK503c, were used in this study for constructing the CRAd-S.RGD vector. The pShuttle-Scs/PA/S-S was generated by Zhu *et al.* (10) and the Ad vector, pVK503c which contains both the E3 gene and a capsid modified RGD motif, was a kind gift from Dr. V. Krasnykh (M.D. Anderson, Houston, TX) (11). After cleavage with *Pme I*, the shuttle vectors were recombined with *Cla I* linerized pVK503c to generate a CRAd genome with a RGD-modified fiber. The resultant plasmid encoding the survivin promoter was linearized with *Pac I* and transfected into 911 cells using lipofectamine (Invitrogen, Carlsbad, CA). The viruses generated, then propagated in D65 cells (a glioma cell line in which survivin gene is over-expressed), and purified by double CsCl density gradient centrifugation, followed by dialysis against phosphate-buffered saline (PBS) containing 10% glycerol. The viruses were titrated by plaque assay in 293 cells, and v.p. number was determined spectrophotometrically based on absorbance at a wavelength of 260 nm. The viruses were stored at -80° C until use.

***In vitro* Analysis of Cytocidal Effects**

In vitro, the cytocidal effects of the CRAd-S.RGD were analyzed by determining the viability of the cells using the MTT assay after infection. Briefly, cells (5.0×10^3 cells per well) were plated on 96-well plates and the next day the cells were infected A) at multiplicities of infection (MOI) ranging from 0.01, 0.1, 1.0, 10 and 100 pfu/cell of CRAd-S.RGD in infection medium and B) for three groups: group A, infected with 10 pfu/cell of CRAd-S.RGD alone; group B, treated with 10 μg/ml of CDDP alone; group C, infected with 10 pfu/cell of CRAd-S.RGD for 3 h plus treated with 10 μg/ml of CDDP post 24 h-infection. Each point was performed as triplicate. Ten days later, the cell viability was determined using the MTT assay as described (12). Briefly, cells were stained with 20 μl sterile MTT dye (5mg/ml; Sigma, USA) at 37˚C for 4 h, then culture medium was removed and 150 μl of Me_2SO was added and thoughly mixed in for 10 min. Spectrometric absorbance at 570 nm was measured by using a microplate reader. The inhibitory rate on cell proliferation was evaluated using the following formula: Inhibitory rate = $(A_{control}–A_{sample})/(A_{control}-A_{blank})$ x 100%. $A_{control}$, absorption of cells without treatment; A_{sample}, absorption of cell treated with Ad agent, CDDP or Ad/CDDP; A_{blank}, absorption of medium.

***In vivo* studies**

Female athymic mice (Balb/c, 6–8 weeks old) were purchased from Shanghai SLAC Laboratory Animal Co. Ltd (Shanghai, China). SKOV3 cells were counted with a Coulter Counter and 97% of cells were viable. 0.3 ml (2.0×10^7 cells) of the cell suspension was injected subcutaneously into the right flank of the nude mice. On tumor volumes reaching 300-500 mm^3, the mice were randomly sorted into 4 groups (n = 12/group) as follow: 1) CRAd group, in which tumors were injected with 100μl CRAd (5×10^8 pfu/ml) of for 5 consecutive days (days 1–5); 2) CDDP group, in which CDDP (4 mg/kg/day) was administered by i.p. for three days (day 1, 3, 5); 3) combination treatment group, in which animals were used i.t. adminstrations of 100 μl CRAd (5×10^8 pfu) for 5 consecutive days

(days 1-5) and followed CDDP at dose of 4 mg/kg for every other day (day 7, 9, 11) by i.p.; 4) control group, in which the mice injected with PBS as same as group 1. All animals were observed daily throughout the study for food and water consumption, appearance and body condition. Tumor diameter and the general status of the animal were checked twice weekly. The tumor volume was measured using calipers, and calculated by the formula: $1/2xy^2$, where x is the longest distance and y the shortest distance of the tumor. The tumor volume was shown as mm^3. The animals were maintained to analyze survival.

Measurement of apoptosis

During the course of the study, 3 mice from each group were euthanized and the tumors were harvested (days 14 after the end of treatments). The tumor samples were embedded in paraffin blocks, and 4 μm sections were cut and stained with H&E. The apoptotic degree of the tumor tissues were detected using the Annexin V assay.(13) The tumor tissues were ground into cell suspensions, washed with PBS and stained with conjugated annexin-V and propidium iodide (PI) using the Annexin kit according to the manufacturer's protocol (PharMigen, Germany). Cells were determined by Flow cytometry (FACSCalibur, Becton Dickinson, Franklin Lakes, NJ) to be viable (annexin-V-negative and PI-negative), early apoptosis (annexin-V positive and PI-negative), or late apoptosis (annexin-V-positive and PI-positive). The cells was quantified as degree of apoptotic the annexin-V-positive cells. Data were analyzed with the ModFit LT program (Becton Dickinson).

Statistical analysis

Data were expressed as mean ± SD. from at least three different experiments. two way ANOVA was used to determine the statistical difference between various experimental groups. Cumulative survival rates were calculated with the Kaplan-Meier's method (14) and the differences were

evaluated with the log-rank test. $P < 0.05$ was considered to be statistically significant.

Results

The tumor killing effects of CRAd-S.RGD combined with CDDP in ovarian cancer cells

To determine the tumor cell killing effects of combined therapy on SKOV3 ovarian cancer cells, cell viability was assessed by MTT assay following treatment. The results showed that CRAd-S.RGD kills tumor cells in a dose-dependent manner (Figure.1A). After a 10 day infection, the SKOV3 cell viabilities were, 91.1 (± 7.7), 84.9 (± 4.9), 70.1 (± 5.9), 57.9 (± 6.8) and 30.4 (± 8.9) at MOI of 0.01, 0.1, 1.0, 10 and 100 pfu/cell, respectively, as shown in Figure 1A. In Figure 1B, SKOV3 cell viabilities were 61.8 % (± 5.3) and 66.8 % (± 5.6) after 10 day infection of CRAd-S.RGD at an MOI of 10 pfu/cell or treatment of 10 mg/ml of CDDP alone, respectively. However, the viable rate of SKOV3 cells dropped to 21.3 ± 4.9 % after infection of CRAd-S.RGD plus treatment with CDDP at same doses.

Antitumor efficacy of CRAd-Survivin-RGD combined with cisplatin *in vivo*

SKOV3 animal **x**enograft model was used to assess the therapeutic effects of combined CRAd-S.RGD and CDDP treatment. Tumor volumes were decreased in the three treated groups by a single treatment with either CRAd-S.RGD or CDDP, and combined treatment with CRAd-S.RGD plus CDDP. However, tumor volumes were increase by treatment with PBS in a control group. Compared to baseline tumor volumes at day 1, the average tumor volumes decreased to 54.8 % (443 ± 39 mm^3 at day 1 and 243 ± 35 mm^3) and 41.9% at day 28 (455 ± 67 mm^3 at day 1 and 191 ± 29 mm^3 at day 28) in the single therapy groups treated with either CRAd-S.RGD or CDDP, respectively ($P<0.05$). However, tumor volume dramatically shrank to 26.1 % of the baseline tumor volume (422 ± 63 mm^3 on day 1 and 110 ± 30 mm^3 on day 28) in combined therapy group treated with CRAd-S.RGD plus CDDP, compared to the baseline tumor volume at day one ($P<0.01$). Interestingly, the average tumor volume at day 44 returned to 98.4 % of the baseline tumor volume

(443 ± 39 mm^3 at day 1 and 436 ± 23 mm^3 at day 44) in the single therapy with CRAd-S.RGD, and 105.9 % (455 ± 67 mm^3 at day 1 and 482 ± 22 mm^3 at day 44) in the single therapy with CDDP ($P<0.05$). However, tumor volume dramatically shrank to 18.9 % of the baseline tumor volume at day 44 (422 ± 63 mm^3 on day 1 and 80.0 ± 35 mm^3 on day 44) in the group with CRAd-S.RGD plus CDDP combined therapy ($P<0.01$).

The mice in the combined treatment group had superior survival percentages compared to the mice in single therapy and in PBS control groups (Figure 2B). The 50% survival rates were 40, 50, and 60 days for PBS control group, CDDP and CRAd-S.RGD single treatment groups, respectively, while 70% of mice were still alive 100 days after combined treatment with CRAd-S.RGD plus CDDP ($P<0.01$). No differences in animal weight, behavior, and appearance were observed between single and combined treatment groups.

Analysis of apoptosis in tumor sections

Tumors collected at day 14 post-treatment documented the effect of combination therapy. Apoptosis was measured using an Annexin V based Apoptosis Detection Kit (PharMigen, Germany). Apoptosis was reported as the percentage of annexin stained cells among the total living cells. In Figure 3, the combined therapy group resulted in 42.7 ± 4.2 % apoptotic cells ($P<0.01$) at day 14 compared to 26.6 ± 7.9 % in CDDP and 23.2 ± 2.3 % in CRAd-S.RGD single therapy groups.

Discussion

Despite aggressive chemotherapy regimens after surgical resection, ovarian tumor recurrences are still common. Chemotherapy and radiation therapy is limited due to the inability to effectively treat metastatic lesions in the patients with ovarian cancer. Therefore, more effective strategies are warranted for ovarian cancer treatment. Gene therapy approaches using adenoviral vectors have received wide attention for treatment of human cancer (15). Specifically, oncolytic virotherapy using CRAd has been used in clinical trials (3). However, therapeutic effects were limited because of its poor infectivity, tumor specificity, and high toxicity. Many approaches have reported that the poor infectivity could be overcome by altering viral tropism to utilize CAR-independent pathways. In addition, the tumor specificity could be improved by incorporating a tumor specific promoter, such as the survivin promoter in this study. Further, the toxicity could be minimized by combined treatments to gain the therapeutic index and decrease the individual doses of treatment agents. In this study, we focused on combined treatment.

The tumor specific survivin promoter was used in this approach for driving the luciferase reporter gene in the AdGL3BSurvivin vector, described previously (16). Survivin is a novel member of the inhibitor of apoptosis (IAP) protein family (17), that play an important role in the survival of cancer cells and progression of malignancies (18). Survivin is selectively expressed in some of the most common human neoplasms including ovarian cancer (19), and is undetectable in most normal adult mouse tissue (20). Our previous reports showed that the survivin promoter is a promising tumor-specific promoter exhibiting a “tumor on” and “liver off” profile and has proven to be a good candidate for transcriptional targeting of cancer therapy in a wide variety of tumors, including ovarian cancer (16). As with previous reports (8,9), this group (Zhang et al.) has recently verified that the survivin promoter activity was stimulated by combined treatment with the survivin promoter

based AdGL3BSurvivin vector and cisplatin or radiation, in both ovarian cancer cell lines and primary cells (Submitted to Gynecology Oncology). Thus, the survivin promoter is a cisplatin and radiation responsive promoter in ovarian cancer cells. In this paper, we described the combined effect of using a conditionally replicative adenovirus, CRAd-S.RGD, with CDDP *in vitro* and *in vivo* for ovarian cancer therapy.

The CRAd-S.RGD is a replicative adenovirus vector in which the Ad E1 gene is driven by a tumor specific survivin promoter, resulting in the virus selectively replicating in tumor cells but not in normal host cells (21). This CRAd agent retained the adenovirus E3 gene for a tumor cell killing effect, and an RGD motif was incorporated into the Ad HI loop for enhancement of viral infectivity via a CAR-independent pathway (22). Compared to AdGL3BSurvivin, the CRAd-S.RGD vector is a replicating competent adenovirus and has the advantage to directly observe the therapeutic effects, including tumor cell killing and tumor growth inhibition, *in vitro* and *in vivo* by combined treatment with CDDP.

Cisplatin has been studied as a single agent and in combined regimens for ovarian cancer and is a first-line cytotoxic agent that is often used in therapy to treat platinum-sensitive ovarian cancer. Overall tumor response rates associated with platinum are relatively high and range from approximately 70-80% (23-25). However, 50-70% of responders will relapse within approximately 18 months after completing the first-line therapy and will require further systemic therapy (24). However, cisplatin is associated with several cumulative toxicities, including dose-dependent renal tubule toxicity and neurotoxicty (26). Therefore, a strategy for minimizing toxicity of cisplatin treatment is warranted.

Although the CRAd-S.RGD is a promising oncolytic virus for multiple tumor targeting (10), the current generation of virotherapy agents, including CRAd-S.RGD, have not been successfully applied in clinical trial because of its safety when administered via a systemic delivery route, specifically, lethal liver dysfunction (5). Alternatively, Khuri et al. applied conditionally replicative adenovirus in combination with cisplatin (27). Their study validated the concept of virotherapy/chemotherapy-combined therapy. In addition, the rationale was established to further explore combinations of conventional anti-tumor modalities which might operate synergistically with replicating viral agents. Further to this end, virotherapy has been combined with conventional anti-neoplastic modalities, including chemotherapy (28) and radiation therapy (29) with anecdotal reports of synergistic gains. On the other hand, many approaches of combined therapy have been frequently used in the clinic, and have been proved to be effective (30, 31).

In our study, CRAd-S.RGD killed SKOV3 tumor cells in a dose-dependant manner and cell killing was dramatically increased. Cell viability decreased to 21.3% by combined treatment with CRAd-S.RGD plus CDDP, compared to 61.8% and 66.8% by single treatment of either CRAd-S.RGD or CDDP alone *in vitro*, respectively. The same tumor inhibition and survival curve effects were observed in SKOV-3 xenograft mice. Tumor growth was inhibited by the combined treatment and the tumor volume shrank to 26.1% compared to pre-treatment at day 28 compared to 54.8% and 41.9% in single treatment of CRAd-S.RGD and CDDP, respectively. Interestingly, tumor growth was continually inhibited by the combined treatment and the tumor volume shrank to 18.9% compared to pre-treatment at day 44, but not in single treatment groups in which the tumor volumes returned to pre-treatment levels. Apoptotic analyses of tumor sections collected from the combined therapy group revealed obvious enhancement in the percentage of apoptosis, compared with tumors collected from mice treated with either agent alone. This data is similar to that described by

Geoerger *et al.* in which AdΔ24-P53 was associated with extensive cell lysis, apoptotic cell death, and fibrous fascicle in the tumor (32), however, is in conflict with data from Abou El Hassan *et al.* (33), which showed no evidence for the involvement of the p53-Bax apoptotic pathway in response to CRAd agents. Moreover, no significant body weight loss was observed in the combined treatment group. These results showed that CRAd-survivin-RGD combined with cisplatin had an improved oncolytic activity and no added toxicity.

When we apply two drug agents to a system, we can obtain either the same response as the sum of the two agents individually (additive), a greater response (synergistic) or a smaller resoponse (if one drug blocks the effects of the other). Synergy was examined in this study based on tumor inhibition rate using combined treatment divided that using single treatment method of Zhang (34). From data summarized in Table 1, the additive effect was observed from day 16 to day 36, due to the percentage from last column of table 1 less than 100% and bigger than tumor inhibition rate (%) from single treatment. The synergistic effect was observed from day 40 to day 44 due to the percentage from last column of table 1 less than tumor inhibition rate from single treatment. The additive effects of combined treatment were obtained at day 10 for Figure 1B and day 14 for Figure 3, respectively. The mechanisms of synergistic activity of the combination treatment are not clear, however, the possibilities, however, are as follows: 1) the antitumoral mechanism of each agent was independent in ovarian cancers and cross-resistance occurs between the viral therapy and chemotherapy; 2) cisplatin could improve viral replication; 3) CRAd-S.RGD augmented the antitumor activity of cisplatin. Of the possibilities, the most important to the current study is that cisplatin could improve viral replication. Previous studies from other groups indicated that survivin expression was increased during cisplatin treatment (35, 36). Our group also indicated that the survivin promoter is a cisplatin and radiation responsible in the context of the adenoviral vector.

The survivin promoter activity was increased with treatment of cisplain in glioma, ovarian cancer cell lines and in primary tumor cells (8, 9, Zhang *et al.*). Replication of the CRAd agent, CRAd-Survivin, is under the control of a tumor specific promoter, survivin, which is stimulated by the treatment of cisplatin. To explain the synergistic effect in this study, it is possible that cisplatin stimulates the activity of the survivin promoter, resulting in more E1 protein production that enhances viral replication of the CRAd agent. The E1 level is critical for viral replication, although, Hitt *et al.*(37) indicated that very low levels of E1 protein are sufficient for virus product in cultured cells, while wild-type Ad5 produces E1A protein in excess of that required.

Cisplatin not only increases the activity of the survivin promoter in the CRAd agent, but also increases endogenous survivin gene expression (35, 36), which reduces the activity of apoptosis and allows tumor resistance to cisplatin-induced apoptosis (38, 39). Thus, the synergistic effect described in this study is a sum of the effects of amplified viral replication and the decrease of the cisplatin-induced apoptosis. Synergistic tumoricidal activity is the key to minimizing the toxicity of both virotherapy and chemotherapy. In this study, the synergistic effect allows dosage reduction for both agents while achieving the same therapeutic efficacy.

In conclusion, our current findings clearly showed that CRAd-S.RGD combined with cisplatin significantly improved cytotoxicity *in vitro* and synergistically increased the efficacy in the xenograft tumor model without a concomitant increase in toxicity. These results suggest that CRAd-S-RGD combined with cisplatin would be a promising therapy for ovarian cancer and this combined therapy has great potential for translation into effective clinical therapy.

Acknowledgement

We thanks Dr. Justin C. Roth for his helpful advices and review the manuscript, Dr. F. Li for his providing the vector, pLuc-cyc1.2, which was used to construct AdGL3BSurvivin and Dr. Jingahua Wang for the gift of the ovarian cancer tissues. This study was supported by Nanjing Medical University Grant (CX2004006), NIH-R01CA083821 and DOD-W81XWH-05-1-0035.

Reference

1. Mathis, J. M., M. A. Stoff-Khalili and D.T. Curiel. (2005). “Oncolytic adenoviruses - selective retargeting to tumor cells.” Oncogene **24**(52): 7775-91.
2. Todo, T., R. L. Martuza, Rabkin, S. D. and Johnson, P. A. (2001). “Oncolytic herpes simplex virus vector with enhanced MHC class I presentation and tumor cell killing.” Proc Natl Acad Sci U S A **98**(11): 6396-401.
3. Heise, C. and D. H. Kirn (2000). “Replication-selective adenoviruses as oncolytic agents.” J Clin Invest **105**(7): 847-51.
4. Reynolds, P., I. Dmitriev, Curiel, D. (1999). "Insertion of an RGD motif into the HI loop of adenovirus fiber protein alters the distribution of transgene expression of the systemically administered vector." Gene Ther **6**(7): 1336-9.
5. van der Eb, M. M., S. J. Cramer, Vergouwe, Y., Schagen, F. H., van Krieken, J. H., van der Eb, A. J. Rinkes, I. H., van de Velde, C. J. And Hoeben, R. C. (1998). "Severe hepatic dysfunction after adenovirus-mediated transfer of the herpes simplex virus thymidine kinase gene and ganciclovir administration." Gene Ther **5**(4): 451-8.
6. Adusumilli, P. S., M. K. Chan, Chun, Y. S., Hezel, M., Chou, T. C., Rusch, V. W. and Fong, Y. (2006). "Cisplatin-Induced GADD34 Upregulation Potentiates Oncolytic Viral Therapy in the Treatment of Malignant Pleural Mesothelioma." Cancer Biol Ther **5**(1).
7. Lu, B., Y. Mu, Cao, C., Zeng, F., Schneider, S., Tan, J., Price, J., Chen, J., Freeman, M. And Hallahan, D. E. (2004). "Survivin as a therapeutic target for radiation sensitization in lung cancer." Cancer Res **64**(8): 2840-5.
8. Arafat, W.O. et al. A Novel Radiation/Tissue-Specific Promoter for Gene Therapy of Brain Tumor. I.J.Radiation Oncology.Biology.Physics. 2003, 57:S146.
9. Arafat, W.O. et al. Survivin as a novel radiation/CIS platinum/tumor specific promoter for conditional oncotytic therapy. 2004, J. Clin Oncology, 2004 ASCO Annual Meeting Proceedings, 22:1535.
10. Zhu, Z. B., S. K. Makhija, Lu, B., Wang, M., Rivera, A. A., Kim-Park, S., Ulasov, I. V., Zhou, F., Alvarez, R. D., Siegal, G. P. and Curiel, D. T. (2005). "Incorporating the survivin promoter in an infectivity enhanced CRAd-analysis of oncolysis and anti-tumor effects in vitro and in vivo." Int J Oncol **27**(1): 237-46.

11. Suzuki, K., Fueyo, J., Krasnykh, V. Reynolds, P. N., Curiel, D. T. and Alemany, R. A conditional replicative adenovirus with enhanced infectivity shows improved oncolytic potency. Clin Cancer Res 7:120-126, 2001.
12. Tim Mosmann. Rapid colorimetric assay for cellular growth and survival: Application to proliferation and cytotoxicity assays . Immunol Methods 1983; 65:55.
13. Ormerod MG. The study of apoptotic cells by flow cytometry. Leukemia 1998; 2: 1013 ~ 25.
14. Kaplan EL, Meier P. Nonparametric estimation from incomplete observations. J Am Stat Assoc 1985; 53: 457-81.
15. Curiel, D. T. and C. Rancourt (1997). "Conditionally replicative adenoviruses for cancer therapy." Adv Drug Deliv Rev **27**(1): 67-81.
16. Zhu, Z. B., S. K. Makhija, Lu, B., Wang, M., Kaliberova, L., Liu, B., Rivera, A. A., Nettelbeck, D. M., Mahasreshti, P. J., Leath, C. A., Barker, S., Yamaoto, M., Li, F., Alvarez, R. D. and Curiel, D. T. (2004). "Transcriptional targeting of tumors with a novel tumor-specific survivin promoter." Cancer Gene Ther **11**(4): 256-62.
17. Ambrosini, G., C. Adida and Altieri, D. C. (1997). "A novel anti-apoptosis gene, survivin, expressed in cancer and lymphoma." Nat Med **3**(8): 917-21.
18. Wu, Y., G. Wang, Wei, J. And Wen, X. (2005). "Survivin protein expression positively correlated with proliferative activity of cancer cells in bladder cancer." Indian J Med Sci **59**(6): 235-42.
19. Zhang, S. L., C. Q. Zhao, Lin, B., Li, Y. and Gao, H. (2003). "[Expression of survivin gene and its relation with the expression of bcl-2 and bax protein in epithelial ovarian cancer]." Zhonghua Fu Chan Ke Za Zhi 38(4): 203-6.
20. Bao, R., D. C. Connolly, Murphy, M., Green, J., Weinstein, J. K., Pisarcik, D. A. and Hamilton, T. C. (2002). "Activation of cancer-specific gene expression by the survivin promoter." J Natl Cancer Inst **94**(7): 522-8.
21. Kruyt FA, Curiel DT. Toward a new generation of conditionally replicating adenoviruses: pairing tumor selectivity with maximal oncolysis. Hum Gene Ther 2002; 13: 485-95
22. Dmitriev, I., V. Krasnykh, et al. (1998). "An adenovirus vector with genetically modified fibers demonstrates expanded tropism via utilization of a coxsackievirus and adenovirus receptor-independent cell entry mechanism." J Virol **72**(12): 9706-13.

23. Bookman MA, McGuire, W. P., 3rd, Kilpatrick, D., Keenan, E., Hogan, W. M., Johnson, S. W., O'Dwyer, P., Rowinsky, E., Gallion, H. H. and Ozols, R. F. Carboplatin and paclitacel in ovarian carcinoma: a phase I study of the Gynecologic Oncology Group. J. Clin. Oncol 1966;14:1895-902.
24. McGuire WP., Hoskins WJ, Brady MF, Kucera PR, Partridge EE, Look KY, Clarke-Pearson DL, Davidson M.. Cyclophosphamide and cisplatin compared with paclitaxel and cisplatin in patient with stage III and stage IV ovarian cancer. N Engl J Med 1996;334:1-6.
25. Ozols RF, Bundy, B. N., Greer, B. E., Fowler, J. M., Clarke-Pearson, D., Burger, R. A., Mannel, R. S., DeGeest, K., Hartenbach, E. M. and Baergen, R. Phase III trial of carboplatin and paciltaxel compared with cisplatin and paclitaxel in patients with optimally resected stage III ovarian cancer: a Gynecologic Oncology Group study. J. Clin. Oncol 2003;21:3194-200.
26. Ozols, R. F. and R. C. Young (1985). "High-dose cisplatin therapy in ovarian cancer." Semin Oncol **12**(4 Suppl 6): 21-30.
27. Khuri, F. R., J. Nemunaitis, I. Ganly, J. Arseneau, I.F. Tannock, L. Romel, M. Gore, J. Ironside, R.H. MacDougall, C. Heise, B. Randle, A.M. Gillenwater, P. Bruso, S.B. Kaye, W.K. Hong, D.H. Kirn. A controlled trial of intratumoral ONYX-015, a selectively-replicating adenovirus, in combination with cisplatin and 5-fluorouracil in patients with recurrent head and neck cancer. Nat Med 2000; 6: 879-85.
28. Chu, R. L., D. E. Post, F.R. Khuri and E.G. Van Meir. Use of replicating oncolytic adenoviruses in combination therapy for cancer. Clin Cancer Res 2004; 10: 5299-312.
29. Dilley, J., S. Reddy, D. Ko, N. Nguyen, G. Rojas, P. Working and D.C. Yu. Oncolytic adenovirus CG7870 in combination with radiation demonstrates synergistic enhancements of antitumor efficacy without loss of specificity. Cancer Gene Ther 2005; 12: 715-22.
30. Nemunaitis J, Khuri F, Ganly I, Arseneau J, Posner M, Vokes E, *et al*. Phase II trial of intratumoral administration of ONYX-015, a replication-selective adenovirus, in patients with refractory head and neck cancer. J Clin Oncol 2001; 19: 289–98.
31. Freytag SO, Stricker H, Pegg J, Paielli D, Pradhan DG, Peabody J, *et al*. Phase I study of replication-competent adenovirus-mediated double-suicide gene therapy in combination with conventional-dose three-dimensional conformal radiation therapy for the treatment of newly diagnosed, intermediate- to high-risk prostate cancer. Cancer Res 2003; 63: 7497–506.

32. Geoerger, B., V. W. van Beusechem, et al. (2005). "Expression of p53, or targeting towards EGFR, enhances the oncolytic potency of conditionally replicative adenovirus against neuroblastoma." J Gene Med **7**(5): 584-94.
33. Abou El Hassan, M. A., I. van der Meulen-Muileman, et al. (2004). "Conditionally replicating adenoviruses kill tumor cells via a basic apoptotic machinery-independent mechanism that resembles necrosis-like programmed cell death." J Virol **78**(22): 12243-51.
34. Wang H, Nan L, Yu D, Lindsey JR, Agrawal S and Zhang R: Anti-Tumor Efficacy of a Novel Antisense Anti-MDM2 Mixed-Backbone Oligonucleotide in Human Colon Cancer Models:p53-Dependent and p53-Independent Mechanisms. Molecular Medicine 8:185-199, 2002.
35. Ikeguchi, M., J. Liu, et al. (2002). "Expression of survivin mRNA and protein in gastric cancer cell line (MKN-45) during cisplatin treatment." Apoptosis **7**(1): 23-9.
36. Belyanskaya, L. L., S. Hopkins-Donaldson, et al. (2005). "Cisplatin activates Akt in small cell lung cancer cells and attenuates apoptosis by survivin upregulation." Int J Cancer **117**(5): 755-63.
37. Hitt, M. M. and F. L. Graham (1990). "Adenovirus E1A under the control of heterologous promoters: wide variation in E1A expression levels has little effect on virus replication." Virology **179**(2): 667-78.
38. Nomura, T., M. Yamasaki, et al. (2005). "Expression of the inhibitors of apoptosis proteins in cisplatin-resistant prostate cancer cells." Oncol Rep **14**(4): 993-7.
39. Li, H., J. Y. Niederkorn, et al. (2006). "Downregulation of survivin expression enhances sensitivity of cultured uveal melanoma cells to cisplatin treatment." Exp Eye Res **83**(1): 176-82.

Legends

Figure 1

Cell viability determined by MTT assay. A) Viability of ovarian cancer SKOV-3 cells were infected with different concentrations of CRAd-S.RGD (0.01, 0.1, 1.0, 10 and 100 pfu/cell); B) Viability of ovarian cancer SKOV-3 cells were treated with 10 pfu/cell of CRAd-S.RGD, 10 μg/ml of cisplatin, 10 pfu/cell of CRAd-S.RGD combined with 10 μg/ml of cisplatin, and PBS, respectively. Data were presented as mean ± S.D. , n = 3.

Figure 2

Antitumor efficacy of treatments in SKOV-3 ovarian cancer cell xenograft model. Mice with s.c. SKOV-3 flank tumors (10/group) received CRAd-survivin-RGD4C (i.t. 10^8 pfu /d, days 1-5), cisplatin(i.v. 4 mg/kg/d, days 1, 3, 5), CRAd-S.RGD (i.t. 10^8 pfu /d, days 1-5) followed by cisplatin (i.v. 4 mg/kg/d, days 7, 9, 11) and neither (i.t. PBS), respectively. A) SKOV3 tumor volumes change after treatments. Data were presented as mean ± S.D. , n = 3; B) Kaplan-Meier survival of animals following the above treatments.

Figure 3

The apoptosis rate of mice tumor tissues were detected by TUNNEL assay after 14 days treatments. Data were shown as means ± SD, n = 3. $^{*}P$ <0.01, *vs*. PBS. $^{\#}P$ <0.05, $^{\#\#}P$ <0.01, *vs*. CRAd or cisplatin.

Table 1. Therapeutic effectiveness of combination treatment in animal bearing SKOV3 xenograft.

The ratio 3:2 or 1 can be used to illustrate the potential additive or synergistic effects when the CRAd-S.GRD was given in combination with cisplatin. When the ratio for combination therapy is less than 100% (compared to agent alone), an effect of an additive effect is indicated. If the ratio for combination therapy is significant less than that of single therapy, a synergistic effect is indicated.

Figure 1A

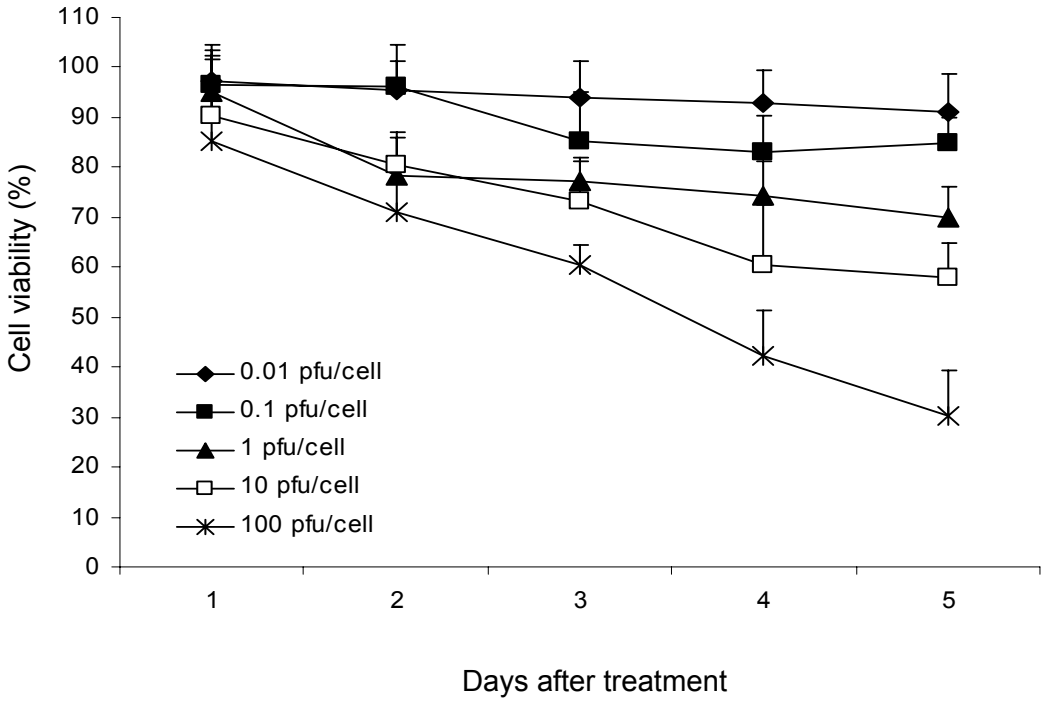
Cell viability (%)
110
100
90
80
70
60
50
40
30
20
10
0
1
2
3
4
5
Days after treatment
0.01 pfu/cell
0.1 pfu/cell
1 pfu/cell
10 pfu/cell
100 pfu/cell

Figure 1B

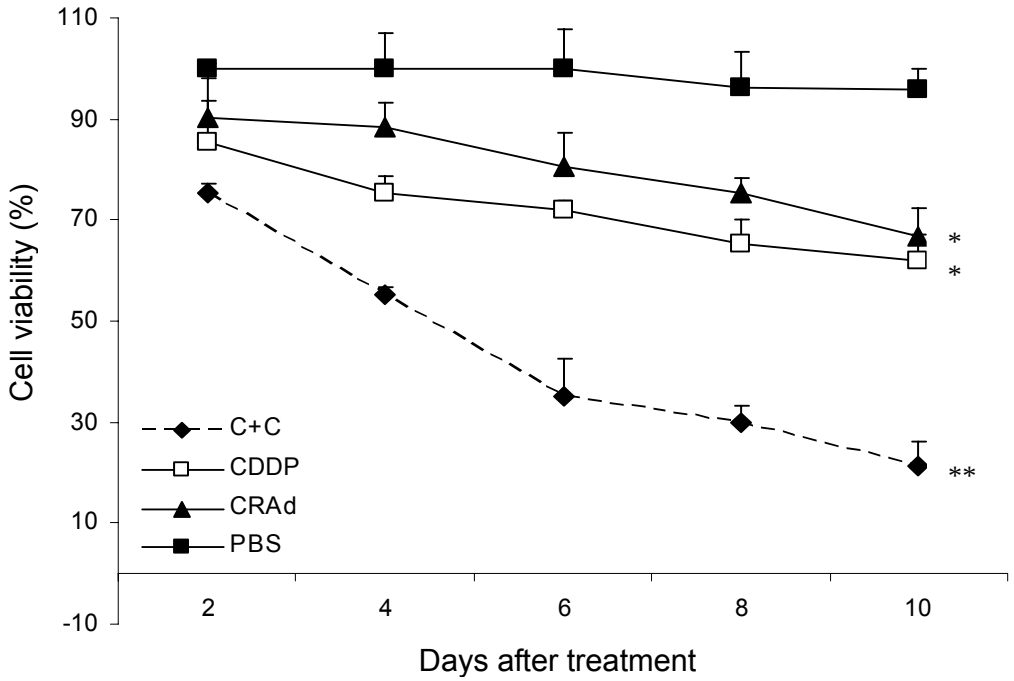
110
90
70
50
30
10
-10
Cell viability (%)
2
4
6
8
10
Days after treatment
C+C
CDDP
CRAd
PBS
*
*
**

Figure 2A

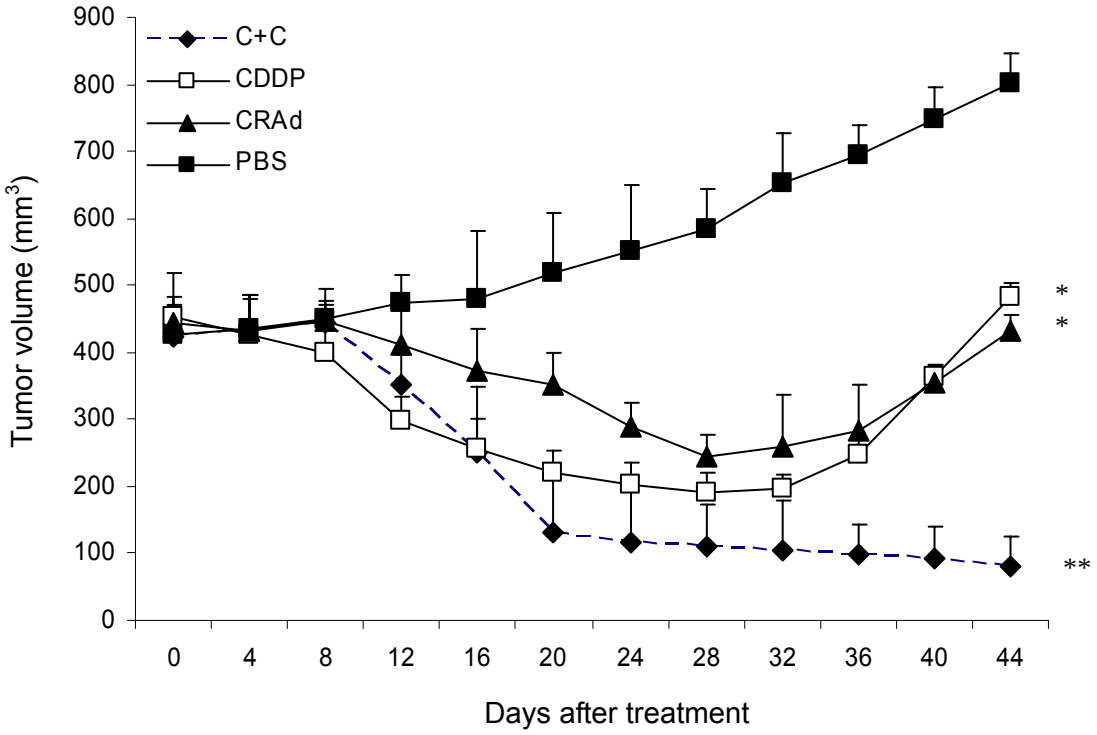
C+C
CDDP
CRAd
PBS
Tumor volume (mm3)
900
800
700
600
500
400
300
200
100
0
0
4
8
12
16
20
24
28
32
36
40
44
Days after treatment
*
*
**

Figure 2B

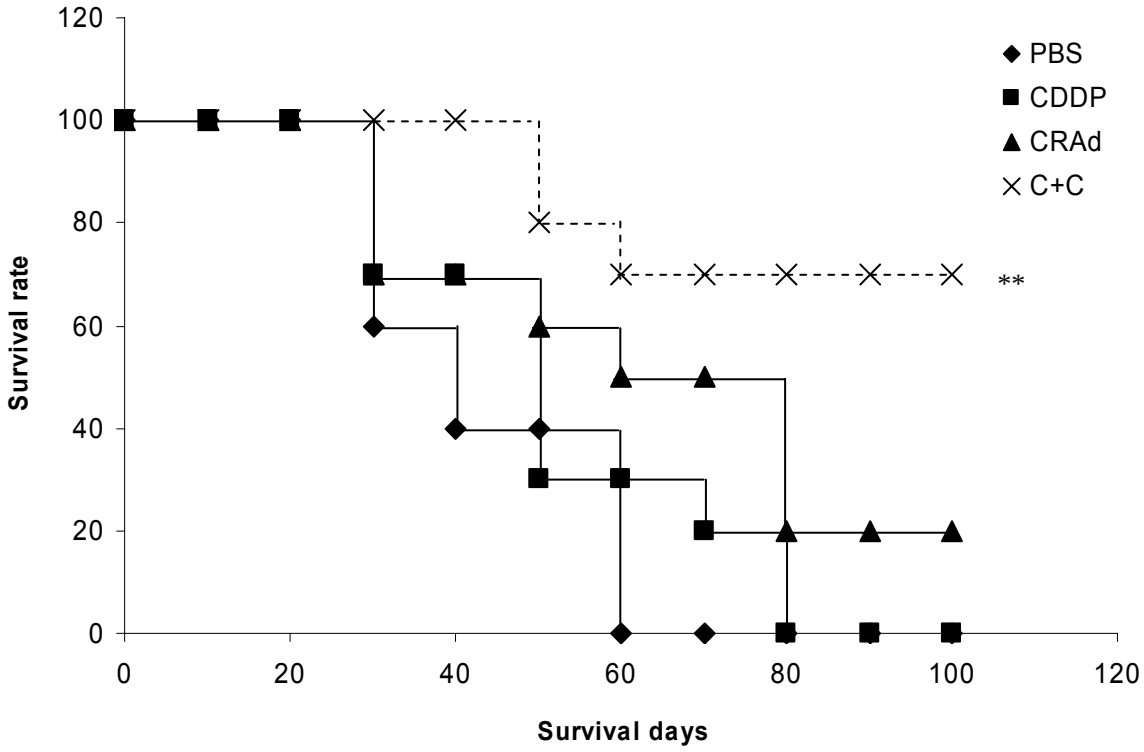
120
100
80
60
40
20
0
Survival rate
0
20
40
60
80
100
120
Survival days
PBS
CDDP
CRAd
C+C
**

Figure 3

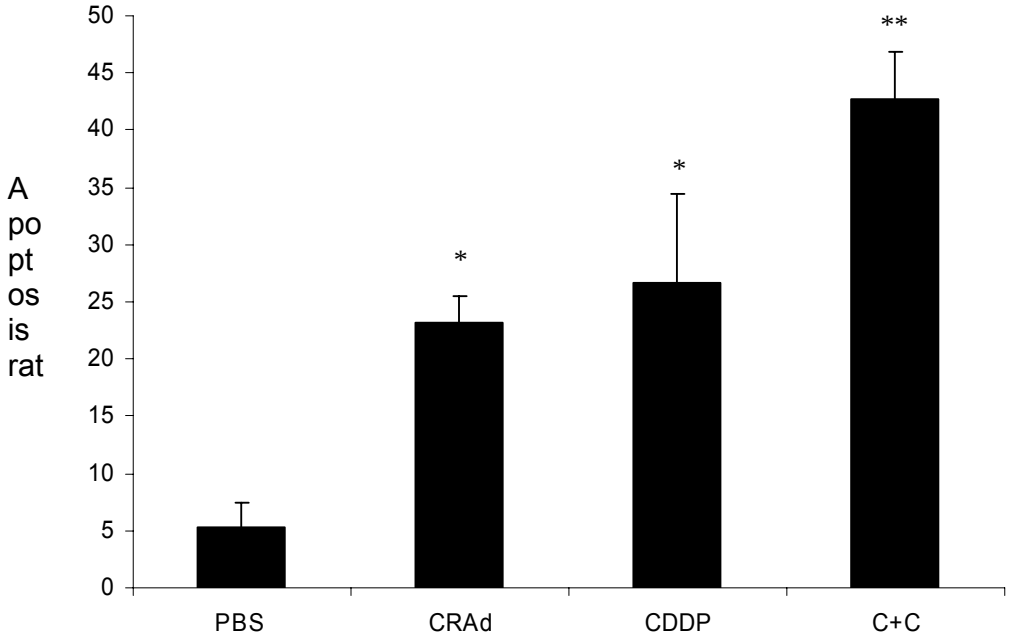

Table 1. Therapeutic effectiveness of combination treatment in animal bearing SKOV3 xenograft

Day after treatment	Treatment	Tumor vol. mean (mm3)	ratio (%) T: C		Ratio (%) 3:2 or 1
0	PBS	427	100.0		
	CDDP	452	105.9	1	93.4
	CARD	443	103.7	2	95.3
	C+C	422	98.8	3	
4	PBS	434	100.0		
	CDDP	427	98.4	1	101.6
	CARD	432	99.5	2	100.5
	C+C	434	100.0	3	
8	PBS	450	100.0		
	CDDP	389	86.4	1	114.4
	CARD	448	99.6	2	99.3
	C+C	445	98.9	3	
12	PBS	437	100.0		
	CDDP	298	68.2	1	118.1
	CARD	412	94.3	2	85.4
	C+C	352	80.5	3	
16	PBS	481	100.0		
	CDDP	255	53.0	1	98.0
	CARD	372	77.3	2	67.2
	C+C	250	52.0	3	
20	PBS	520	100.0		
	CDDP	221	42.5	1	59.3
	CARD	353	67.9	2	37.1
	C+C	131	25.2	3	
24	PBS	552	100.0		
	CDDP	203	36.8	1	57.6
	CARD	288	52.2	2	40.6
	C+C	117	21.2	3	
28	PBS	583	100.0		
	CDDP	191	32.8	1	57.6
	CARD	243	41.7	2	45.3
	C+C	110	18.9	3	
32	PBS	652	100.0		
	CDDP	197	30.2	1	52.3
	CARD	259	39.7	2	39.8
	C+C	103	15.8	3	
36	PBS	693	100.0		
	CDDP	247	35.6	1	40.1
	CARD	283	40.8	2	35.0
	C+C	99	14.3	3	
40	PBS	747	100.0		
	CDDP	365	48.9	1	24.9
	CARD	354	47.4	2	25.7
	C+C	91	12.2	3	

44	PBS	801	100.0		
	CDDP	482	60.2	1	16.6
	CARD	432	53.9	2	18.5
	C+C	80	10.0	3	